Chemical reactions catalysed by metal nanoparticles under sustainable conditions

		
Doctor of Philosophy in Environmental, Territorial, Building Risk and Development	***POLITECNICO DI BARI***	03
Coordinator: Prof. Michele Mossa		2019
XXXII CYCLE Curriculum: CHIM/07		
DICATECh Department of Civil, Environmental, Building Engineering and Chemistry		
	Chemical reactions catalysed by metal nanoparticles under sustainable conditions	
	Prof. Piero Mastrorilli ***DICATECh, Polytechnic University of Bari*** ***Prof. Rinaldo Poli*** ***LCC CNRS, Toulouse***	
	Prof. Maria Michela Dell'Anna ***DICATECh, Polytechnic University of Bari***	
	Ambra Maria Fiore	

		
Dottorato in Rischio e Sviluppo ambientale, Territoriale ed Edilizio	***POLITECNICO DI BARI***	03
Coordinatore: Prof. Michele Mossa		2019
XXXII CYCLE Curriculum: CHIM/07		
DICATECh Dipartimento di Ingegneria Civile, Ambientale, del Territorio, Edile e di Chimica		
	Chemical reactions catalysed by metal nanoparticles under sustainable conditions	
	Prof. Piero Mastrorilli ***DICATECh, Polytechnic University of Bari*** ***Prof. Rinaldo Poli*** ***LCC CNRS, Toulouse***	
	Prof. Maria Michela Dell'Anna ***DICATECh, Polytechnic University of Bari***	
	Ambra Maria Fiore	

“ La scelta di un giovane dipende dalla sua inclinazione,
ma anche dalla fortuna di incontrare un grande maestro.”

Rita Levi-Montalcini

A mio padre

EXTENDED ABSTRACT

Metal nanoparticles (NPs) and nano-catalysts are largely investigated given their unique properties. With the recent advances in nanochemistry and particularly in the synthesis of new highly active catalyst, nanocatalysis is now recognized as a full and rich part of catalysis. In the present research, an environmentally friendly synthetic method was developed for preparation of a new polymer supported Ni NPs (Ni-pol), generated by calcination under nitrogen of Ni(II) containing polyacrylamide. Ni-pol catalysed the hydrogenation of nitroarenes to anilines in aqueous medium, the one pot stepwise reductive amination of arylaldehydes with nitroarenes and the upgrade of bio-oils. The catalyst was fully characterized by STEM, IR and elemental analysis before, during and after several catalytic runs. In the second part of this thesis, strategies of synthesis of metal nanoparticles (M-NPs) confined on triphenylphosphine (TPP) functionalized and organized (amphiphilic core-shell) polymers, termed core cross-linked micelle (CCM) were developed. TTP@CCMs were first loaded with complexes of Rh, Ru, Ir, Pt, Pd, Au, and then reduced under H_2 at different temperatures (depending on the metal) to give polymer stabilized metal NPs. Turning several parameters a metal nanoparticles embedded in polymeric nanoreactors were obtained with uniform distribution. NPs were employed as catalysts in acetophenone, as model reaction, and in styrene hydrogenation. The NPs morphology was studied by TEM analyses before and after the catalytic applications.

Keywords: Nanoparticles, Polymer supported nanoparticles, Recyclability, Water confined nanoreactors

EXTENDED ABSTRACT

Negli ultimi anni l'interesse della comunità scientifica si è focalizzato sullo studio di nuovi nanomateriali e nanocatalizzatori, materiali molto promettenti per diverse applicazioni. Con lo sviluppo delle nanoscienze, la nano chimica ha fatto passi da gigante in particolare per la sintesi di nuovi catalizzatori attivi e selettivi, in condizioni eco sostenibili. In questo lavoro di tesi è stato messo a punto un nuovo metodo di sintesi pulito per la preparazione di un nuovo polimero supportante nanoparticelle (NPs) di nickel (Ni-pol). Queste ultime sono state ottenute per mezzo di una riduzione termica del polimero supportante il complesso di Ni(II), contenente poliacrilammide, sotto flusso di azoto. Ni-pol è risultato attivo nell'idrogenazione dei nitroareni per ottenere le corrispondenti aniline; nella riduzione amminica delle aldeidi con i nitroareni e nell'upgrade dei bio-oil. Il catalizzatore è stato caratterizzato mediante analisi elementari, STEM e IR, durante e dopo diversi cicli catalitici. Nella seconda parte di questo lavoro di tesi è stata messa appunto una nuova strategia per la sintesi di nanoparticelle metalliche confinate nel cuore idrofobico di nanoreattori polimerici. Il nanoreattore è stato caricato con diversi precursori metallici i quali sono stati ridotti sotto flusso d idrogeno a diverse temperature, a seconda del metallo impiegato. Modificando diversi fattori le NPs sono state confinate all'interno del nanoreattore polimerico con una distribuzione uniforme delle stesse. Le nanoparticelle metalliche ottenute sono state impiegate nell'idrogenazione dell'acetofenone, reazione di riferimento, e dello stirene. La morfologia delle nanoparticelle è stata studiata mediante analisi TEM prima e dopo l'applicazione in catalisi.

Parole Chiave: Nanoparticelle, Polimeri supportanti nanoparticelle, Reciclabilità, Nanoreattori confinati in acqua

GENERAL INDEX

INTRODUCTION

Nanoscience has recently evolved as a major research way of our modern Society resulting from an ongoing attempt to develop at the nano-scale processes that presently use microsystems. Towards this end, it is well admitted that new cheap and clean approaches replaced the old ones, a strategic choice that is common to several areas of nanoscience including medicine, optoelectronics, and catalysis. The latter one, without doubt, is the key one for the development of starting chemicals, fine chemicals and drugs from raw materials. During the twentieth century, chemists have made considerable attainments in heterogeneous catalysis, while homogeneous catalysis processed after the Second World War (with hydrophormilation) and especially since the early 1970s (with hydrogenation). Heterogeneous catalysis, which benefits from easy removal of catalyst materials and possible use of high temperatures, endured for a long time from lack of selectivity and understanding of the intrinsic aspects that are necessary for improvement the parameters. Homogeneous catalysis is very efficient and selective, and is used in a few industrial processes, but it suffers from the difficulty of removal of the catalyst from the reaction media and its limited thermal stability. Green catalysis aspects now clearly require that environmentally friendly catalysts be designed for easy removal from the reaction media and recycling many times with very high efficiency. These demanding conditions lead a new research impetus for catalyst development in the middle of homogeneous and heterogeneous catalysis. However, the considerable knowledge gained from the past researches in homogeneous, heterogeneous, supported, and biphasic catalysis, should now help establish the desired optimized catalytic systems. In this content the use of transition metal nanoparticles in catalysis is crucial as they mimic metal surface activation and catalysis at the nanoscale and thereby bring selectivity and efficiency to heterogeneous catalysis.

In this context, the current thesis is based on the development of new strategy for the synthesis of metal nanoparticles used as active and recyclable catalysts in several chemical reactions. The search project needs a broad range of know-how from organometallic complexes, polymer and nanoparticles synthesis, heterogeneous and biphasic catalysis. Considering the multidisciplinary approaches and their implementation, the research program was developed in a collaboration between our team, specialized in the synthesis characterization and catalytic application of polymer supported metal nanoparticles as highly active, selective and recyclable catalysts, and another team at “Laboratoire de Chimie de Coordination” (LCC) CNRS, headed by Prof. Rinaldo Poli, specialized in ligand design, architectures complexes and catalysis.

The first chapter will provide an overview of role of nanoparticles in catalysis, the available catalyst recovery strategies, followed by a description of the developed search on new nano-catalysts, which will be considered as the starting point for the new research, including the role of support for nano-catalysts. This bibliographic chapter also includes a section detailing various methods for biphasic catalysis and the known examples of the well-defined polymeric nanoreactors with their use in catalysis.

The second chapter will describe all the synthetic efforts realized during this thesis, starting with the synthesis and characterization of polymer supported Ni(II)complex, [known as *Ni(II)-pol*], obtained by co-polymerization of $Ni(AAEMA)_2$ ($AAEMA^-$ = deprotonated form of 2-acetoacetoxyethyl methacrylate) with suitable co-monomer (*N,N*-dimethylacrylamide) and crosslinker (*N,N*-methylenebisacrylamide), including the description of the method used for the calcinations of Ni(II)-pol to give polymer supported Ni(0)-nanoparticles (Ni-pol), and their characterization. This part is followed by catalytic applications of Ni-pol in the synthesis of primary and secondary anilines, followed by the comparison between the catalytic activity of Pd-pol and Ni-pol in the upgrade of bio-oils.

The third chapter will describe the synthesis of metal nanoparticles embedded in polymeric nanoreactors. Starting with a recently developed synthesis of triphenylphosphine (TPP) functionalized and hierarchically organized (amphiphilic core-shell) polymers, termed core cross-linked micelle (CCM), containing a neutral shell, the metal coordination was carried out inside the nanoreactors, extending this method to six metal precursors (Rh, Pd, Pt, Ir, Ru, Au). The metal centres located in the CCM core were reduced under hydrogen gas to give metal nanoparticles. This part is followed by the strategies developed for the nanoparticles confinement in the polymeric nanoreactors, including their catalytic application as recyclable aqueous biphasic catalyst for the hydrogenation of acetophenone, taken as model reaction.

All the synthetic protocols, the full characterization data for the products, and a description of the equipment and instrumentation used for the preparation, characterization and evaluation of the polymeric nanoreactors is detailed in chapter IV.

CHAPTER I
State of art

TABLE OF CONTENTS

CHAPTER I
State of the Art

1.1 Chemistry and the Environment

1.1.1 Green chemistry

Chemistry affects our lives every day. While we enjoy the attractive price to performance ratio of chemical products such as new materials for everyday life, cheap stuff for the apartment, plastic bottles and so on, the accumulation of plastic garbage makes more and more people realise the importance of product life cycle. This factor leads to slow changes. Two words are the symbol of these changes: sustainability and sustainable development. Sustainability can be considered as a society which tries to find a common solution for both the needs of the current humanity and the needs of future generations. Sustainable development is a strategic goal that can be reached using green chemistry rules. Figure I.1 shows the relationship between sustainable development and practical approaches. Each practical approach exploits precise tools in order to contribute to the sustainable development. Green chemistry is just one step, but the most important on the road to sustainability. An operational tool of green chemistry is catalysis, on which we will focus shortly.

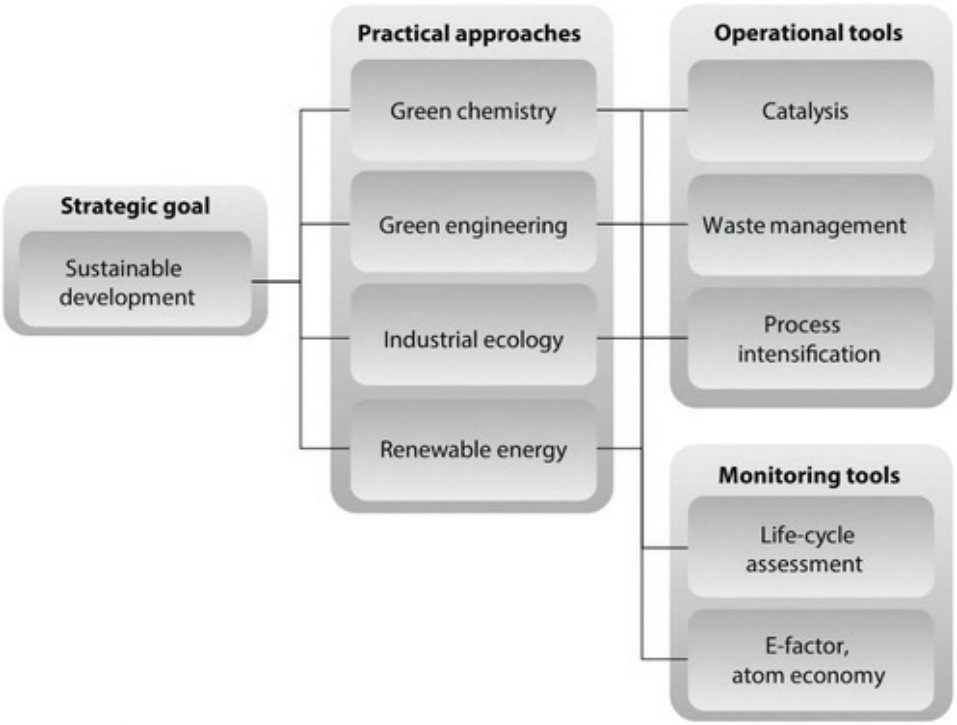

Figure I.1 - The strategic goal of sustainable development relies on practical approaches, such as green chemistry, industrial ecology, renewable energy and green engineering. These approaches use various operational and monitoring tools.[1]

In the 1990s, the concept of green chemistry was introduced in both USA and Europe and it has been widely adopted by chemical industry. Green chemistry deals with designing chemical products and processes that generate and use less hazardous substances. Indeed, the green chemistry message is simple "Seek prevention, not cure". Green chemistry offers an alternative to the traditional environmental protection agenda, mainly because it deals with avoiding hazardous, rather than with treating and solving exposure problems.

Three forces drive the green chemistry initiative: government legislation, societal pressure, and economic benefit. The economic benefit is the most important aspect because if you use less solvent, your reactor space-time yields go up. If you replace costly reagents with cheaper and more abundant ones by using smaller and safer equipment, the production cost decreases. Eliminating waste also eliminates the need for waste treatment and disposal, replacing tox-

ic reagents with benign ones saves on safety costs during transportation and storage. Thus, more and more companies are adopting green chemistry practices simply because it improves their bottom-line performance. By applying the principles of green chemistry, companies start to use cleaner and more efficient technologies, aiming at keeping the environment cleaner and healthier.

So Green Chemistry or Sustainable Chemistry changes the traditional concept of process efficiency, passing from the scope of a high chemical yield to an objective that assigns economic value to eliminating waste at source and avoiding the use of toxic and hazardous substances. The most important focus of this approach is the environmental impact of both chemical products and the processes used for their production. Anastas[2] demonstrated that the guiding principle is the start point for the environmentally friendly products and processes. Ideally the processes should respect the fundamental principles of green chemistry, reported in Table I.1. Maximizing all 12 principles of Green Chemistry simultaneously is the most important objective. Anyway, it might be impossible. The optimization of the various criteria can lead to high benefits.

Trying to respect these principles in every process is the main goal of chemical industries. In this framework, a crucial point is, for example, the implementation of green chemistry in the production of omnipresent materials such as polymers and plastics, and the use of catalysts.

Table I.1 - The 12 principles of Green Chemistry

1. It is better to prevent waste than to treat or clean up waste after it is formed
2. Synthetic methods should be designed to maximize the incorporation of all materials used into the final product
3. Wherever practicable, synthetic methodologies should be designed to use and generate substances that possess little or no toxicity to human health and the environment
4. Chemical products should be designed to preserve efficacy of function while reducing toxicity
5. The use of auxiliary substances (e.g. solvents, separation agents, etc.) should be made unnecessary wherever possible and, innocuous when used
6. Energy requirements should be recognized for their environmental and economic impacts and should be minimized. Synthetic methods should be conducted at ambient temperature and pressure
7. A raw material of feedstock should be renewable rather than depleting wherever technically and economically practicable

8. Unnecessary derivatization (blocking group, protection/de-protection, temporary modification of physical/chemical processes) should be avoided whenever possible
9. Catalytic reagents (as selective as possible) are superior to stoichiometric reagents
10. Chemical products should be designed to preserve efficacy of function while reducing toxicity
11. Analytical methodologies need to be developed to allow for real-time, in-process monitoring and control prior to the formation of hazardous substances
12. Substances and the form of a substance used in a chemical process should be chosen so as to minimize the potential for chemical accidents, including releases, explosions and fires

1.1.2 Catalysis Role

More than 75% of all chemical industry transformation employs catalysts in different areas, such as production of polymers, pharmaceuticals, agrochemicals, and petrochemicals.[3]

Use of catalysts represents a primary tool for achieving the principles of Green Chemistry. Scientific results demonstrated that very often catalytic processes can follow at the same time several principles of Green Chemistry. The field of catalysis science can be considered as a full scientific area.[4] In addition, catalysis is also a powerful instrument to solve environmental problems related to chemical waste storage, processing and disposal (Table I.2).[5] The most common chemical waste is the so called mixed waste, containing organic and inorganic compounds. The generally used method for destroying combustible hazardous waste is flame incineration, which has different disadvantages linked to the formation of pollutants such as NO_x and CO, hydrocarbons and aerosol toxic particles.[6] Selective catalytic reduction of NO_x is an example of use of catalysts for environmental remediation.

More, storage of high level liquid entail the formation of hydrogen which forms explosive mixtures with air;[7] catalytic oxidation of hydrogen ensures the safety of the liquid waste storage.

Table I.2 - Applications of catalysis for treatment of different type of wastes.

Application of catalysis in radioactive waste processing

Type of waste	Method of processing or storage	Problem	Application of catalysis
Mixed organic waste	Incineration in flame	Air pollutants, radioactive aerosols	Alternative process—catalytic fluidized bed oxidation
Mixed organic waste	Molten salt oxidation	High temperature, corrosionand NO_x formation	Application of catalytically active melts
Mixed waste	Plasma arc destruction	High NO_x concentration up to 10 000 ppm	Selective catalytic reduction of NO_x
High level waste containing nitrates	Vitrification	High NO_x concentration over 10 000 ppm	Selective catalytic reduction of NO_x
High level waste containing nitrates	Vitrification	High NO_x concentration over 10 000 ppm	Reduction of nitrates to N_2 and NH_3 followed by catalytic NH_3 oxidation to N_2
Liquid high level waste	Storage in tanks	H_2formation at explosive concentrations	Catalytic oxidation of H_2
Contaminated soil and groundwater	Remediation of nuclear sites by stripping of soil and groundwater with air or steam	Formation of VOCs	VOC catalytic oxidation

On the other hand, industries have developed a great interest in the use of catalysts for the synthesis of fine chemicals used as intermediates for the preparation of a wide range of materials. Unfortunately, chemical industries still employ toxic solvents, expensive materials and strong reaction conditions (such as high temperature, pressure and so on). Recently, the efforts of academic and industrial communities are focused in minimizing cost and toxicity catalytically promoted processes.[8]

1.2 Catalysis

The notion of catalysis was introduced for the first time by Elizabeth Fulhame in 1794, based on her work in oxidation-reduction.[9] In 1836 Berzelius used for the first time the term "catalyst" in order to describe a new entity able to promote the chemical reaction using a "catalytic contact".[10]

Based on the collision theory, a chemical reaction occurs when the collision between particles is successful. This happens when, beside other requirements, the reagent particles have enough energy to break bonds in order to start chemical reaction. The minimum energy needed for a reaction to take place is called activation energy (Figure I.4). Particles energy varies even at fixed temperature; this suggests that only some particles will have enough energy in order to promote the chemical reaction (Figure I.2). Increasing the reaction temperature provide the effect of increasing the number of particles that have enough energy to react.

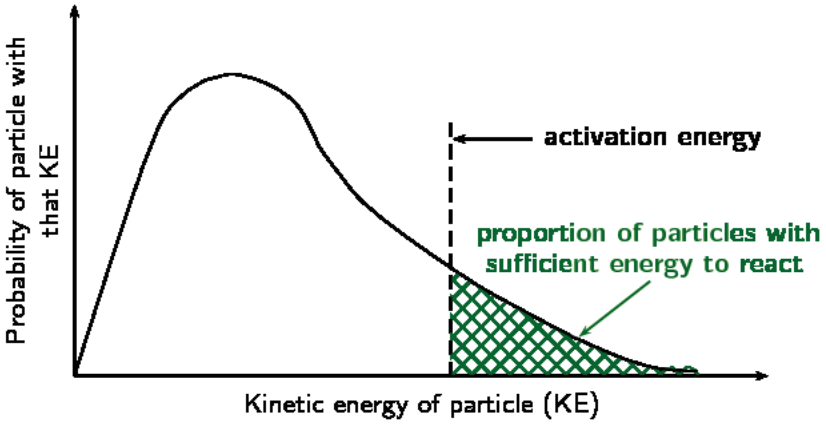

Figure I.2 - The distribution of particle kinetic energies at a fixed temperature.

A catalyst increases reaction rates by lowering the activation energy, thus increasing the number of particles able to react (Figure I.3), because it forms with the reactant a transition state (the activated complex) more stable than the transition state formed in the absence of the catalyst (Figure I.4). The catalyst mass remains unchanged at the end of the reaction, this suggests that the catalyst does not appear in the reaction stoichiometry. A catalyst does not need to be added in stoichiometric quantity in the reaction. A small amount of it, in moles, compared to the substrates, is enough to promote the reaction.

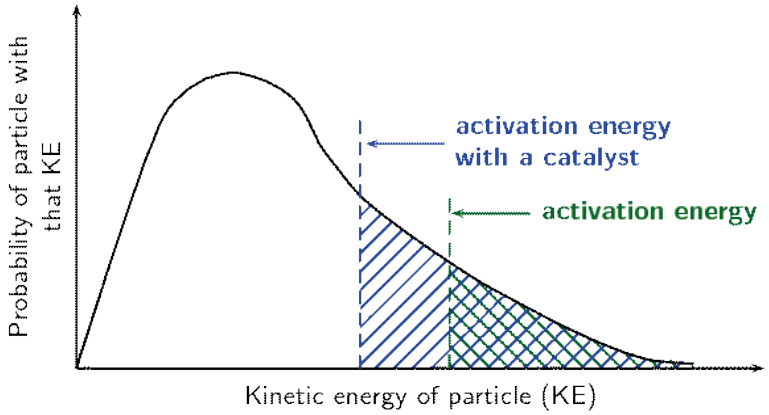

Figure I.3 – The number of particles that have enough energy to react increases with a catalyst.

Energy diagrams (Figure I.4) are useful to illustrate the effect of a catalyst on reaction rates. Catalysts decrease the activation energy required for a reaction to proceed, and therefore increase the reaction rate. In the presence of a catalyst, the average kinetic energy of the molecules remains the same but the required energy decreases.

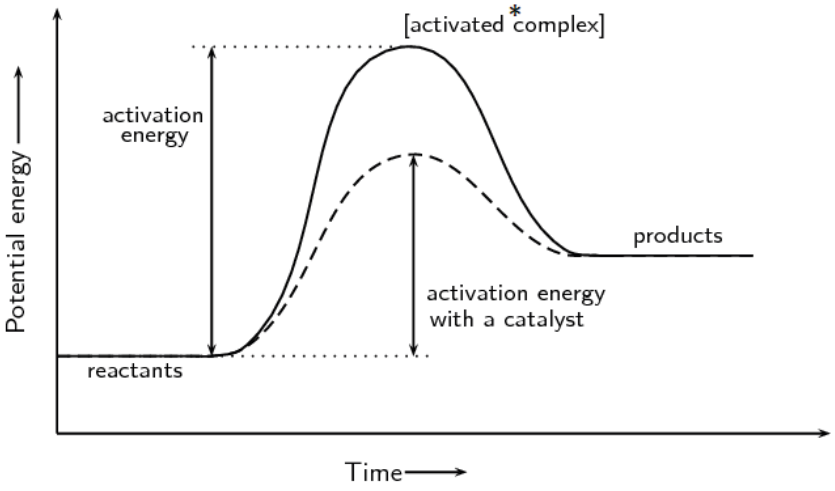

Figure I.4 - The effect of a catalyst on the activation energy of reaction.

Many years after the Berzelius observation, in 1895 Ostwald came up with the definition that we use until today: a catalyst is a substance which increases the rate at which a chemical reaction approaches equilibrium without becoming itself permanently involved.

Catalysis can be homogeneous or heterogeneous: in the first case the catalyst and all reactants and the solvent are in the same phase, while in the second one they are in different phases.

1.2.1 Homogeneous and heterogeneous catalysis

Homogeneous catalysis, by definition, refers to a catalytic system in which the substrates for a reaction and the catalyst components are brought together in one phase, most often the liquid phase.

To recycle the homogeneous catalyst is necessary to separate it from the homogeneous phase containing the reaction products. The recovery and recycling of homogeneous catalysts are important issues from the economic and environmental points of view. The problem related to the recovery of the catalyst arises because the most commonly used separation method is distillation which requires elevated temperature unless the product is volatile. Several homogeneous catalysts are thermally sensitive, so the thermal stress caused by product distillation usually decomposes the catalyst. Using the traditional distillation method to do separation, low pressure is often necessary in order to lower boiling temperature and avoiding catalyst deactivation. However, this method is often energy intensive and can deactivate the catalyst. Other different methods such as chromatography or extraction also lead to catalyst loss.

To overcome the separation problems, chemists and engineers investigate a wide range of strategies for catalyst recovering that can broadly be grouped into three types. The first one consists in anchoring the catalyst onto a soluble support (polymer or a dendrimer) that can be more easily separated from the products phase at the end of the reaction by precipitation, after addition of a second solvent in which the supported catalyst is insoluble. The second and third strategies consist of immobilizing the homogeneous catalyst onto a second phase, solid and liquid respectively, thus the catalytic process becomes heterogeneous. When the catalyst is confined in a second liquid phase, immiscible with the product phase, it can be recovered at the end of the reaction by simple decantation.

Catalytic processes, in which the catalyst and the reactants are not in the same phase, are known as heterogeneous catalytic reactions. They include reactions between gases or liquids or both at the surface of a solid catalyst. The surface is the place at which the reaction occurs, in fact it is generally prepared in ways that produce large surface areas per unit of catalyst; finely divided metals, metal gauzes, metals incorporated into supporting matrices, and metallic

films have all been used in modern heterogeneous catalysis.

Unlike what has emerged for homogeneous catalysis, in the case of heterogeneous catalysis the catalyst recovering can take place in easy way by removing the insoluble catalyst from the reaction mixture at the end of the use.

Table I.3 reports the main differences between homogeneous and heterogeneous catalysis. Most of the homogeneous catalytic reaction occurs in a liquid phase and the catalyst is a well-defined molecular compound whereas the heterogeneous ones involve the use of a solid catalyst and the reaction occurs on the solid surface. The fact that the catalyst is in a different phase with respect to the reaction medium is the main advantage of the catalytic heterogeneous processes. In this case separation and recycling are easier and less costly. On the other side, in the homogeneous catalysis the use of a well-defined molecular compound that is in the same phase as the catalyst, makes homogeneous catalysts more active and selective. On the other hand, heterogeneous catalysts are characterized by an irregular shape surface that has a multiple sites. If on one side homogenous catalysis gives a very good results in terms of yield and products, on the other the heterogeneous catalysis permits to recover and reuse catalyst, sometimes without loss activity.

Table I.3 - Comparison between homogeneous and heterogeneous catalysis.

	Homogeneous	**Heterogeneous**
Active Centers	All atoms	Only surface atoms
Selectivity	High	Low
Mass Transfer Limitations	Very rare	Can be severe
Structure/Mechanism	Defined	Undefined
Catalyst Separation	Tedious/Expensive (extraction or distillation)	Easy
Applicability	Limited	Wide
Cost of Catalyst Losses	High	Low

During the last years, the increasing attention for the environment causes wide development in the methodologies used for catalysts recycling. This aspect is one of the key scopes in green chemistry, where chemical efficiency should be combined with economic and environmental needs. Thus, the development of recyclable heterogeneous catalysts is highly desirable not only for a facile separation but also for devising novel chemical processes, even if there are some disadvantages such as strong reaction conditions that they require to be efficient.

1.3 Nanoparticles

In the framework of catalysis, nanoparticles recently have gained great importance. Nanoparticles are defined as particulate dispersions or solid particles with a size in the range of 1-100 nm.[11] They are used in a wide range of applications, such as cosmetics, optoelectronic and semiconductor devices, catalysis and so on. Nanocomposites made up of inorganic nanoparticles and organic polymers; represent a new class of materials that exhibit improved performance when compared with their microparticle counterpart.[12] Surface modification of inorganic nanoparticles has attracted a great deal of attention because it produces excellent integration and improved interface between nanoparticles and polymer matrices. The nanocomposites obtained by incorporation of these types of materials can lead to improvements in several areas. However, the nanoparticles have a strong tendency to undergo agglomerations followed by insufficient dispersal in the polymer matrix. To improve the dispersion stability of nanoparticles (NPs) in aqueous media or polymer matrices, it is necessary that the particle surface modification, involving polymer surfactant molecules or other modifiers, generates a strong repulsion between nanoparticles.

Nanoparticles may be synthesized from many materials by various physical and chemical methods. They can be classified depending on morphologies, shape, size[13] and chemical or physical properties.[14] The physical methods generally involve vapour deposition and depend on the principle of sub-dividing bulk precursor materials into smaller nanoparticles. The chemical approach generally involves reduction of metal ions into metal atoms in the presence of stabilizing agents, followed by the controlled aggregation of atoms.[15] The synthesis of nanoparticles by chemical methods has proved to be more effective than the use of physical methods.

Nanoparticles are generally classified into the organic, inorganic and carbon based. Organic nanoparticles, also known as polymers, are micelles, dendrimers, liposomes and so on (Figure I.5). These NPs are biodegradable, non-toxic and in the case of micelles they have an empty core; they are sensitive to thermal and electromagnetic radiation such as light. For these particular properties, they are ideal nanomaterials for drug delivery.[16]

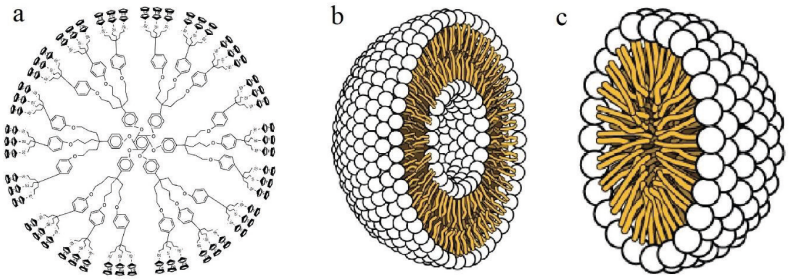

Figure I.5 - Organic nanoparticles: a – Dendrimers, b – Liposomes and c – micelles.

Inorganic nanoparticles are particles that are not made up of carbon. Nanoparticles based on metal and metal oxide are considered as inorganic NPs. Two most important differences must have to consider for the metal and metal oxide nanoparticles. In the first one, NPs are synthesized from metals to nanometric sizes through destructive or constructive methods. Almost all the metals can be synthesised into their nanoparticles.[17] These NPs have particular interesting surface characteristics like high surface area to volume ratio, pore size, surface charge, crystalline and amorphous structures, shapes like spherical and cylindrical and colour, reactivity and sensitivity to environmental factors such as air, heat etc. The second ones, instead, are synthesised to modify the properties of their respective metal based nanoparticles. For example nanoparticles of iron (Fe) instantly oxidise to iron oxide (Fe_2O_3) in the presence of oxygen at room temperature, this increases their reactivity compared to iron nanoparticles. Metal oxide nanoparticles are synthesised mainly due to their increased reactivity and efficiency.[18] These nanoparticles have posses' exceptional properties when compared to their metal counterparts. There is also the possibility to obtain nanoparticles made completely of carbon, called as carbon-based NPs.[19] They are classified into fullerenes, graphene, carbon nanotubes (CNT), carbon nanofibers and carbon black, sometimes activated carbon in nanosize. They are presented in Figure I.6.

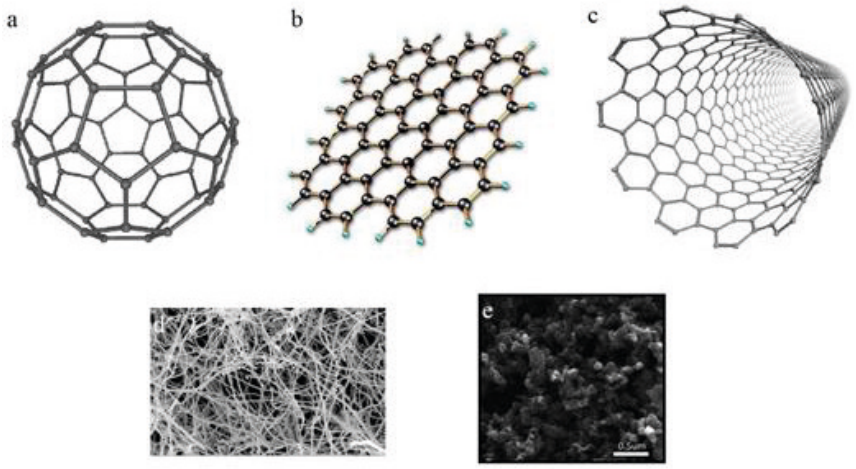

Figure I.6 - Carbon based nanoparticles: a – fullerenes, b – graphene, c – carbon nanotubes, d – carbon nanofibers and e – carbon black.

The properties of nanoparticles are divided into physical and chemical properties. The physical properties include optical such as the colour of the nanoparticles, absorption and reflection capabilities, reflection abilities in a solution or when coated onto a surface. It also includes the mechanical properties such as elastic, strengths and flexibility that play a significant factor in their application. Other properties like hydrophilicity, hydrophobicity, suspension, diffusion and settling characteristics have found their way in many modern everyday things. The chemical properties such as the reactivity of the nanoparticles with the target, their stability and sensitivity to factors such as moisture, atmosphere, heat and light, determine their application. The high surface are make nanoparticles catalytically active. In fact, NPs result as efficient catalyst in the production of chemicals, due to their extremely large surface.[20]

In the last years, indeed, the goal for most of the research and development efforts in nanoscience is to create new materials and technologies for practical use. The nanostructured materials have long been regarded as promising heterogeneous catalysts, thanks to their high surface, to volume ratio and the possibility of maximizing active facets by manipulating the morphology of the nanocrystals. Zaera examines the major synthetic approaches for producing nanostructures with well-defined sizes, shapes, and compositions for heterogeneous catalysis, and provides a few examples to illustrate their usefulness for such application.[21]

Therefore, the control of size, shape, architecture, composition and so on, plays an important role on revealing their new or enhanced functions and application potentials. The kind properties of metal nanomaterials make them ideal building blocks for

engineering and tailoring nanoscale structure for specific technological applications. At nanoscale dimensions, the properties of the material may change significantly to differ completely from their bulk counterparts. As the size of the material decreases, the proportion of surface atoms increases, which increases the reactivity and makes them highly reactive catalysts. The surface atoms of the catalyst are the active centres for elementary catalytic processes. Thus, the nanoparticles possess unique electronic, magnetic and mechanical properties that depending on their nanometer scale size. Several studies are not only focused on the synthesis of these nanoparticles, but also on their surface modification by chemical treatment in order to improve the dispersion stability of NPs in various liquid media. The modified nanoparticles show different behaviour within organic solvents or polymer matrices compared to unmodified nanoparticles, e.g., the modified nanoparticles show comparatively better dispersion in both media.[22]

For their unique properties, NPs are considered as new promising material. In addition, in the catalytic context, the effort for the synthesis and use of these new materials opened a new avenue of research.

1.3.1 Nanoparticles (NPs) in catalysis

Since at the end of 1990s, the development of nanosciences left nanocatalysis emerge as a domain at the interface between homogeneous and heterogeneous catalysis, which offers unique solutions to answer the demanding conditions for catalyst improvement. The main focus is to develop well defined catalysts, which may include both nanomaterials and metal nanoparticles.

Nanoparticles were considered the new material at the interface between homogeneous and heterogeneous catalysis. The use of transition metal nanoparticles (NPs) in catalysis is crucial as they mimic metal surface activation and catalysis at the nanoscale and thereby bring selectivity and efficiency to heterogeneous catalysis. Metal NPs are clusters containing from few tens to several thousand metal atoms stabilized by ligands, surfactants polymers and so on, protecting their surfaces. The most active NPs in catalysis are nanoparticles of one or few nanometres in diameter. The nanoparticles approach is also relevant to homogeneous catalysis, because there is a full continuum between small metal clusters and large metal clusters, the latter being also called colloids, sols or NPs. Moreover, NPs are well soluble in classic solvents. Thus the field of NPs catalysis involves both the homogenous and heterogeneous catalysis communities, and these catalysts are sometimes therefore called semi-heterogeneous.

This field has attracted a considerable amount of attention, as demonstrated by the large number of publications in all kinds of catalytic reactions, because NPs catalysts are selective efficient, recyclable and thus meet the modern requirement for green catalysis. Applications are already numerous, and the use of these catalysts in industry will obviously considerably expand in the last years.

Transition metals have a well-established history of being efficient catalysts for selective molecular transformations. Two examples are enough to explain how much important they become during the last years. In 2005 Nobel Prize in Chemistry was won by Yves Chauvin, Robert H. Grubbs and Richard R. Schrock for the synthesis of Mo-and Ru based catalyst that were used for metathesis reactions.[23] In 2010 a Nobel Prize has been conferred to F. Heck, E. Negishi and A. Suzuki with palladium catalysts.[24] It was exploited for C–C bond forming reactions well known as Heck, Negishi, or Suzuki reactions. Accordingly, noble metals like silver, gold, platinum and iridium are widely studied.

Recent studies were focused on the developing a chemical approach for the controllable synthesis of noble metal nanomaterials with a rich variety of shape, e.g. single-component Pt, Pd, Ag and Au nanomaterials, multi-component core/shell, intermetallic or alloyed nanomaterials, etc.[25] Several studies have been done on different applications of noble metal nanoparticles.

Metal NPs nanostructure, size, morphology and composition determine the physical and chemical properties of them.[26] Some metal NPs, such as Ir and Rh NPs can be synthesized in an ionic liquid that results to be an outstanding medium for their preparation.[29] They have been used as catalyst for various reactions. For instance, the development of Shell 405 represented a milestone catalyst to catalyze the decomposition of hydrazine for hydrogen production, providing enough energy and power for launching satellite.[27] Ir NPs were applied in the hydrogenation reaction of cyclohexene and phenylacetylene under mild reaction conditions. They result to be highly active and reusable catalyst. [28] Ir NPs generated in 1-n-buyl-3-methylimidazolium based ionic liquids constitute an outstanding recyclable catalytic system for the hydrogenation of simple alkenes and arenes under very mild reaction conditions (temperature and hydrogen pressure). These catalytic systems can be recovered and re-used several times.[29,30] Rhodium NPs were recycled 20 times in the hydrogenation reactions of benzene and cyclohexene.[31] Ceria (CeO_2) supported Rh NPs, Rh^0/CeO_2 was found as reusable catalyst preserving 67% of their initial catalytic activity even after the fifth use in hydrogen generation from the hydrolysis of ammonia borane at room temperature.[32] Nanoparticles of rhodium inserted into polyvinylpyrrolidone (PVP) were used as catalyst in the hydrogenation of different substrates such as phenylacetylene, quinoline, benzene,

norbornene and adiponitrile. These Rh NPs can work as heterogeneous catalyst or as a soluble heterogeneous catalyst in biphasic conditions (liquid/liquid) when the catalyst was dissolved in water. The [Rh-PVP] catalyst has shown an efficient activity for the catalytic hydrogenation of different molecules.[33]

In the field of catalysis, palladium appears to be particularly important among the noble metals.[34] As an efficient catalyst in organic reactions, it can offer the most favourable combination of activity and selectivity.[35] One of the well-known reactions catalyzed by palladium is the Suzuki coupling reaction, which is a powerful and convenient synthetic method in organic chemistry to generate biaryls, conducting polymers, and liquid crystals.[36,37,38.] The first example of heterogeneous Palladium catalyzed C-H arylation was reported by Nakamura et al. in 1982.[39] Afterwards different examples of C-H arylation by palladium were reported[40,41] that demonstrated the vast application field of Pd as heterogeneous catalysis.[42]

The research group led by prof. Sastry has developed a simple and general procedure for the synthesis of palladium and platinum nanoparticles. The noble metal nanoparticles were immobilized on the surface of amine-functionalized zeolite and they were evaluated as heterogeneous catalysts for hydrogenation and Heck reactions. These new catalysts exhibit excellent selectivity, and reusability for both hydrogenation and carbon-carbon bond formation reactions (as Heck reactions).[43] Another efficient catalyst based on Pd NPs was also synthesized, immobilized on amine-modified $NiFe_2O_4$ and Fe_3O_4 nanoparticles. The Pd-catalyst was applied for the hydrogenation of aromatic nitro and azide compounds to their respective amines as well as saturation of different unsaturated compounds. The catalyst results to be magnetically recoverable; his activity remains unaltered even after 10 cycles.[44]

Polymer molecules, known as dendrimers that act as hosts for guest molecules, are a new type of potential template for the formation of inorganic nanoclusters.[45] In 2005 Wiston et al. used dendrimers to encapsulate noble nanoparticles. The most important aspect of this study is that they evaluate how the diameter of nanoparticles can influence the rate of reaction. This study demonstrated that this effect is electronic in nature for nanoparticles having diameter smaller than 1.5 nm; for larger particles it depends on their geometric properties.[46]

Moreover, the use of Pd-catalysts found broad space also in streamlining processes such as biomass refining. Depositing Palladium onto carbon nanotube-inorganic oxide hybrid nanoparticles, biphasic hydrodeoxygenation and condensation catalysis can be done.[47]

For many researchers the goal is to replace homogeneous catalysts with heterogeneous and recyclable catalysts, and to synthesize nanoparticles keeping

their stability during the reaction. In addition, many efforts were done to developed new supports for NPs that can be able to provide new nanoparticles properties and therefore different applications of them. Countless studies have been carried out to develop new synthetic methods to stabilize nanoparticles. If on one side homogeneous catalyst can be immobilize onto inert inorganic materials or organic polymers, in order to overcome the problem related to their recovery and reuse; on the other side the role of the support for nanoparticles is to avoid the problem of aggregation.

1.3.2 Support for nanocatalysts

The synthesis of nanoparticles with controllable nanoscale sizes and shapes and the prevention of aggregation are the most important challenges for catalyst preparation. In addition, the preparation method of supported catalysts significantly affects their activity, selectivity, and lifetime.[48] With the aim to maximize the metal surface area for a given weight of metal, it is usually desired to synthesize nanoparticles catalysts anchored to a thermally stable, high-surface-area support, such as alumina (Al_2O_3), silica (SiO_2), titania (TiO_2), or carbon (C).

Schwarz described two main routes to synthesize supported metal nanoparticles: in solution with "three-dimensional chemistry," after which they can be deposited onto catalyst supports, or by "two-dimensional chemistry" involving deposition of metal precursors at the liquid–support interface, after which the precursors can be thermo-chemically converted to metal particles.[49]

The common criteria for a high-performance catalyst are narrow size distribution and high dispersion on support. According to these criteria, several innovative and cost-effective preparation methods have been developed beyond the oldest, the most common method of impregnation. They show promise for reaching performance optimization by controlling synthetic procedures and conditions.

Detailed studies of co-precipitation have provided new insights into the precipitation mechanism and effect of subsequent thermal activation treatments, while alternative precursors, precipitating agents, and thermal treatments provide promising alternatives for "greener" co-precipitation methods. Deposition and precipitation is used to produce highly loaded metal catalysts, but shows an increased usage for the preparation of low-loaded, highly dispersed (noble)-metal catalysts. Impregnation and drying remains the most studied preparation technique. Detailed study of impregnated ordered materials has

shown complete pour filling with aqueous solutions and oxide supports, and an enhanced understanding of adsorption on support surfaces has improved the ability to rationally synthesize well-dispersed supported metal catalysts. In addition, the development of the nanoscale metal distribution, which has been a long-standing challenge in the synthesis of catalysts, was recently studied. Thermal decomposition of the metal salt precursor, in particular the role of the gas composition or use of chelating agents, has also been systematically studied to elucidate the effects on particle size and particle distribution.

Besides these, several new approaches were noticed. First, melt infiltration is a promising and facile technique for the preparation of catalysts with high metal loadings that bears many similarities to impregnation and drying, and as such could benefit from the extensive knowledge obtained recently on this method.[50] Second, the synthesis of colloids in solution leads to unique control over particle size, shape, and composition and yields extensive literature.[51] However, deposition of the formed colloids onto a support is critical but has been less studied. Third, the kinetics of particle growth in the presence of a support has been studied in real time for the first time using in situ catalytic measurements of the emerging catalyst. Fourth, atomic layer deposition is showing promise especially for deposition of nanoparticles, but also for deposition of a stabilizing layer onto supported catalysts, for which further insight into the stabilizing effect and ability to obtain porous layers is desired.

On the basis of literature, it is clear that single (monometallic) particle properties can be largely controlled. To further advance the field of catalyst preparation, more detailed studies on the kinetics of particle formation,[52] as well as systematic studies to control the collective properties of the nanoparticles,[53] and the controlled formation of bimetallic and core–shell particles,[54] are greatly desired.

The idea of using polymeric supports in synthesis and catalysis has generated great interest and has encouraged the use of functionalized cross-linked polystyrene to support transition metal catalytic species, for instance complexes of Rh, Co and Ir[55] in heterogeneous reactions such as hydrogenation of arenes, and the preparation of polymer-supported reagents for organic synthesis.[56] More recently the concept of polymer- supported triphasic catalysis, which involves the use of polymeric reagents in triphasic mixtures such as solid/solid/ liquid or solid/liquid/liquid phases, has been used in order to catalyze reactions between immiscible reagents, or between reagents soluble in immiscible solvents (water and organic solvents).

Polymeric supports can play a wide variety of roles, depending on the system. In some cases polymer supports act only as carriers for the appropriate catalyst dispersed on the surface. In other cases the macromolecular network contains tethered

active sites, in the form of functional groups or ligands of metal complexes. Sometimes the catalyst is encapsulated within polymeric membranes, in a way that is reminiscent of enzymatic activity in natural systems. In all cases the primary advantage that has encouraged the use of polymeric supports is the facile separation, carried out normally by filtration of the products from the reagents. Moreover, the rich variety of polymeric supports and the ability to functionalize them at will, can provide a range of properties that are limited only by the creativity of the researchers. Most polymeric supports are insoluble, non volatile, non toxic, and often recyclable, properties that are especially attractive in an area of enhanced environmental awareness. In spite of these advantages, polymeric supports have so far been of limited use in industrial processes. The reasons for this situation are due to the remaining problems of polymeric supports: limited chemical stability, especially at temperatures above 100 °C; poor mechanical properties; the reactions are often typical of heterogeneous catalysis, where the active site is buried inside the cross-linked support and the reactions are diffusion limited; and finally, the supported catalysts can lose their activity, as is the case for rhodium complexes attached to phosphine groups in cross-linked polystyrene, where the loss of the metal by ligand exchange prevented its industrial application.[57] Some approaches to overcome these problems include preparation of macroporous support systems, where the active sites are attached to the surface and are therefore accessible to reactants;[58] or synthesis of soluble supports, where the selectivity and reaction rates are high, and where nature and structure of the active sites can be probed.[59] The preparation of polymer supported metal complex can also be carried out by the synthesis of a metal-containing monomer (MCM). It is polymerized with suitable co-monomers and possible cross-linkers. This method consents to obtain materials that have a uniform distribution of catalytically active sites and the same features for both homogeneous and heterogeneous catalysts. In 2004 Mastrorilli and Nobile report the methodology and the synthetic procedure for organic polymers obtained by copolymerization of MCMs.

1.3.3 Pd nanoparticles in catalysis: the new research

With the aim to develop innovative catalytic processes that enable chemical transformations to be performed under mild and sustainable conditions with high efficiency, in the laboratory of Chemistry of Politecnico di Bari, where I carried out my thesis work, several polymers supported metal complexes have been synthesised and used as efficient catalysts. Among them, the polymer supported palladium catalyst (Pd-pol) assumed great importance. In order to obtain a material with a uniform distribution of the

catalytically active sites, the catalyst was not synthesised by classical immobilization of palladium centres onto a pre-fabricated support, but it was prepared by co-polymerization of the metal-containing monomer $Pd(AAEMA)_2$ [$AAEMA^-$ = deprotonated form of 2-(acetoacetoxy)ethyl methacrylate] with suitable co-monomer (ethyl methacrylate) and cross-linker (ethylene glycol dimethacrylate) to give a polymer supporting Pd(II) centres, i.e. Pd-pol pre-catalyst (Scheme I.1).[60] Pd-pol pre-catalyst was then reduced under reaction conditions to obtain polymer supported Pd NPs (Pd-pol, Figure I.7).

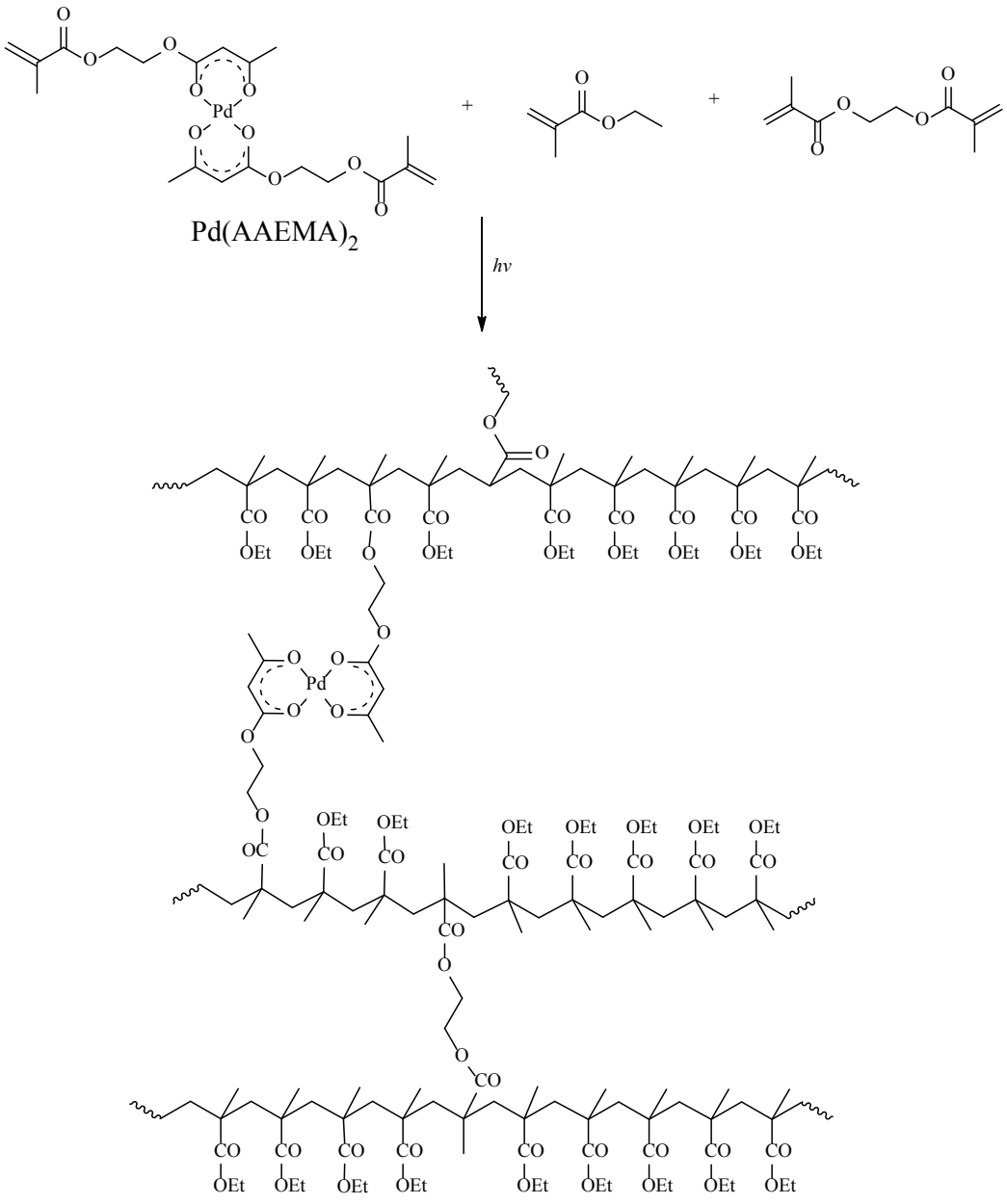

Scheme I.1- Synthesis of Pd-pol pre-catalyst. In situ reduction during duty in catalysis.

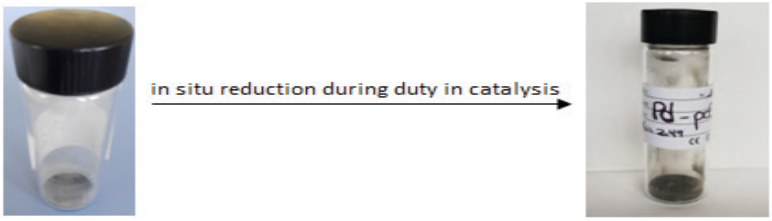

Figure I.7- In situ reduction of Pd-pol pre-catalyst.

Pd-pol was already found active and recyclable in several palladium promoted reactions. [61,62,63,64,65] The reticular and macro porous polymeric support of Pd-pol is able to immobilize and stabilize palladium nanoparticles (formed under reaction conditions by reduction of the pristine Pd(II) anchored complex), suitable for the Suzuki cross coupling of arylhalides with arylboronic acids in water (Scheme I.2),[61] for the aerobic selective oxidation of benzyl alcohols in water (Scheme I.3),[62] for the selective hydrogenation of quinolines in aqueous medium under mild conditions (Scheme I.4),[63] for the reductive amination reaction under 1 atm of H_2[64] and nitrobenzenes hydrogenation into anilines in water in the presence of sodium borohydride (Scheme I.5).[65]

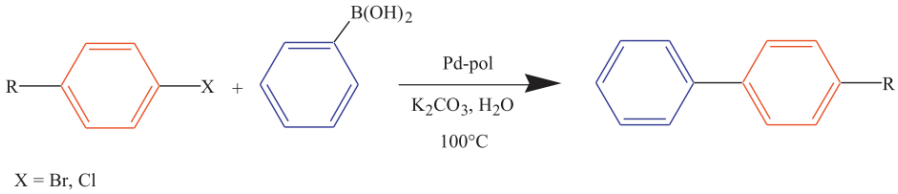

Scheme I.2 - Suzuki–Miyaura coupling reactions of aryl halides in water catalyzed by Pd-pol.

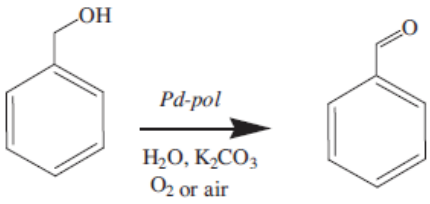

Scheme I.3 - Aerobic oxidation of benzyl alcohol under aerobic conditions in the presence of Pd-pol.

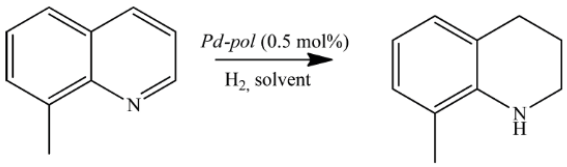

Scheme I.4 - Reductive hydrogenation of quinoline catalyzed by Pd-pol.

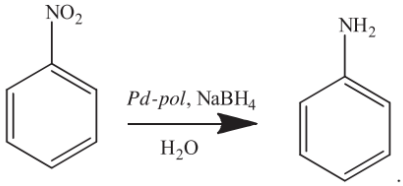

Scheme I.5 - Reduction of nitroarenes to aniline catalyzed by Pd-pol in water.

Furthermore, its good swellability in water renders Pd-pol an ideal potential catalyst for reactions carried out in aqueous solvent, since the migration of the reagents to the active sites would be not hampered by the solid support. In addition, a deep morphological study on Pd NPs supported onto Pd-pol was carried out by TEM, EDS and micro-IR techniques. These analyses were performed on such material before, during and after its exposition to prolonged catalytic runs, under green conditions in water solvent, in the following organic reactions: the Suzuki-Miyaura coupling between aryl bromides and phenyl boronic acid and the hydrogenation of nitroarenes and quinolines, using dihydrogen or $NaBH_4$, as reducing agent. This study explained the morphological features of both metal NPs and polymeric insoluble support. Micro-IR analyses showed that the support was chemically stable during all the re-cycles of the catalyst in all the reactions tested. TEM techniques showed that the macro-porosity of the resin remains constant after each run, well swelling in water. This is an important requirement for insoluble catalytic materials capable of facilitating the migration of reactants towards active sites. Moreover, TEM analyses revealed that in all cases the pristine Pd(II) polymer supported complex, which is the pre-catalyst, was in situ reduced to Pd(0) forming nanoparticles, the real active species, under reaction conditions. The organic polymer was always able

to stabilize Pd NPs with the re-cycles; this is confirmed by metal NPs detected by TEM analysis which show ever negligible agglomeration. NPs were recycled from 5 to 12 times depending on the reaction. In all cases, after several re-uses the percent amount of the smallest Pd NPs, ranging from 2-8 nm, still remained high, while the presence of larger NPs (10–15 nm diameter) might indicate the growth but no agglomeration, of the smallest Pd NPs with the re-cycles. However, the level of NPs growth that was observed with the re-uses was not enough to cause a significant decrease of the catalytic activity. The Pd NPs average size and morphology resulted affected by several parameters, such as: temperature, presence of a tetralkyl ammonium salt, reducing agent. High temperature (80-100°C) favoured the thermal reduction of Pd(II) with formation of NPs of 9 nm average size, while at room temperature a greater amount of smaller NPs (2-6 nm diameter) was observed.

On the basis of these previous studies, I decided to synthesize polymer supported Ni NPs, in order to obtain a catalyst (Ni-pol) similar to Pd-pol, thus replacing a noble metal (Pd) with a cheaper one (Ni) of the same periodic table group.

1.3.4 Nickel catalysts

The idea of using cheap transition metals, like nickel, copper, cobalt and so on, providing a cost-effective alternative to palladium and other precious metals, that have somewhat monopolised this field of chemistry, is of great interest.

Nickel has emerged as a very promising alternative to palladium. At the first time it was considered as a low-cost replacement for cross-coupling reactions. An increasing number of reports on exclusive catalytic properties exhibited by nickel catalysts in processes such as C-C coupling, carbon dioxide sequestration, or C-H activation have appeared in the literature in the last decade.[66,67]

Nevertheless, in the above cases, as in most of the metal-catalysed organic reactions, there is still work pending: to reduce the catalyst amount ever more, to develop different modes of activation for metal pre catalyst, to avoid the use of stoichiometric amounts of toxic transmetallating agents, or to discover more environmentally friendly procedures.[68]

C-H activation of aromatic compounds by nickel was made as early as the 1960s. In 1963 Dubeck and co-workers prepared an oxidative adduct of a C-H bond on an aromatic ring onto a nickel complex,[69] obtaining the complex product, shows in the upper part of the Scheme I.6. Thereafter, for more than 50 years there were no reports

describing the C–H nickelation of aromatic C–H bonds. Liang and co-workers in 2006 reported pincer nickel complex 4 that is able to react with benzene (5) to give complex 6.[70]

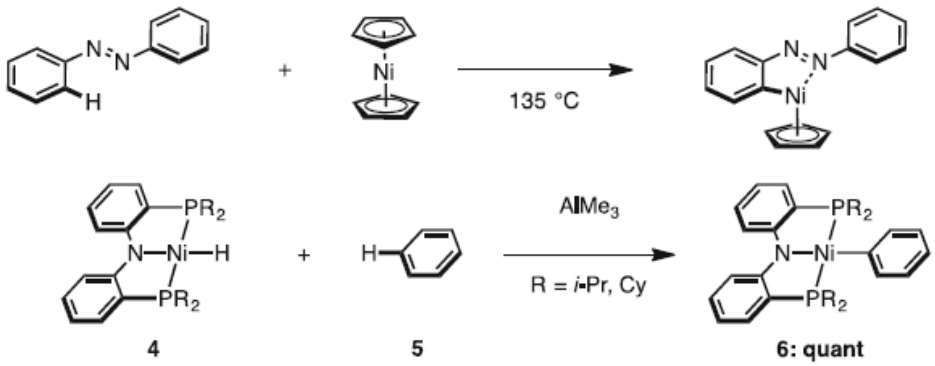

Scheme I.6 - Pioneering work for C–H activation using nickel complexes.

The first example of nickel-catalyzed C-H arylation of 1,3-azoles with aryl halides was reported in 2009 by Itami and Miura. In these reaction conditions the use of LiOt-Bu as base is necessary in order to obtain the desired product.[71,72] Afterwards cheaper and light alternative to LiOt-Bu was proposed in 2011 by Itami et al (Scheme I.7).[73]

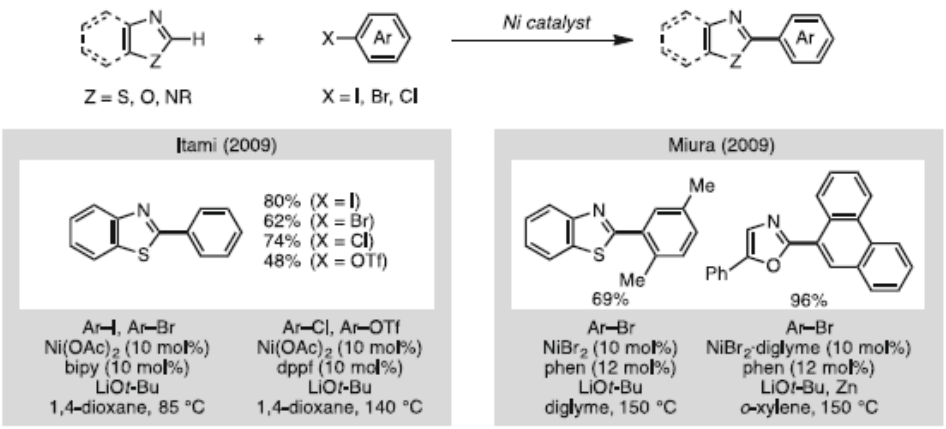

Scheme I.7 - Nickel-catalyzed C-H arylation of 1,3-azoles with aryl halides using LiOt-Bu as base.

Hereafter different works were reported about the use of Ni catalyst in C-H reactions. It was used for: C-H alkynylation of heteroarenes in 2009 for the first time

(Scheme I.8);[74] for aromatic C-H alkylation in 2010 (Scheme I.9);[75,76] for oxidative C-H arylation in 2010 (Scheme I.10)[77] and also for alkenylation (Scheme I.11)[78] and so on.

At the same time, numerous efforts were also made to optimize the reaction conditions for the use of mild and less expensive reagents.[73,79,80]

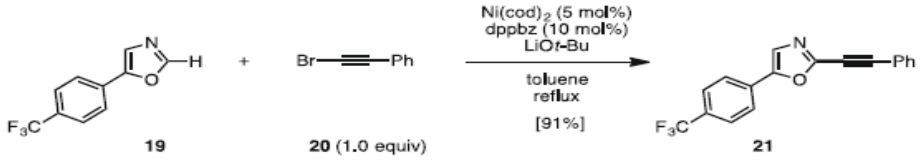

Scheme I.8 - C-H alkynylation of azoles with alkynyl bromides.

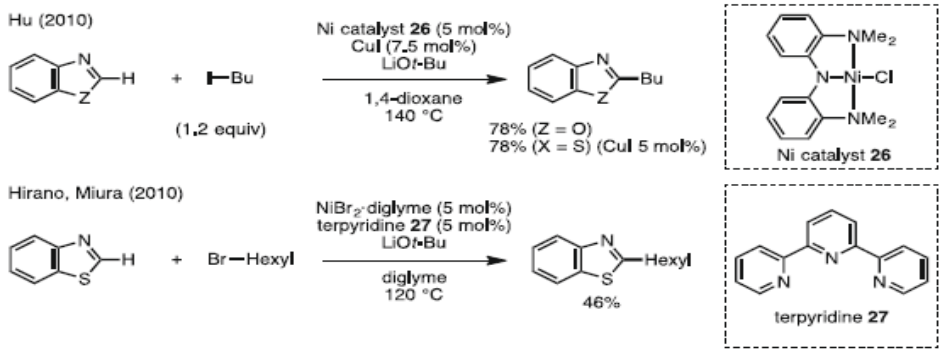

Scheme I.9 - C-H alkylation of 1, 3-azoles and alkyl halides.

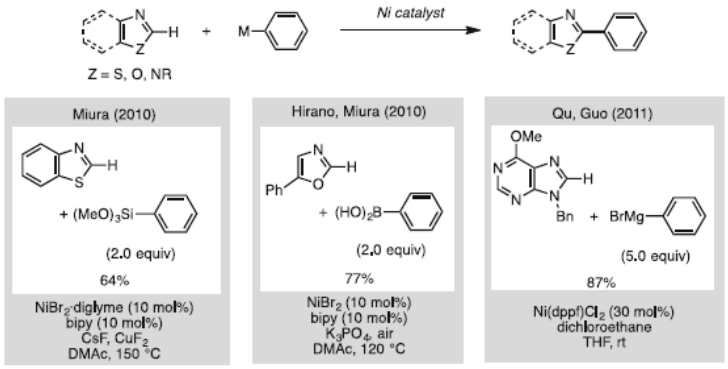

Scheme I.10 - Ni-catalyzed direct C-H arylation and alenylation of azoles with organosilicon, boron and Grignard reagents.

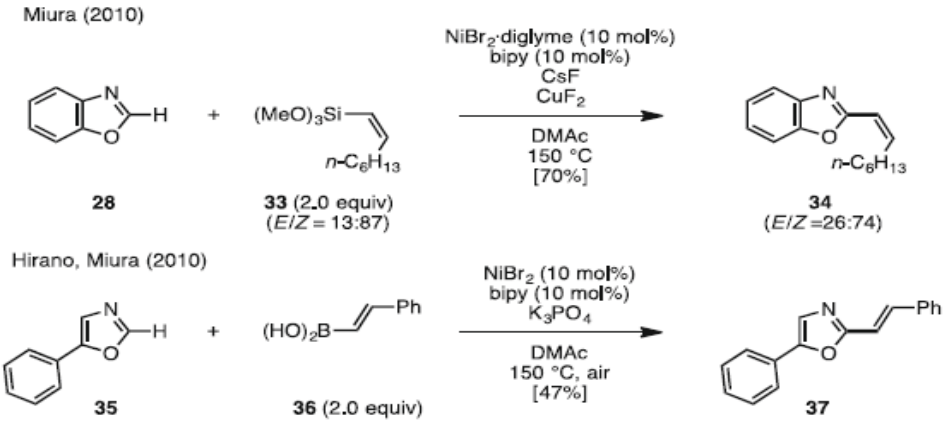

Scheme I.11 - Oxidative C-H arylation of azoles with organosilicon and boron reagents.

After the discoveries of reductive elimination reaction of organo-nickel complexes by Yamamoto[81] in 1971 and the cross-coupling reaction catalyzed by Kumada and Tamao[82] (1972) and Corriu[83] (1972), nickel was used as one of the catalysts most promising for carbon-carbon bond formation reactions.

The C-C reaction of unsaturated electrophiles was widely studied and during the last two decades much effort has been devoted to the development of new transition metal catalyst for the cross-coupling reaction of alkyl electrophiles, as well as alkyl nucleophiles. For such transformations, Pd catalysts were often employed with a combined use of bulky trialkylphosphines[84] or N-heterocyclic carbenes[85] as the ligands.[86] Nickel has also received considerable attention as promising catalyst for the cross-coupling reaction of alkyl halides and pseudo-halides.[87,88,89,90] The first discovery was made in 1995 by Knochel. He observed that the cross-coupling reaction of alkyl iodides and bromides with dialkylzinc reagents can be facilitated by intermolecular coordination of an olefin[91] or keto group[92] to, as reported in Scheme I.12.

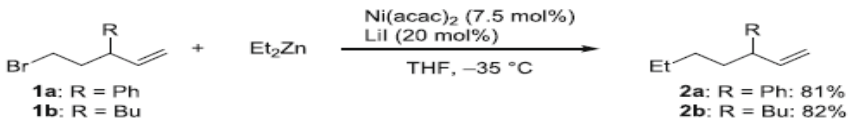

Scheme I.12 - Cross-coupling of alkyl bromides bearing an alkene moiety with Et_2Zn.

It was also discovered that the C-C reaction of Negishi can be catalyzed by Ni and it preceded efficiently by using acetophenone or styrene derivates as the additive. In the Scheme I.13 is reported one example of this reaction. The reaction between an alkyl iodide 5 with di-pentylzinc reagent using

$Ni(acac)_2$ as catalyst afforded only 20% yield of the coupling product 6, whereas the addition of one equivalent of acetophenone improved the yield to 71%. [93,94]

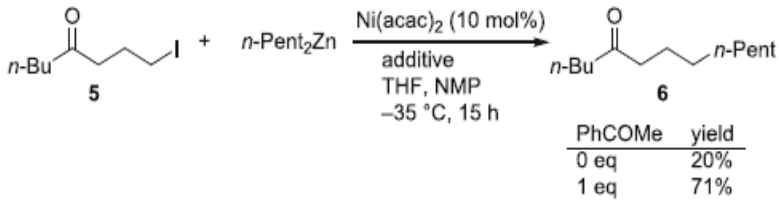

Scheme I.13 - Cross-coupling of an alkyl iodide with alkylzinc reagent using acetophenone as an additive.

Starting from here, excellent results have been obtained with the optimization not only of the reaction conditions but also of the morphology and structure of catalyst used.[95,96,97] Different type of Ni-catalyst were used for C-C coupling reaction such as Negishi coupling (Scheme I.14)[98], Kumada-Tamao-Corriu cross-coupling reaction using a phosphine ligand.[99] It was also used in Hiyama[100] and Stille[101] coupling reactions of primary and secondary alkyl halides with aryl trifluorosilane and trichloro stannane reagents (Scheme I.15, Scheme I.16).

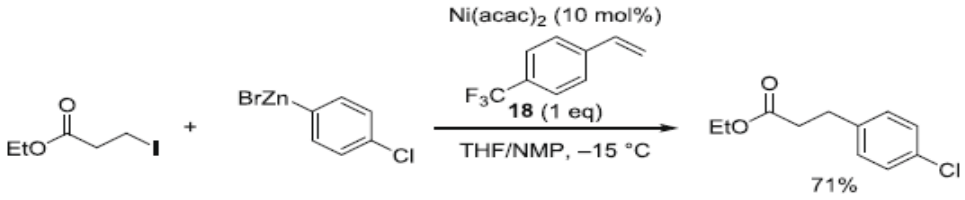

Scheme I.14 - Negishi coupling aìof an alkyl iodide with PhZnBr.

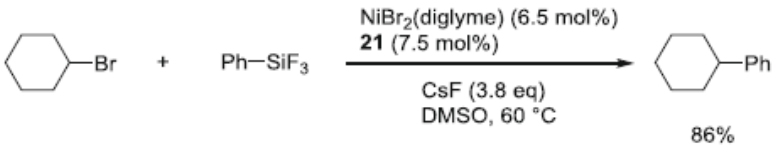

Scheme I.15 - Hiyama coupling of a secondary alkyl bromide.

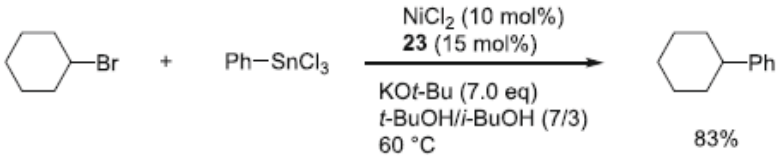

Scheme I.16 - Stille coupling of secondary alkyl bromide.

While the use of nickel as a catalyst has found ample space replacing palladium with excellent results, to the best of our knowledge, recycling[102,103] and the tolerance towards sensitive functional groups have not yet been demonstrated for heterogeneous nickel catalysts able to hydrogenate nitroarenes efficiently.[104,105,106]

Undoubtedly, the precious metal-based catalysts are still remain the leading catalysts for hydrogenation such as palladium,[107] platinum,[108,109] rhodium,[110] ruthenium,[111] aurum-based systems,[112,113] even though their widespread applications are limited by their low earth abundance and high cost. Various non-precious metal-based catalysts, especially nickel-based catalysts[114,115] have been developed as economical alternatives.

In this framework, during my doctoral research work I synthesized a polymer supported Nickel catalyst (Ni-pol) similar to Pd-pol (described in paragraph 1.3.3) aiming at using it as efficient and recyclable catalyst.

1.4 Aqueous biphasic catalysis

Previously, it was emphasized that despite of the several advantages offered by heterogeneous catalysis in industrial catalyzed processes, homogeneous catalysis remains attractive in terms of activity and selectivity. One of the outstanding challenges in catalysis is to develop efficient method for reusing the catalytic system. One method is the utilization of the so called two-phase catalysis in aqueous medium, where one liquid phase contains the substrate/product and the catalyst is confined in a different liquid phase. Although the use of fluorous organic solvents[116] and ionic liquids[117], for catalyst confinement, has attracted great interest, water remains the most interesting choice in view of its lower cost and hazards.[118] The special properties of water, such as lack of odour, non-flammability, non-toxicity, etc. make it suitable for environmental and safety reasons, as a "green" reaction solvent for industrial applications.

The first definition of biphasic catalysis was made by Manassen[119] in 1975-1979, but only in 1984 it was used for the first time in industrial field, in the hydroformylation of propylene in the plants of Ruhrchemie AG,[120,121] allowing an easy separation of the catalyst from the organic products at the end of the reaction.

In conclusion, this technique merges the advantages of the use of homogeneous catalysis, such as, high activity and selectivity, possibility of tailoring organometallic complexes as catalysts and so on, with the main convenience of the use of heterogeneously catalysed systems, i.e. easy catalyst separation from the reaction mixture.[122] Furthermore, this separation is the most effective and successful method of immobilizing homogeneous catalysts, thus making them "heterogeneous".

1.4.1 Approaches for aqueous biphasic catalysis

Different strategies for catalyst recovery include distillation, precipitation, extraction, and ultrafiltration. Among them, without doubt, the least costly and most easily implemented process is decantation, provided that the catalyst and the reaction product are in two different liquid phases at the end of the reaction and decantation is rapid. So by developing biphasic catalytic protocols, an extraction solvent can be avoided. Even if biphasic catalysis has several advantages, the mass transport becomes its major problem.

Aqueous biphasic catalysis can operate according to four different principles depending on the localization of the catalyst, such as at the interface, in the bulk phase or in the core of micelles. All of them require decantation of the organic product from the aqueous phase, where the catalyst remains confined. In order to avoid the catalyst

losses, the solubility of the latter in the organic phase should be negligibly small. In interfacial catalysis, the reactants are insoluble in water and the reaction occurs at the interface. The reaction rate increases upon increasing the interfacial area by using surfactants. In the bulk catalyst phase, the substrate should be sufficiently soluble in the catalyst phase, which severely limits this approach especially for aqueous biphasic catalysis. At this regard, the most relevant example is Rh-catalyzed hydroformylation with water-soluble phosphines as supporting ligands,[123] used at industrial scale. However, this process can be used only for small molecules, such as propene and butene, due to water insolubility of longer chain α-olefins. In order to overcome this problem, additives such as cosolvents (alcohols)[124] and cyclodextrins[125] have been used to improve the solubility of organic substrate in the aqueous phase. Another approach consists of transferring the catalyst reversibly to the substrate/product phase, but in this case the relevant problem is the catalyst loss at the separation stage. In order to overcome this disadvantage, an interesting approach is to anchor the homogeneous catalyst to thermomorphic polymers. They are completely water soluble at room temperature but become more lipophilic and migrate toward the organic phase at the high temperatures used for the catalytic reaction.[126]

Finally, the catalyst may also be anchored onto the hydrophobic part of surfactants or amphiphilic diblock copolymers that are able to self assemble as micelles at low concentration over the critical micelle concentration (CMC). This self organization sets the catalyst inside the hydrophobic core of the micelle in which the reaction takes place. In this method the substrate can migrate from the organic phase to the micellar core (aqueous phase) and the products can migrate back to the organic phase (Figure I.8 b),[127] instead the micellar catalyst remains confined in water phase. The micellar catalysis is not to be confused with micellar effect in interfacial catalysis in which surfactants generate micelles but the reaction occurs only at the water/organic interface through the action of a water-soluble catalyst (Figure I.8 a).[128,129]

Micellar catalysis method has different advantages: versatility, due to the possibility to choose the size and functionality of polymers, fast kinetics, thanks to the high local concentration of catalyst, low mass transport limitations.[130]

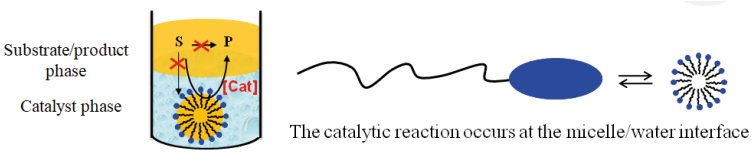

a)

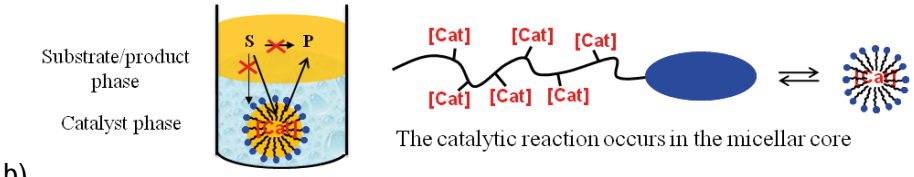

b)

Figure I.8 - a) Interface catalysis process; b) core micellar catalysis process.

Two major limitations can occur by using this methodology at the industrial scale. The first one is the formation of stable emulsion by excessive swelling of the micellar core (Figure I.9, 1), due to the high affinity between the micellar core and organic phase. The second one is the possible presence of free surfactant molecules or polymers (so called "free arms") at the water /organic interface placed as Langmuir-Blodgett film. This causes the formation of inverse micelles, even for surfactants that have a very low CMC, which in turn causes catalyst losses (Figure I.9, 2).

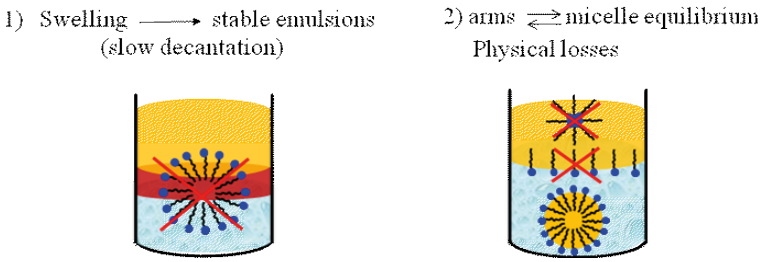

Figure I.9 - Simulation of: excessive swelling of core (1) and micelle equilibrium (2).

1.4.2 Unimolecular core shell nano-object

In order to avoid both limitations, recently a new approach has been introduced, consisting of turning the self-organized micellar architecture into a unimolecular core-shell nano-object by cross-linking all surfactant molecules, so the swelling of the particles is limited. Recent developments in reversible-deactivation radical polymerization (RDRP) now allow the formation of polymer particles with elaborate and precise architectures, including unimolecular core-shell polymers with narrow size dispersion.[131]

A few examples of unimolecular macrostructures, that achieve a favourable environment for efficient catalysis in water, are available in the literature. Using natural polyphenols as amphiphilic ligands, Mao et al. could prepare noble metal complexes and noble metal nanoparticles catalysts for the biphasic hydrogenation of cinnamal-

dehyde and quinoline. They observed some decrease of conversion upon recycling.[132] Gong et al. synthesized four water-soluble dendritic phosphonated ligands starting from poly(amido amine) (PAMAM) dendrimers. Their application to the hydroformylation of 1-octene led to significant loss of metal used, rhodium.[133] Terashima et al. proposed a different approach to incorporate monophosphine units into a star polymer. They used controlled radical polymerization mediated by ruthenium. The simultaneous introduction of a monomer functionalized with a phosphine, an amphiphilic macro initiator, and a cross-linking agent ensures the confinement of the phosphine ligands within the obtained polymer microgel core, which can entrap the ruthenium metal.[134] These catalysts were successfully used for the hydrogenation of different unsaturated compounds under a thermomorphic approach.[135] O'Reilly et al. have developed nanoreactors containing a hydrophilic poly(acrylic acid) (PAA) shell and a hydrophobic polystyrene (PS) core in which terpyridine ligands coordinate catalytic Cu (I) centers.[136] O'Reilly et al. proposed L-Proline functionalized poly(methyl methacrylate) (PMMA) nanogel particles as catalysts for aldol reactions in water.

Their studies demonstrated that, more hydrophobic is the nanogel core, higher the observed enantioselectivity.[137] These examples prove that the performance and stability of such macrostructures require suitable loading and location of the catalytic moieties, as well as a good match between the hydrophobic character of the substrate and the polymer core. Zhang et al. developed a new strategy in order to synthesized phosphine-functionalized core-shell polymer in which the hydrophobic shell is designed to limit or completely avoid transfer of the nano-objects to the organic phase and, also, they improved a new methodology giving direct access to a metal-free polymer.[138] Weck et al. have developed shell cross-linked micelles using a strategy of catalyst confinement. Their new system consists by a hydrophobic block, a photo cross linkable block and a functionalized block with enantiomerically pure salen ligand. After metalation of the core with Co (III), these catalysts were applied as nanoreactors in the hydrolytic kinetic resolution of epoxides and they could also be successfully recycled eight times by ultrafiltration. These objects showed slightly lower catalytic activity than analogous non-cross-linked objects due to a less permeable shell towards the organic reagents in the cross-linked particles.[139]

In principle, mass transport should be less affected, or not at all, by cross-linking at the hydrophobic end of the surfactant or amphiphilic polymer (Figure I.10). This polymeric architecture was elaborated for the first time, for application as catalytic nanoreactor, with the catalyst located on flexible linear arms in a unimolecular core–shell nano-object.

Sawamoto et al.[140,132] prepared a phosphine-functionalized core-shell polymer by $[RuCl_2\text{-}(PPh_3)_3]$-catalyzed atom-transfer radical polymerization (ATRP). A convergent

synthetic strategy was applied, starting with hydrophilic and thermo responsive chains made from poly(ethylene oxide) methyl ether methacrylate (PEOMA) monomer, which were subsequently extended with the ligand monomer-diphenylphosphinostyrene (DPPS) and simultaneously cross-linked with ethylene glycol dimethacrylate (EGDMA).[141] Due to the synthetic methodology, the ATRP catalyst remained entrapped in the nanoreactor core, coordinated by the phosphine groups, although it was possible to subsequently remove the metal from the polymer. These objects were applied to Ru-catalyzed transfer hydrogenation in a thermomorphic approach.[154] Hence, in these nano-objects the anchoring sites for the catalyst are located inside a cross-linked network rather than on flexible arms.

The research group headed by prof. R. Poli, where I carried out research work for a 6-month internship period during my thesis, synthesized nanoreactors[138,142,143] that differ from the polymers described by Sawamoto in two aspects. The first one: the hydrophilic shell is designed to limit or completely avoid transfer of the nano-objects to the organic phase at the operational temperature of the catalytic application. The second one: with their innovative methodology they prepare a metal-free nano-object, as potential nanoreactor, for general use without any metal. These polymers can be referred as core-cross-linked micelles (CCM, Figure I.10) amphiphilic diblock copolymers, which are ligand-functionalized in the hydrophobic part. The copolymers are cross-linked at the hydrophobic chain end, resulting in star-block unimolecular nano-objects where the ligands are placed on the flexible arms, outside of the cross linked part.

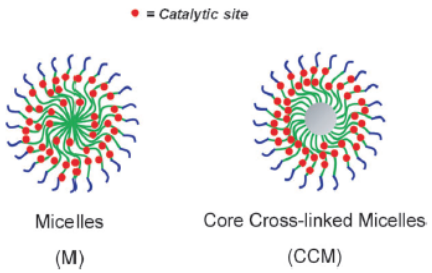

Figure I.10 - Transposition of the micellar catalysis concept to unimolecular core-shell nano-object.

This synthetic protocol is based on a convergent one-pot polymerization in water using reversible addition-fragmentation chain transfer radical polymerization (RAFT) as the controlling method, whereby following the controlled growth of the hydro-soluble block, chain extension with the hydrophobic monomer in water, leads to polymerization-induced self-assembly (PISA). [144,145]

The obtained nano-objects consist of triphenylphosphine (TPP)-functionalized core cross-linked micelles (TPP@CCM), assembled in a convenient and scalable one-pot process in three steps and obtained as latex directly usable in catalysis (Scheme I.17).

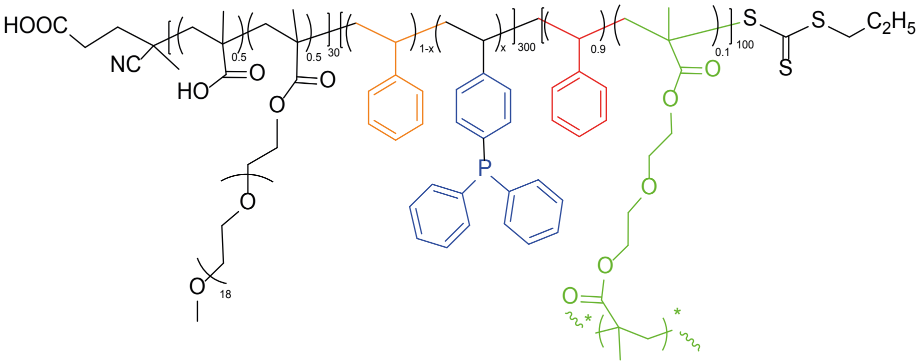

Scheme I.17 - TTP functionalized core cross-linked micelles, TPP@CCM with neutral shell.

In 2016, Chen et al. loaded TPP@CCM with the complex [Rh(acac)(CO)$_2$]. They observed an interparticle molecular migration of the rhodium complexes from a core to another one.[146] In 2017, A. Joumaa et al. demonstrated that this TPP@CCM is a convenient ligand for the biphasic rhodium-catalyzed hydroformylation of 1-octene and of styrene (Scheme I.18).[147]

a)

b)

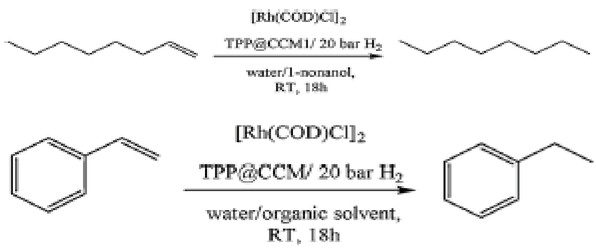

Scheme I.18 - a) Hydrogenation of 1-octene under biphasic conditions; b) Hydrogenation of styrene under biphasic conditions.

Following the research work of Professor Rinaldo Poli group in the field of CCM and nano-reactors, during my research work at Laboratoire de Chimie de Coordination (LCC) CNRS in Toulouse (France), I synthesised metal nanoparticles embedded in polymeric nanoreactors TPP@CCM aiming at using them as efficient and recyclable catalysts for hydrogenation reactions.

Aim and scope of the present work

As shows in the previous section, the catalytically active noble metal nanoparticles offer advantages in terms of activity and selectivity, even if their high cost limits their practical use. This problem can be solved only by replace them with cheaper base metal catalysts. However, compared with precious metal-based catalysts, the non-precious metal-based systems usually exhibit relatively low activity, require higher temperatures and consume more energy in the process. Hence, it is of great interest to develop new recyclable low-cost base metal systems, able to catalyse organic reactions under mild and sustainable conditions.

This thesis aims at synthesizing new nano-catalysts based on no-precious metal nanoparticles supported on polymeric matrix, and at studying their catalytic activity and recyclability in some important organic reactions, such as hydrogenations of different substrates of industrial interest, pharmaceutical and so on. In particular, I focused my study on the synthesis of Nickel nanoparticles supported on polymeric matrix (Ni-pol). Ni-pol was obtained by reduction of polymer supported Ni(II) complex (Ni(II)-pre catalyst). The catalytic activity of this new catalyst was tested in the reduction of nitroarenes in order to obtain the corresponding anilines and secondary amines under suitable reaction conditions, as well as in the partial hydrogenation of poly-unsaturated fatty acid methyl esters for the upgrade of biodiesel.

Moreover, in collaboration with the Equipe G headed by prof. Rinaldo Poli, at the Toulouse LCC-CNRS, I synthesised new catalytic systems based on metal nanoparticles embedded in polymeric nanoreactor TPP@CCM (M-NPs). These nanoparticles were obtained after the synthesis of unimolecular core-shell-nano objects (CCM), functionalized with tryphenylphoshine (TPP) as ligand, within the hydrophobic core, in order to coordinate the metal pre-catalyst. The confinement of nanoparticles embedded in polymeric nanoreactors and their activity, as new aqueous biphasic catalysts, was studied in the reduction of acetophenone, taken as model reaction, and styrene under aqueous biphasic conditions.

CHAPTER II

Synthesis, Characterization and catalytic application of polymer supported Ni nanoparticles

TABLE OF CONTENTS

CHAPTER II

Synthesis, characterization and catalytic application of polymer supported Ni nanoparticles

2.1 Introduction

Supported metal complexes attract the interest of a huge part of the scientific community for the advantages that they offer compared to the soluble counterparts.[148] Some advantages are the robustness, the increased air and moisture stability, easy separation and the recyclability, when used as heterogeneous catalysts.

Two different kinds of supports can be used: inorganic or organic polymers. Inorganic supports are oxides that carry surface hydroxyl group. They work as ligand for suitable metal containing moieties.[149] The use of organic co-polymers as support for the trans-metal complexes lead to combine a controllable flexibility of the matrix with the possibility to fine-tune the physical properties, such as polarity, morphology, etc., of the material by combination of co-monomers and cross-linkers.

The synthetic route for the synthesis of organic polymer supporting metal complex is reported in Scheme II.1. It consists of the synthesis of a macromolecular ligand and the subsequent anchoring of complex or metal salt (route a). It results to be the most used strategy which has led to uncountable examples about the use, for example, of polystyrene as support.[150,151] An interesting alternative that is not most considered is the incorporation of metal onto a support by polymerization of a suitable metal containing monomer (MCM) (route b). With this approach there is the possibility to study the MCM as homogeneous catalyst before polymerization[152,153] and it is also possible to use MCM for the synthesis of material with controllable "outer sphere" morphology.[154]

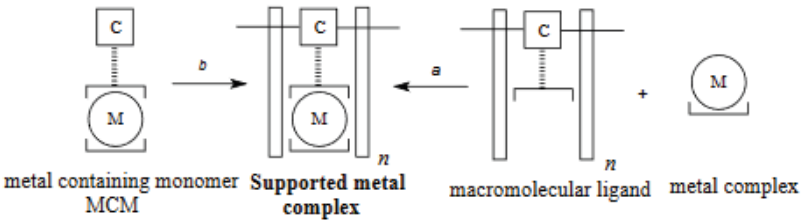

Scheme II.1 - Synthesis of supported metal complexes.

Moreover, this strategy leads to a uniform distribution of the metal complex in matrix, a higher dispersion of the metal, the knowledge about the metal centre that can

be interesting for the catalytic route in the heterogeneous catalysis.[155] Supported metal complexes obtained from MCM polymerization have been proposed for other potential applications than catalysis, such as nanosized technology,[156] biomimetic systems,[157] materials science[158] and chromatographic separations.[159]

Following our studies on polymer supported metal complexes, I prepared an acryl amidic polymer supported nickel catalyst (Ni-pol) and I evaluated its catalytic activity in different reduction reaction, such as: 1) the hydrogenation of nitroarenes in aqueous medium;[281] 2) the reductive amination of aldehydes;[160] 3) the partial hydrogenation of fatty acid methyl esters for the upgrade of biodiesel. In any case, the real active species were Ni nanoparticles with a peculiar nanostructure stabilized by the insoluble support, which were active, selective and recyclable.

2.2 Synthesis and characterization of Ni(II)complex: $Ni(AAEMA)_2$

The synthesis of nickel containing monomer was carried out by reacting the deprotonated form of 2-(acetoacetoxy) ethyl methacrylate (HAAEMA) with $Ni(NO_3)_2.6H_2O$ in ethanol (Scheme II.2). A precipitation of $Ni(AAEMA)_2$ (Figure II.1) as a pale green solid was obtained. The solution was left under stirring for 1h and then the solid was filtrated and washed with water for the first time, then with ethanol and pentane. The resulting green solid was left under vacuum for all night.

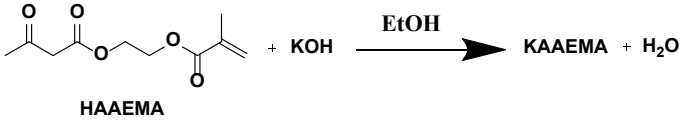

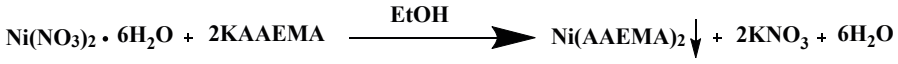

Scheme II.2 - Synthesis of the metal containing monomer $Ni(AEEMA)_2$.

The product was characterized by HRESI-MS, IR, UV-vis and elemental analyses. The ESI spectrum (Figure II.2) shows that the exact mass is 485.0952 da. The mean error between observed and calculated isotopic patterns is -1.3 ppm: this suggests that the complex obtained is compatible to the expected one. The formation of Ni-complex was also confirmed by UV-vis spectrum (Figure II.3).

The synthesis of this metal containing monomer followed the procedure already used for the synthesis of different metal containing monomer, as reported in literature.[161]

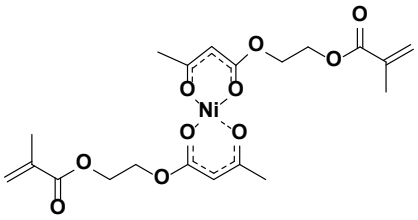

Figure II.1 - Structure of Ni(AAEMA)$_2$.

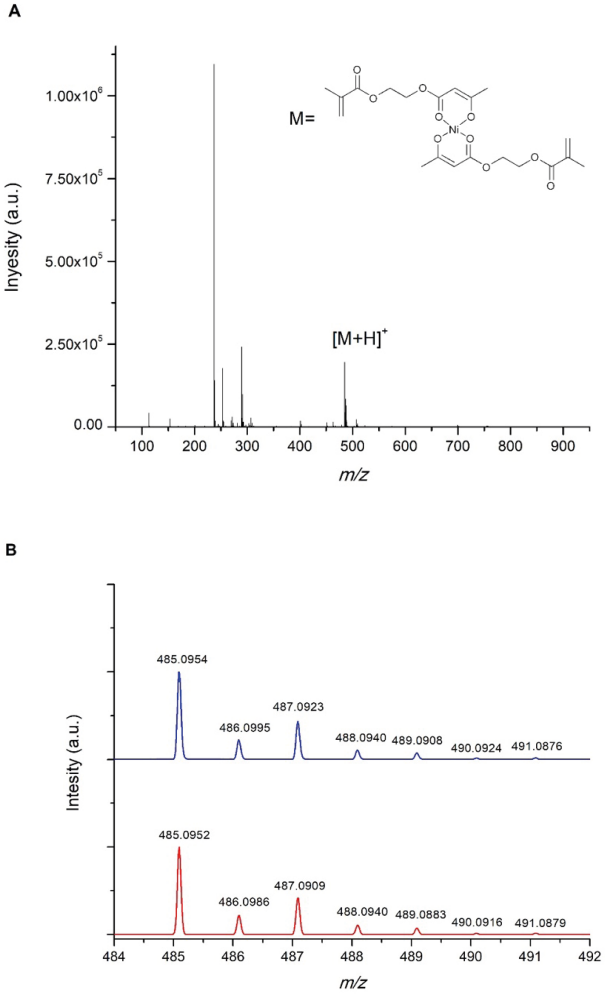

Figure II.2 - A: Experimental HRMS (ESI+) of Ni(AAEMA)$_2$ in CH_3OH. B: Experimental (top) and calculated (bottom) isotopic patterns of [Ni(AAEMA)$_2$+H]$^+$.

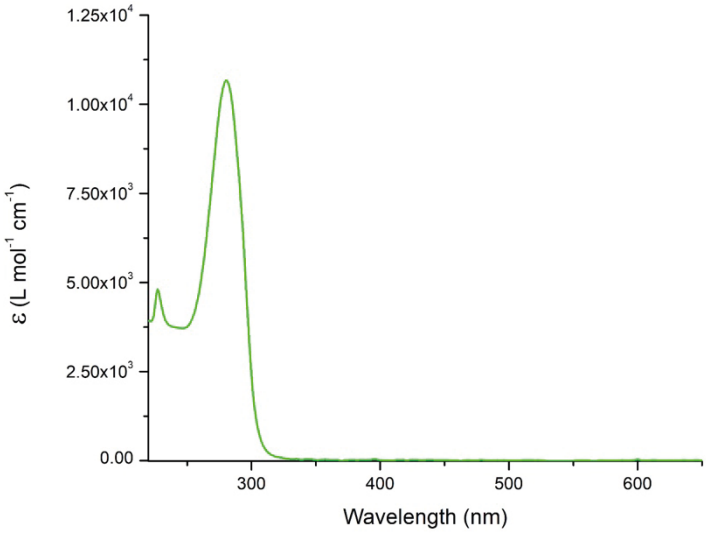

Figure II.3 - UV-vis spectrum of 6.9 x 10-5 M $Ni(AAEMA)_2$ in dichloromethane solution.

2.3 Synthesis of polymer supported Ni catalyst

The polymer supported nickel catalyst was synthesized in unconventional way. In order to obtain a uniform distribution of Ni(II) centres, a copolymerization of metal containing monomer $Ni(AAEMA)_2$ with suitable co-monomer and cross-linker (Scheme II.3) was carried out. A green jelly solid was formed in the reaction flask, it was filtered, heated all night and then grinded with a mortar in order to recover a pale green powder. The metal-containing polymer was a non-hygroscopic green powder, insoluble in all solvents. It swelled well in water, acetone, halogenated solvents and dioxane and shrink when treated with diethyl ether, ethyl acetate or petroleum ethers. It was characterized by IR and elemental analysis. Its IR spectra in KBr (Figure II.4) showed the features of the coordinated β-ketoesterate moiety (1527 and 1622 cm^{-1}) at the same wave numbers of the corresponding $Ni(AAEMA)_2$ complex (1531 and 1623 cm^{-1}), thus substantiating that the metallorganic units in both soluble and supported materials are similar. The elemental analysis revels that: Ni 3.69; C 57.06; H 7.94; N 9.91%. The amount of Ni in the final polymer was 5.48%.

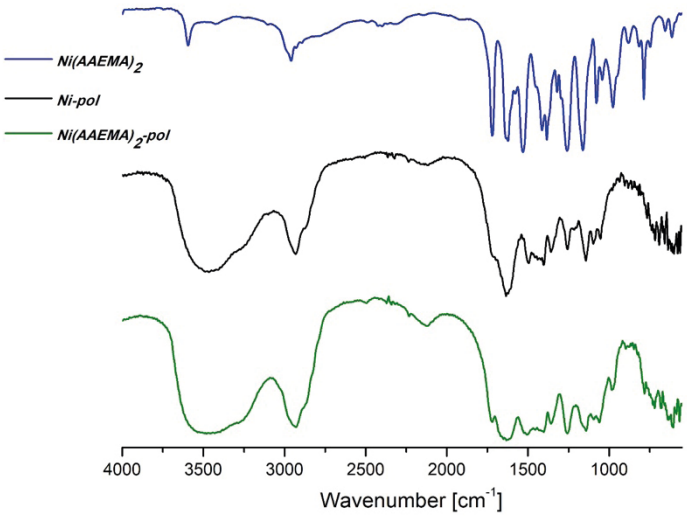

Figure II.4 - FTIR of $Ni(AAEMA)_2$, $Ni(AAEMA)_2$-pol and Ni-pol.

The polymer supporting Ni-complex obtained is reported in Scheme II.3. It was synthesized using the same strategy used for the synthesis of already obtained $Pd(AAEMA)_2$ with methacrylic monomers. The Pd polymer was found active, selective and recyclable in several palladium catalyzed reactions, as reported in the introduction. The Pd(II) based polymer was reduced under reaction conditions, obtaining Pd(0) nanoparticles supported on methacrylate based resin. The polymer matrix was able to immobilize, stabilize and retain Pd NPs, the real catalytically active species. The good swell ability in water of the methacrylic insoluble support makes the catalyst a good system for reactions carried out in aqueous medium, since the migration of reagents to the active sites is not hampered by the solid matrix.

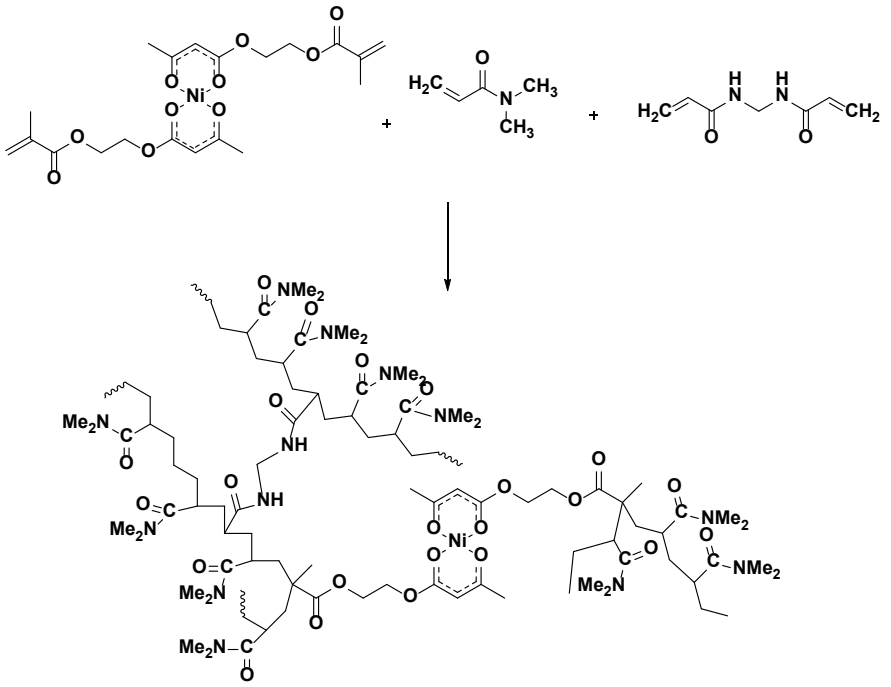

Scheme II.3 - Synthesis of polymer supported Ni(II) complex.

2.4 Synthesis of Ni-pol as Ni-NPs

Calcination under hydrogen or nitrogen atmosphere is a well-known technique used for preparing metallic nanoparticles anchored to an insoluble support by thermal reduction of supported metal ions. Depending on the calcination temperature, the thermal treatment modifies also the insoluble matrix (which may lose water, crystallization solvent molecules and/or carbon-based moieties), thus enhancing or depressing the ability of the support in stabilizing and retaining the so formed metal nanoparticles. For example, Qiu and coworkers found that the calcination temperature is the key factor affecting the structure, morphology and the catalytic performance of their Ni/C catalyst in the hydrogenation of nitroarenes. They identified in T = 300 °C the best calcination temperature for their catalyst in terms of activity.[104] Thermal Gravimetrical Analyses (Figure II.5) suggested us to set the calcination temperature for our system at 300 °C as well, because over 300 °C the loss in weight of the polymeric material exceeded 5% of the initial mass, due to important structural modification of the support. Therefore, by annealing Ni(AAEMA)$_2$-pol under nitrogen flow for 30 min at 300 °C, we obtained Ni-pol as a black powder (Scheme II.4).

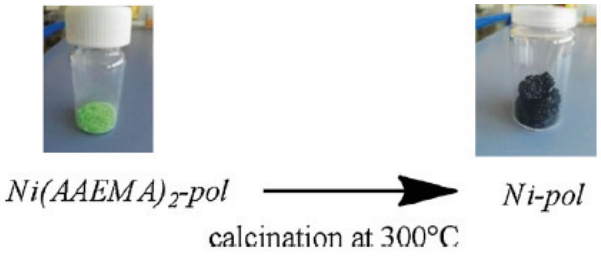

Scheme II.4 - Reduction of Ni(II)-pol into Ni-pol by calcination under N_2 at 300 °C.

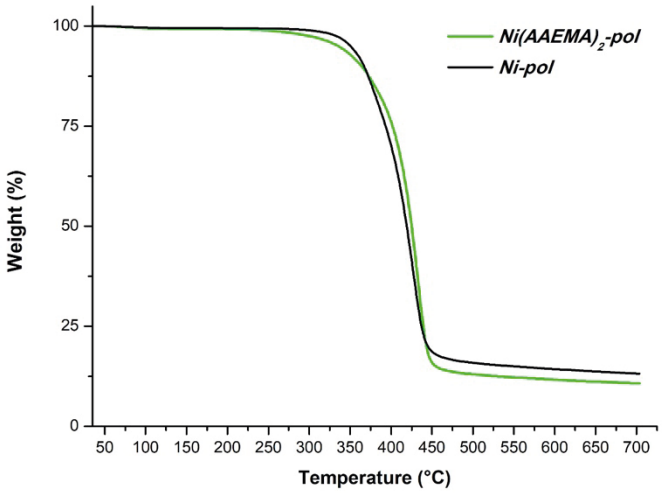

Figure II.5 - TGA of Ni(AAEMA)$_2$-pol, and Ni-pol.

2.5 Study of the catalytic activity of Ni-pol: the reduction of nitroarenes to anilines in aqueous medium

2.5.1 Introduction

The hydrogenation of nitroarenes to give the corresponding aromatic amines is a basic chemical reaction used both for removing toxic nitro aromatics from aqueous medium and for synthesising anilines. In fact, aromatic amines are important bulk chemicals and intermediates to produce fine chemicals, pharmaceuticals, polymers, herbicides, and more.[162] The industrial hydrogenation of nitrobenzene for the synthesis of aniline uses copper, palladium or palladium-platinum, supported on carbon or inor-

ganic oxides, as catalysts, under high pressure (up to 3 MPa) and high temperature (up to 300 °C), and it is not able to avoid the formation of noxious azo- and azoxyderivatives, which lowers the yield into anilines.[162] Aiming at overcoming the above reported weaknesses, the scientific community tried to develop alternative protocols for the reduction of aromatic nitro compounds,[163] including the use of different reducing agents, such as hydrazine,[164] silane[165] and sodium borohydride[166] in the presence of Cu,[167] Pd,[168] Au,[169] Ru,[170] Ag, [171] and, more recently, Co[172] and Ni[173] catalysts.

In 2006 Corma and Serna applied Au nanoparticles, supported on TiO_2 as catalyst, in the hydrogenation of nitroarenes.[174] NPs were selective over 95% for the reduction of the nitro group in 3-nitrostyrene, 4-nitrobenzaldehyde, 4-nitrobenzonitrile, and 4-nitrobenzamide.

The use of transition metal in this reaction was recently reported in the presence of different hydrogen donors such as alcohols or formic acid and its salts.[175]

Recently Yan and coworkers reported a new novel transfer hydrogenation system,[176] in which twelve "active hydrogens" can be transferred from water/ethanol mixture over Ru-Fe/C catalyst for the hydrogenation of halogenated nitrobenzene, obtaining o-chloroaniline with 98.0% selectivity at 99.8% conversion without dehalogenation. Beller and co-workers used cobalt catalyst[177] and related iron catalyst[178] in the hydrogenation of nitroarenes with high selectivity.[179,180] Until now cheap metal catalysts, such as Ni, have not been used for the hydrogenation reactions.[181,182]

In 2006, for the first time, Kempe et al. reported that Ni@SiCN nanocatalyst hydrogenated nitroarenes selectively to anilines in the presence of highly sensitive functional groups such as C=C bonds and nitrile, aldehyde, and iodo substituents. It was recycled and reused over multiple runs without a decrease in activity and selectivity. The critical reaction conditions, such as high temperature (110 °C) and high hydrogen, limits its applications.[183]

2.5.2 Catalytic study of Ni-pol in hydrogenation of nitroarenes

Nevertheless, the major problems remain still unsolved and designing new systems with different chemical and physical compositions and morphologies for catalytic reduction of nitroarenes under sustainable conditions is an urgent topic of current research.

In this context, I studied the catalytic activity of our acrylamidic polymer supported nickel catalysts [$Ni(AAEMA)_2$-pol and Ni-pol for the hydrogenation of nitroarenes in aqueous medium, knowing that the real catalytically active species are Ni NPs.

Due to the analogy between $Pd(AAEMA)_2$ and $Ni(AAEMA)_2$ supported polymers,

I decided to test the catalytic activity of Ni(AAEMA)$_2$-pol in a benchmark reaction in which Pd-pol was particularly active and recyclable: the transfer hydrogenation of nitrobenzene in water using $NaBH_4$ as the reducing agent, hoping that Ni(II) centers could turn into Ni(0) nanoparticles under reaction conditions, as it happened for Pd-pol. Preliminary catalytic tests were carried out using nitrobenzene as the representative substrate. By employing the same optimized conditions used for the palladium catalyzed nitroarene reduction,[64] the yield into the desired aniline was poor (24% after 1 h and 47% after 4 h, entries 1 and 2 of Table II.1, respectively), but it significantly increased by increasing $NaBH_4$/substrate molar ratio up to 20 (entry 3,Table II.1). However, attempting in recycling Ni(AAEMA)$_2$-pol failed, since the yield into aniline dropped to 27% already in the second run with the same catalyst (entry 4,Table II.1). We observed also that the resin turned from green to black during reaction (presumably due to Ni reduction from +2 to 0 oxidation state) and, then, from black to white at the end of the reaction, probably due to metal leaching into solution (which in turn became green).

Table II.1 - Preliminary catalytic tests for the reduction of nitrobenzene[a]

Entry	Ni Catalyst	$NaBH_4/PhNO_2$ molar ratio	Solvent	Reaction time (h)	Yield[b] (%)
1	*Ni(AAEMA)$_2$-pol*	10	H_2O	1	24
2	*Ni(AAEMA)$_2$-pol*	10	H_2O	4	47
3	*Ni(AAEMA)$_2$-pol*	20	H_2O	2	93
4	*Ni(AAEMA)$_2$-pol*[c]	20	H_2O	2	27
5	*Ni-pol*	20	H_2O	2	88
6	*Ni-pol*[c]	20	H_2O	2	80
7	*Ni-pol*	20	H_2O/Et_2O	2	90
8	*Ni-pol*[c]	20	H_2O/Et_2O	2	90

[a] Reaction conditions: 0.5 mmol of nitrobenzene, 10.2 mg of Ni-pol (Ni%w = 5.35) or 17.5 mg of Ni(AAEMA)$_2$-pol (Ni%w = 3.12), solvent (5 mL, H_2O or H_2O/Et_2O, v/v = 1/1) and given amounts of $NaBH_4$ were stirred at room temperature under nitrogen.
[b] Yield determined by GLC with the internal standard (biphenyl) method.
[c] Catalyst recovered from the reaction of the previous entry.

Concerning Ni-pol, it resulted active and recyclable in the reduction of nitrobenzene (entries 5-8,Table II.1), although in neat water the reusability of the catalytic system dramatically decreased after the second run. Figure II.6 summarizes the recyclability over five runs of Ni(AAEMA)$_2$-pol and Ni-pol in neat water and in water/diethyl ether (v/v = 1/1), as the solvent.

It can be seen from Figure II.6 that the best catalytic performance in terms of catalytic activity and recyclability was shown by Ni-pol in H_2O/Et_2O as the solvent. The biphasic reaction medium on one side facilitates the access of the water insoluble sub-

strate to the catalytically active sites and on the other side renders more workable the acrylamide based catalyst, becoming the latter too jelly in neat water. In addition, the polymeric support seems to better retain the nickel centers by swelling (in water) and shrinking (in diethyl ether) at the same time. Furthermore, Zhao and coworkers demonstrated that water solvent rapidly deactivates Ni supported catalyst in the hydrogenation of nitroarenes by forming catalytically inactive $Ni(OH)_2$ species.[184] This problem has been resolved by coating the catalyst with a hydrophobic layer of carbon.[27] In our system, the hydrophobic property of diethyl ether might help to prevent catalyst deactivation. Additionally, it can be deduced that the catalytically active species are metallic Ni nanoparticles rather than Ni(II) sites. Therefore, high attention should be paid to the size and morphology of Ni sites, as well as to their distribution in the polymeric support and their modification after the use in the reaction media.

On the bases of the above results, we concluded that the optimum reaction conditions to be used for converting 0.5 mmol of nitrobenzene into aniline in the presence of 10.2 mg of Ni-pol (containing 5.35%w Ni) were the ones reported in entries 7 and 8 of Table II.1.

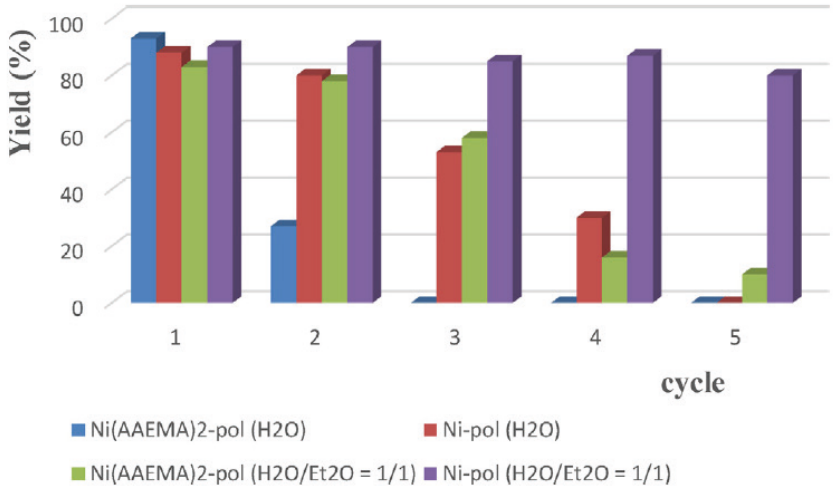

Figure II.6 - Reusability of Ni(II)pol, Ni-pol in water and water/diethylether (v/v=1/1).

The catalytic system was then used for the reduction of different various nitroarenes under the optimized reaction conditions (Table II.2). Ni-pol catalyzed the reduction of substrates that are electron withdrawing and electron donating substituent in the aromatic ring. 2-, 3- and 4-Nitrotoluene, as well as 3- and 4-methoxynitrobenzenes, gave very high yields into 2-, 3- and 4-toluidine, and 3- and 4-anisidine, respectively, in 2–5

h (entries 1–5). Both nitro groups were converted in 12 h (entry 6), and 2-nitro-aniline was detected only insight amount during the reaction course. Due to the absence of steric hindrance, 2,4-dinitrotoluene reacted faster (entry 7) than its isomer reported in entry 6. This is interesting because the o- and p-diaminobenzene are notoriously important in the industry of azodyes.[185,186]

Table II.2 - Transfer hydrogenation reaction of nitroarenes catalyzed by Ni-pol[a].

Entry	Substrate	Product	Time(t)	Yield(%)[b]
1	2-nitrotoluene	2-methylaniline	4	99
2	4-nitrotoluene	4-methylaniline	2	90
3	3-nitrotoluene	3-methylaniline	2	87
4	3-methoxynitrobenzene	3-methoxyaniline	4	91
5	4-methoxynitrobenzene	4-methoxyaniline	5	83
6	1,2-dinitrobenzene	1,2-Diaminobenzene	12	90
7	2,4-Dinitrotoluene	2,4-Diaminotoluene	5	(82)
8	Nitrobenzene	Aniline	3	73

[a] Reaction Conditions: 0.5 mmol of nitroarene, 10.0 mmol of $NaBH_4$ and Ni-pol (9.3·10-3 mmol of Ni) were stirred in 2.5 mL of double deionized water and 2.5 mL of diethyl ether at room temperature for the appropriate amount of time.
[b] Yield determined by GLC with the internal standard (biphenyl) method. Isolated yield after column chromatography in parenthesis.

2.5.2.1 Ni-pol as catalyst for the selective reduction of halo-nitroarenes to halo-anilines

In the field of the hydrogenation of unsaturated compounds the catalytic hydrogenation of aromatic halo nitro compound to yield halo-anilines is a very important reaction. Halo-anilines are a class of industrially interesting compounds. They are important building block and intermediates for the synthesis of fine chemicals, such as dyes, drugs, pharmaceuticals, cosmetic products, polymers, herbicides, and more.[187]

The most common catalysts employed in the hydrogenation of halonitroarenes are based on transition metals such as noble metals and Raney nickel that is sensitive toward the moisture in air. Metals usually used are copper, palladium or bimetallic system such as Pd-Pt, supported on carbon or inorganic oxides. They were used as catalyst

under high pressure (up to 3 MPa) and high temperature (up to 300 °C). This strategy makes the formation of azo and azoxyderivates, which lowers the yield into anilines.[188] In order to overcome this problem, the scientific community tried to develop alternative methods for the reduction of aromatic nitro compound.[163f] Different reducing agents, such as hydrazine,[189] silane[190] and sodiumborohydride[191] with Cu,[192] Pd,[193] Au,[194] Ru,[195] Ag,[196] and, in the last years, Co[197] and Ni[198,199] catalysts were used.

The major problems remain still unsolved: the tendency towards hydro-dehalogenation during the hydrogenation reaction of halo-substituted nitroaromatic compounds. At the same time there was an increasing interest in the development of a new sustainable method for the reduction of halonitroarenes. Different hydrogenation methods have been proposed using Pd,[200] Pt[201,202,203] and Ru[204] as metal based heterogeneous catalysts, all aimed at improving the selectivity towards the corresponding haloanilines and at minimising the dehalogenation process. Pd-based noble metal catalysts are attractive because they can work under atmospheric hydrogen pressure at room temperature.[205,206]

Using the optimized reaction conditions, the selectivity of the Ni-pol catalyst was tested in the reduction of different halonitrobenzenes, i.e. a reaction for which the major challenge is avoiding the undesired hydrodehalogenation reaction, a side-reaction favoured by the electron withdrawing effect of the nitro group in para and/or ortho positions (with respect to the halogen), that enhances the rate of the Ar-X (Cl, Br, I) oxidative addition to the metal centre. Selective halonitroarene reductions have been reached by poisoning Pd[207] or Pt[208] nanocatalysts. Our Ni based catalytic system resulted active and selective in the reduction of halonitrobenzenes (Table II.3), even in the case of challenging bromo- and iodo-nitrobenzene (entries 3 and 4,Table II.3). This chemoselectivity, much higher than the one observed with the analogues Pd catalyst (Table II.4), should be ascribable to reluctance of aryl halides to give oxidative addition to nickel active site, which is the well-known first step of the Ni and Pd catalyzed hydrodehalgenation reaction.[209]

Table II.3 - Reduction of various halonitroarenes catalyzed by Ni-pol.

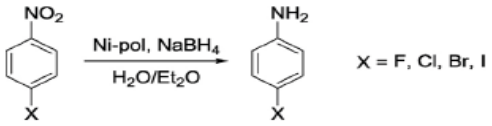

Entry	Substrate	Product	Time (h)	Yield (%)[b]
1	4-fluoronitrobenzene	4-fluoroaniline	5	97
2	4-chloronitrobenzene	4-chloroaniline	5	94
3	4-bromonitrobenzene	4-bromoaniline	12	95(94)
4	4-iodonitrobenzene	4-iodoaniline	5	82

Table II.4 - Comparison between Ni-pol and Pd-pol in the hydrogenation of halo-nitroarenes.

			Pd	Ni
Entry	**Substrate**	**Product**	**Yield**	**Yield**
1	4-Fluoronitrobenzene	4-Fluoroaniline	89	97
2	4-Bromoronitrobenzene	4-Bromoaniline	61	95(94)
3	4-Chloronitrobenzene	4-Chloroaniline	57	94
4	4-Iodonitrobenzene	4-Iodoaniline	/	82

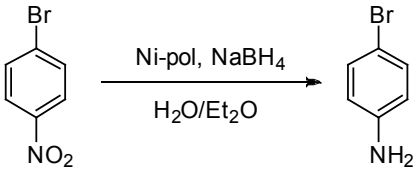

Scheme II.5 - Model reaction for catalytic recycle.

Ni-pol were recycled and reused in several cycles. The model reaction used for the recyclability study is reported in Scheme II.5. The employment of halo-nitrobenzene as model substrates allows us to consider that the catalyst is not only active and recyclable but also that no de-halogenation was observed during any catalytic cycle. The catalytic system showed the same activity and selectivity over five cycles. The recycles were made by easy separation of the organic phase just pipetted out. The remained solution containing the catalyst is a water solution, which was washed three times with diethyl ether in order to remove all organic reactants and products. The catalyst recovered was used for a new hydrogenation reaction adding fresh reagents and diethyl ether to the water mixture. The catalytic system was successfully reused for five subsequent runs, showing the unaltered catalytic activity and selectivity, giving 4-bromoaniline as the product in excellent yield (89–95%) for every cycle (Figure II.7).

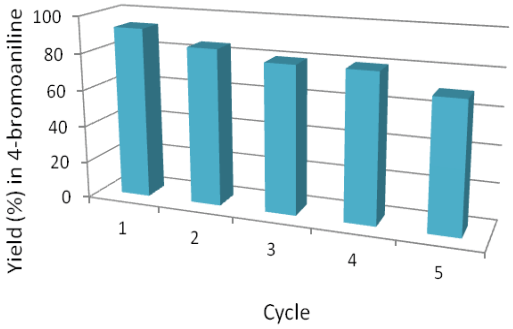

Figure II.7 - Selectivity of Ni-pol towards 4-bromoaniline over five cycles.

2.5.2.2 Heterogeneous or homogeneous mechanism?

In order to be sure that the system works as heterogeneous catalyst, the filtration test was carried out taking the reduction of 4-bromonitrobenzene as the model reaction. The reaction mixture was removed of the supported catalyst by filtration after 3 h stirring. Gas-liquid chromatography analysis (GLC) revealed that the conversion of the substrate was 30% ca. at that stage. The solution collected after filtration of the supported catalyst was left under stirring, after addition of 10.0 mmol $NaBH_4$, in the optimized reaction conditions. The conversion of 4-bromonitrobenzene did not increase even after 9 h stirring. On the contrary, the amount of 4-bromoaniline in the reaction mixture decreased after 9 h stirring. The resulting solution was then mineralized and submitted to atomic absorption spectrometry (AAS) analysis. Results showed that there was a negligible nickel amount. Moreover, the catalyst recovered was also mineralized and analyzed by AAS and it showed the same amount of nickel found in the catalyst before catalytic application. Same results were observed in the sample recovered after the end of the fifth cycle. All these data suggested that the catalysis was truly heterogeneous, since the presence of catalytically active leached nickel species was not observed.

2.5.2.3 Characterization of Ni-pol: STEM analysis

In order to understand how the catalytic reaction conditions can influence the morphology of the catalyst, Scanning Transmission Electron Microscopy (STEM) analyses were carried out on the Ni catalyst before and after calcination, as well as after the first and fifth cycle reaction.

$Ni(AAEMA)_2$-pol was characterized just by Ni(II) species supported on the macroporous polymer, not visible in the STEM micrograph (Figure II.8 a). Ni-pol after reduction under N_2 shows the formation of Ni nanoparticles of diameter ranging between 11-37

nm (Figure II.8 b). Some nanocubes of Ni with side length of 85-200 nm were formed during the thermal reduction.

The STEM image of the catalyst recovered after the first cycle shows Ni nano-twins ranging from 28 to 70 nm in side size (Figure II.8 c). This particular morphology can be attributed to the matrix effect of the polymeric support which controls Ni NPs form and grow. In fact, it seemed that for each nanoparticles a second nano-cube grew up along the preferential direction, diagonal one, giving rise to two compenetrated cubes as final overall nanoparticles.

The catalyst was investigated also after the fifth cycle. After the last recycle the dimension of the Ni nano-twins side sizes are not changed, 27-65 nm, as well as number density of nanoparticles (Figure II.8 d). On the contrary the number of big nanoparticles, having dimension between 45-70 nm in side, seem to decrease if compared with the previous cycles. This phenomenon can be associated to the tendency of the catalyst to dissolve and settle itself in the presence of water,[210] that is able to oxidize Ni(0) to Ni(II),[211] which is reduced again under reaction conditions to form Ni(0) nanoparticles. The fundamental role of the polymer support is to stabilize metal nanoparticles and this characteristic should prevent nanoparticles from aggregation during catalytic cycles. In our study this is confirmed by the observation that NPs size and morphology did not dramatically change with the recycles.

Indeed, some Ni-NPs were formed during reaction because $NaBH_4$, the reductant, works as reducing agent of the metal in two different ways, by providing hydrides and by generating hydrogen gas. The hydrides formed by sodium borohydride can be use in order to displace negatively charged ligands bound to Ni(II), generating Ni-hydrides directly, which upon β-hydride elimination of H_2, give the reduced metal. Besides, the use of water leads to the in situ formation of H_2 (Scheme II.6) in the closeness of Ni(II), thus reducing it to Ni(0).

$$NaBH_4 + 2H_2O \xrightarrow{\text{cat.}} 4H_2 + NaBO_2$$

Scheme II.6 - Metal catalyzed production of H_2 by $NaBH_4$.

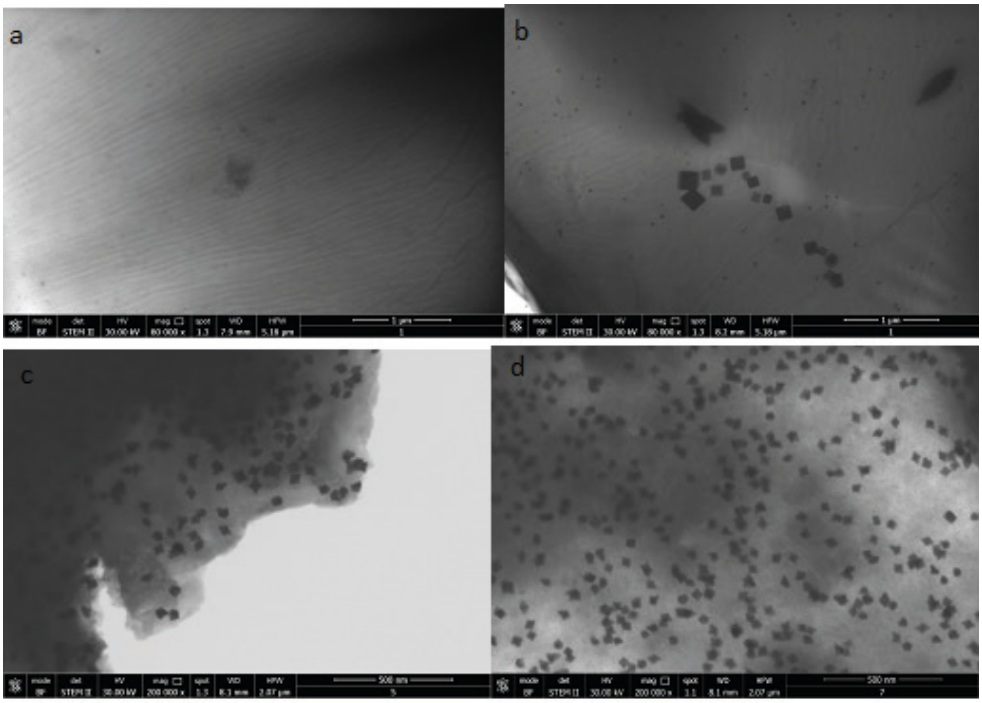

Figure II.8 - STEM images of polymer supported nickel catalyst. a): $Ni(AAEMA)_2$-pol; b): Ni-pol after calcination at 300 °C; c): Ni-pol after 1 cycle reaction; d): Ni-pol after 5 cycle reaction.

2.5.2.4 Mechanism for the reduction of nitroarenes

Under the reaction conditions, when $NaBH_4$ was added to water solution in presence of Ni-pol, a very abundant formation of H_2 gas was observed in the reaction flask, in according with the reaction reported in Scheme II.6.[212] It is well-know that nitroarene (I) hydrogenation can occur in two different pathways: the direct route and the condensation route (Scheme II.7).[213] The first route gives anilines (IV) as final product by the intermediate formation of hydroxylamine (III); the second route forms diazoarene (VI) as reaction intermedium. Basically, catalytic system based on noble metals such as Pd or Au in general prefer the direct route[214,215] even if catalytic system such as Pd/C can be follow other mechanistic ways.[216] In the case of Ni catalyst, a density study was carried out in order to find its preferential route. This study demonstrated that, the direct reduction pathway is more favourable than the indirect one.[217]

Since our catalyst is based on Ni metal, we expected the absence of diazo-compounds during the reaction. On the contrary, monitoring the reaction by GC-MS analysis, the formation of diazo-intermediates (V and VI) and nitroso compound (II) was

observed during the reaction with $NaBH_4$/Ni-pol system. The formation of arylhydroxylamine (III) was never observed. When substrate (I) was totally converted, the concentration of II, V and VI became lower because they were converted into the desired product. Probably, III was never detected because its reduction was faster compared to the one of II and/or because III quickly reacted with II to give V. These results suggest that Ni-pol reducing system might go through both direct and condensation routes (Scheme II.7).

An increasing of diazobenzene (VI) amount and a decreasing of aniline (IV) quantity were observed (GLC Analyses) in the mother liquor removed of Ni-pol during reaction (30% conversion of nitrobenzene) and stirred for additional nine hours after addition of fresh $NaBH_4$. In the absence of the supported catalyst, nitroso benzene (II) and aniline (IV) condensed into diazobenzene (VI) (Scheme II.7), because the hydrogenation of II to give hydroxylamine benzene (III) did not happen without Ni.

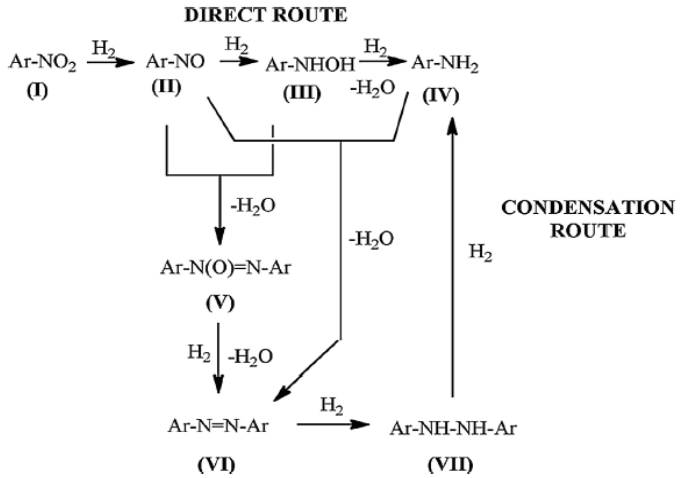

Scheme II.7 - Possible mechanism pathways for the nitroarene hydrogenation.

2.5.3 Final consideration

By comparing Ni-pol catalytic system with the commercial available Raney Ni,[218] it is apparent that the latter dramatically deactivates after few runs and it needs harsh conditions (102 °C and 1.62 MPa of H_2) to obtain high yields. Raney Ni/$NaBH_4$ system has been recently proposed, but no studies on its recyclability have been reported.[219]

Table II.5 displays the reaction conditions employed in catalytic systems based on recent examples of Ni supported catalysts in the hydrogenation of nitroarenes. It is evident that either high temperatures and H_2 pressures or high $NaBH_4$/substrate molar ratio

are needed to get good yield. In addition, to the best of our knowledge Ni-pol system is the second example reported to date[220] of Ni based reusable catalyst, selective in the hydrogenation of halonitrobenzenes to haloanilines.

Table II.5 - Reaction conditions for Ni-based catalyst reported.

Catalyst	**T (°C)**	**Solvent**	**P (MPa) of H_2**	**$NaBH_4$/substrate molar ratio**	**Ref.**
Ni-pol	25	H_2O/Et_2O	_	20	[281]
Ni-NPs/C	25	H_2O	_	847	
Ni/CB	30	H_2O	_	104	
Co-Ni	120	EtOH	3	_	
Ni-53-EN	110	EtOH	2[221]	_	
Ni-B-SiO_2	100	Et[222]OH	1.8	_	

2.6 Catalytic application of Ni-pol: reductive amination of arylaldehydes with nitroarenes

2.6.1 Introduction

Aryl amines are important building blocks and key intermediates in the synthesis of bioactive natural products, pharmaceuticals, dyes, agrochemicals, polymers, and photographic materials.[223,224] In addition, optically active secondary amines have important applications in organic asymmetric synthesis as chiral auxiliaries,[225] catalysts,[226] resolving agents, and fine chemicals.[227]

Traditional methods for the synthesis of aryl secondary amines include reduction of nitroarenes to corresponding anilines[228] and further reaction with alkyl halides, alcohols or carbonyl compounds.[229] However, these processes have several disadvantages, such as the toxicity of reducing or alkylation agents, lack of mono-alkylation selectivity and large amounts of waste produced. Therefore, there is an increasing interest for economical and eco-friendly syntheses of secondary amines.[230] One-pot reductive amination of aldehydes with nitroarenes over heterogeneous catalysts using molecular hydrogen or other "green" reducing agents is an atom-economical and environmentally attractive method for the synthesis of secondary aromatic amines.[231,232,233] This process involves three cascade reactions: hydrogenation of nitroarene into primary aromatic amine, reversible condensation of primary amine with aldehyde to imine, and hydrogenation of imine to the desired secondary amine. In general, the reaction is carried out using metal-based catalysts, such as Pd,[234,235] Pt[236] and Au.[237] Recently, there is an increasing interest in developing a new methodology requiring the presence of no noble transition metals as catalyst. Lately, reductive amination of aldehydes with nitroaromatic compounds, employed Fe- and Co-based catalysts, has been described.[238,236] The catalysts are formed by Fe_2O_3 particles,[239] Co/Co_3O_4 nanocomposites,[240] and Co nanoparticles[241] fixed in mesoporous nitrogen-doped carbon and they were found to be active and selective in this reaction.

The reaction is referred to as *direct* reductive amination, when the amine and the carbonyl compound are mixed together with the proper reducing agent without prior formation of the intermediate imine (or iminium salt), and as *indirect* (*stepwise*) reductive amination, when it involves the pre-formation of the intermediate imine followed by reduction in a separate step.[242]

Thus, a one-pot direct or indirect reductive amination, starting from a nitroarene, is an attractive method as it removes another hydrogenation step, saving both time and costs considering that nitro aromatic compounds are cheaply available starting mate-

rials in organic synthesis.[243] In the last decade several efforts have been addressed to develop an efficient heterogeneous catalytic version of this one-pot direct or indirect reductive amination promoted by supported nanoparticles or nanocomposites of metals such as Ag,[244] Au,[245] Co,[246,243] Cu,[247,248] Fe,[249,242] Pd,[250,251,252] Pt,[253,254] Rh,[255] Ru,[256] as well as by heterobimetallic systems such as AgPd,[257,258,259] AuPd,[260,261] CoRh,[262,263] and NiPd.[264] Several studies were carried out aiming at using no noble metal catalyst. Among them, in 2015 Kalbasi et al. reported the synthesis of secondary ammines in the presence of Ni based-catalyst, Ni/H-mZSM-5, formed by a hierarchical zeolite with mesoporous-microporous structure (Figure II.9). It exhibited good catalytic performance in one-pot reductive amination of benzaldehydes and nitroarenes at room temperature in water in direct pathway (Scheme II.8).[265]

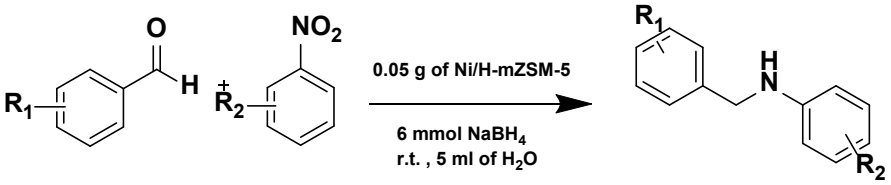

Scheme II.8 - Direct one-pot reductive amination of aldehydes with nitroarenes over Ni/H-mZSM-5.

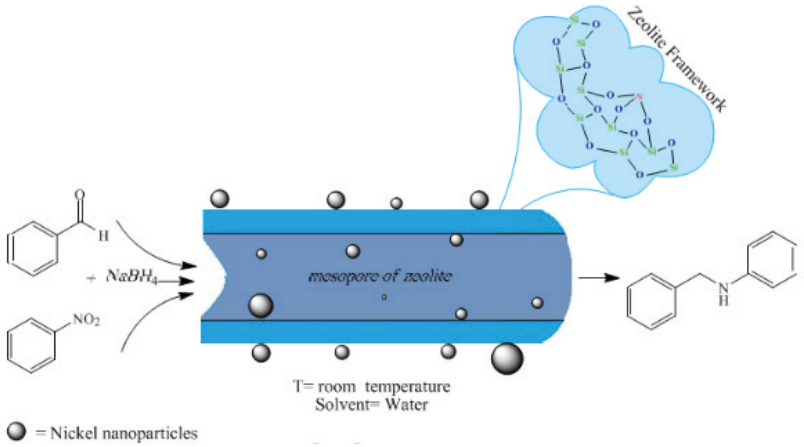

Figure II.9 - Possible mechanism for direct reductive amination using bi-functional catalyst.

The interesting aspect of this work is that the catalyst has acid sites on the zeolite support, thus promoting the formation of the imine. More recently, the same author reported the synthesis of metal–acid bi-functional catalyst based on nickel nanoparticles and polystyrene sulfonic acid chains anchored on ordered mesoporous carbon CMK-8. This catalyst was able to perform direct reductive amination of aldehydes in good

yield in a short reaction time under mild conditions. TEM images of catalyst proved an ordered structure with negligible metal aggregation. Moreover, N_2 adsorption–desorption isotherms declared the Ni–PSSA/CMK-8 as a mesoporous structure with a high surface area and acceptable pore volume even after metal loading and polymerization. The collaboration of acidic and metal sites expedites the performance of the catalyst. Overall, the catalyst could be easy separated from the reaction medium and reused for several runs without any drastic deceleration in the catalyst activity and stability.[266]

2.6.2 Ni-pol catalyzed reductive amination

Encouraged by the results obtained in the nitroarene reduction, Ni-pol catalyst was evaluated as catalyst for the synthesis of other organic molecules. It was employed in the reductive amination reaction starting from nitroarenes in order to obtain N-benzylaniline. We started this study carrying out this procedure in direct way: one pot, one step. Nitrobenzene 1a, benzaldehyde 2a, Ni-pol and $NaBH_4$, as reducing agent, were putted in the same flask. Ethanol/water in equal amount (1:1) was used as the solvent and the reaction was carried out at room temperature. The reaction mixture was monitoring by GC-MS and after 2 h results showed that the conversion of the substrate was quantitative, but the products formed were aniline, as major product, and benzyl alcohol formed for the concurrent reduction of nitrobenzene and benzaldehyde. Very small amount of imine, 2%, and N-benzylaniline were formed. After these results we decided to test the indirect way: one pot, stepwise.[267] The reaction was carried out under the same conditions described before but the benzaldehyde reagent was added after step A (Scheme II.9).

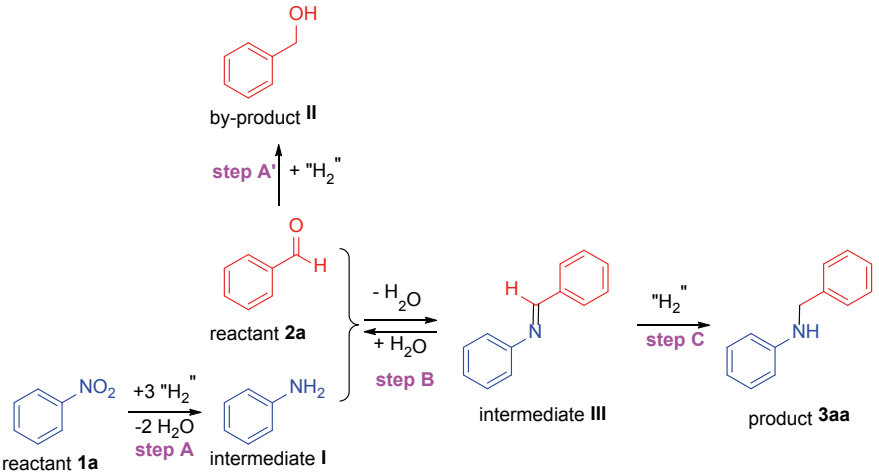

Scheme II.9 - Synthesis of *N*-benzylaniline (3aa) through hydrogenation of nitrobenzene (1a) and reductive amination of benzaldehyde (2a).

In this case the conversion of imine was only 16% and no desirable product was formed. We yet observed that adding 3.0 mmol of $NaBH_4$ in the last step C, 40% of N-benzylaniline can be obtained in 3 h (entry 1 in Table II.6). These results demonstrated that in this catalytic system the formation of imine product was very slow and the most of $NaBH_4$ is lost. It is well known in the literature that there are different factors influencing the equilibrium between the imine and its precursors 1a and 2a. For instance, concentration, solvent, temperature, pH and so on.[268,269] We focused our attention on the pH influence, well knowing that the hydrolysis of $NaBH_4$, that occurs in the first steps, provides an alkaline reaction system,[270,271] on the contrary imines requires a pH value ranging from 4-6 to be formed.[272] First, we reduced the amount of reducing agent added in the step A and let the other parameters unchanged. The results indicated that there was just a little increase of yield, 47% for the formation of the final product (entry 2). Whereas Bronsted acids facilitate the formation of Shiff bases, we decided to check different carboxylic acids. The best results were obtained using HCOOH as additives, attaining 61% yield (entry 3). In order to increase the yield we decided to use methanol as solvent, obtaining 96% of conversion. Methanol, in fact, forms hydrogen by the methanolysis of $NaBH_4$[273,274] and it is able to facilitate the imine formation.[275]

Table II.6 - Preliminary tests to achieve the best reaction conditions.

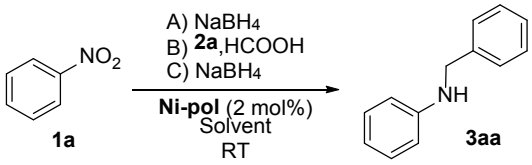

Entry	Molar Ratio $NaBH_4$/1a (step A)	Solvent	Time Reaction (step A+B+C)	HCOOH Addition in step B (2 equiv)	Isolated Yield of 3aa (%)[c]
1	20[b]	H_2O/Et_2O(1:1,v/v)	2 h+40 min+3 h	No	40
2	3[b]	"	3 h+40 min+3 h	No	47
3	3[b]	"	3h+40 min+3 h	Yes	61
4	3[b]	MeOH	3 h+40 min+3 h	Yes	96

[a] Reaction conditions: 0.50 mmol of nitrobenzene (1a), 0.70 mmol of benzaldehyde (2a), Ni 2.0 mol% (11.0 mg of Ni-pol) with respect to 1a, 5.0 mL solvent, room temperature.
[b] 3.0 mmol $NaBH_4$ were added after step B (see Scheme II.9); [c] based on nitrobenzene.

Once have found the optimized reaction conditions, we decided to develop our study

in two different parts. In the first one we carried out the reductive amination of benzaldehyde with different nitroarenes (Table II.7); in the second one the reductive amination of several arylaldehydes with nitrobenzene (Table II.8).

Table II.7 - Reductive amination of benzaldehyde (2a) with different nitroaromatics (1b-j)[a].

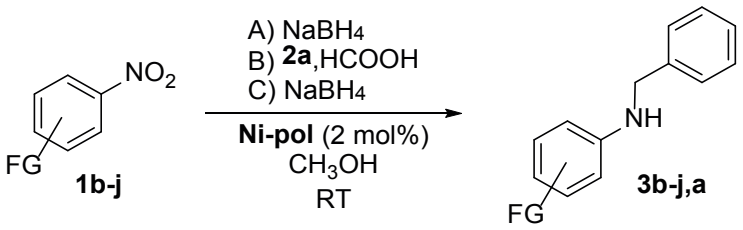

Entry	Nitroarene	Product	Time Reaction (step A+B+C)	Isolated-Yield (%)[b]
1	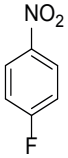 **1b**	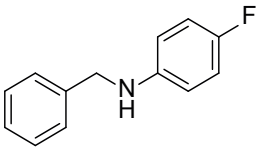 **3ba**	3 h+40 min+3 h	97
2	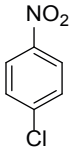 **1c**	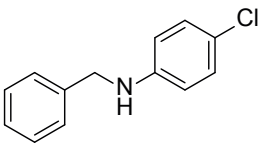 **3ca**	5 h+40 min+3 h	85
3	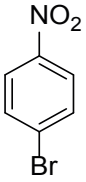 **1d**	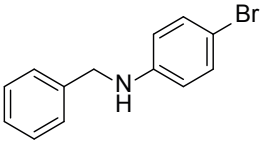 **3da**	6 h+40 min+3 h	80

4	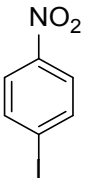 **1e**	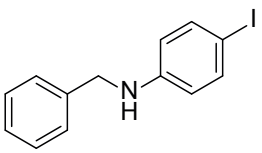 **3ea**	5 h+40 min+3 h	50
5	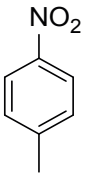 **1f**	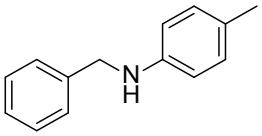 **3fa**	2 h+40 min+3 h	98
6	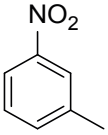 **1g**	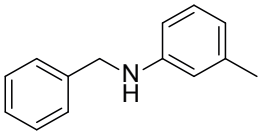 **3ga**	2 h+40 min+3 h	97
7	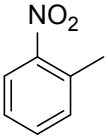 **1h**	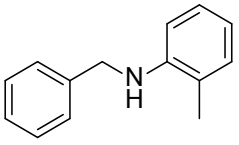 **3ha**	10 h+40 min+3 h	93
8	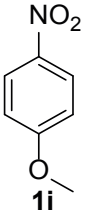 **1i**	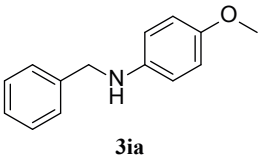 **3ia**	2 h+40 min+3 h	98
9	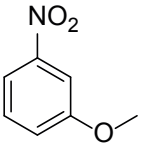 **1j**	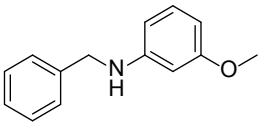 **3ja**	2 h+40 min+3 h	97

Table II.8 - Reductive amination of different arylaldehydes (2b-n) with nitrobenzene (1a)[a].

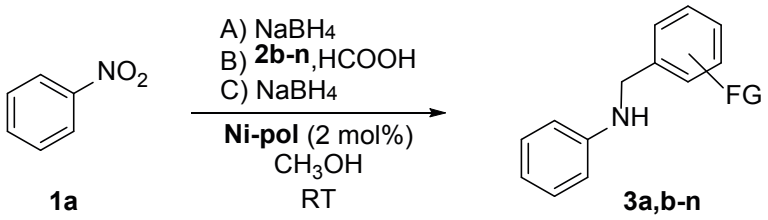

1a **3a,b-n**

Entry	Arylaldehyde	Product	Time Reaction (step A+B+C)	Isolated Yield(%)[b]
1	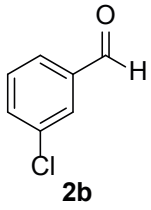 **2b**	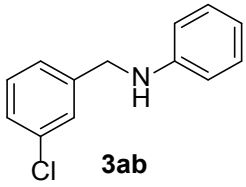 **3ab**	3 h+40 min+3 h	80
2	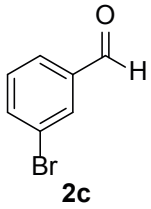 **2c**	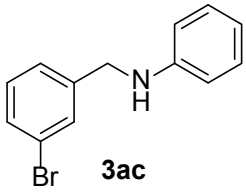 **3ac**	3 h+40 min+3 h	73
3	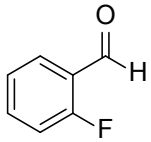 **2d**	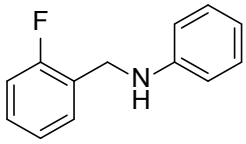 **3ad**	3 h+40 min+3 h	98
4	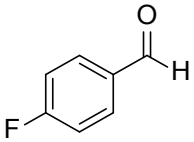 **2e**	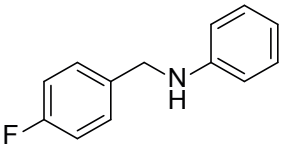 **3ae**	3 h+40 min+3 h	72

5	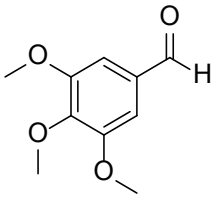 **2f**	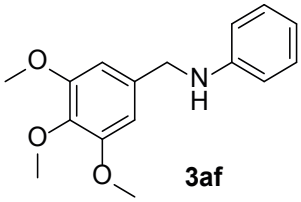 **3af**	3 h+40 min+3 h	93
6	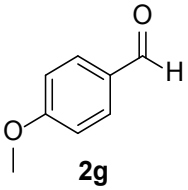 **2g**	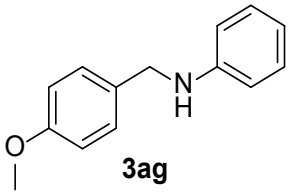 **3ag**	3 h+40 min+3 h	96
7	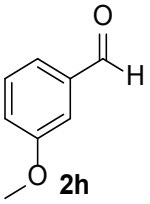 **2h**	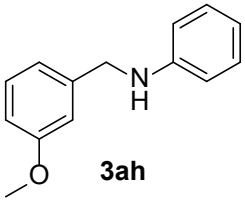 **3ah**	3 h+40 min+3 h	98
8	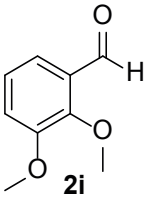 **2i**	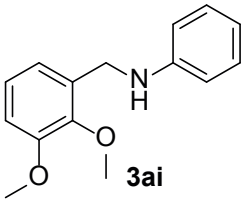 **3ai**	3 h+40 min+3 h	95
9	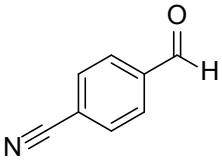 **2j**	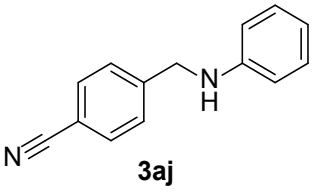 **3aj**	3h+40 min+4h	96
10	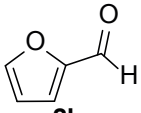 **2k**	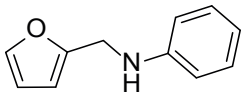 **3ak**	3 h+40 min+3 h	96

11	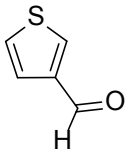 **2l**	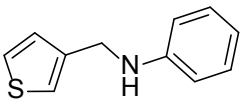 **3al**	3 h+40 min+3 h	98
12	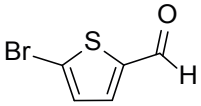 **2m**	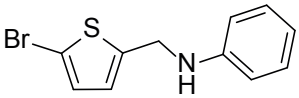 **3am**	3 h+40 min+5 h	93

As shown in Table II.7, in the reductive amination of halonitroarenes the yields reported are different. In fact, we observed that there is the influence of substituent on the reaction time in the step A, but it also influences the yield of secondary amines. With fluorine as substituent, entry 1, the secondary amine was obtained in excellent yield, 97%. With Br and Cl the yield obtained was just little bit lower, about 85 and 80%, and they require longer time for the step A. In the case of iodine, the yield decreases considerably giving a moderate yield (50%). This is due to a partial or consistent de-halogenation of both intermediate imine and target amine that occurs just in the last step C, as confirmed by GC-MS analysis. Given that the role of the catalyst is fundamental in the first and second steps, while the third, the last one, is guaranteed simply by the addition of a reducing agent, the results collected confirm that the catalyst is selective since dehalogenation occurs only in the last step. For the nitrotoluenes substrates (entry 5-7) no significant steric effect was observed on the yield of the final product that was obtained as excellent result for all of them. For 2-nitrotoluene the synthesis of the corresponding secondary amine requests longer reaction time for the step A compared to a very short time related to amines 3ia and 3ja. The same results were reported about methoxy nitrobenzenes (entry 8-9).

In the other part of our study we investigated the reductive amination of arylaldehydes with nitrobenzene, as reported in Table II.8. For halo-derivates was not necessary to use longer times. With m-chloro-benzaldehyde and m-bromo-benzaldehyde partially de-halogenation was observed, unlike 2-fluoro-benzaldehyde for which no de-halogenation has been observed with 93% of yield (entry 3). This yield is very different if compared with yield obtained for 4-fluoro-benzaldehyde, 72% (entry 4). This demonstrated that in our catalytic system the electronic effect is dominating respect to steric ones. This is also confirmed by the methoxy substituted benzaldehydes (entry 5-8). For 2f and 2i, that have a sterically demanding reactants, excellent results were

collected for the corresponding target secondary amines 3af (93%), 3ag (96%), 3ah (98%) and 3ai (95%). Then an arylaldehyde with a potential reducible group (2j) was tested, obtaining a very high yield (96%) although step c requires a longer time (entry 9). Heteroaromatic aldehydes such as furfural (2k) 3-thiophenecarboxaldehyde (2l), and 5-bromo-2-thiophenecarboxaldehyde (2k) were also investigated, obtaining excellent yields of corresponding amines 3ak (96%), 3al (98%), 3am (93%) (entries 9–11). For thiophene based amines (entry 11-12), is relevant to underline that for 3am no debromination was observed.

Ni-pol recyclability was tested in the reductive amination of benzaldehyde with nitrobenzene. The reaction was scaled up to 3.0 mmol in order to reduce the loss of catalysts and to recycle it better. Ni-pol was recycled for five cycles and, as show in Figure II.10, the yield slightly decreases in the second run (from 96% to 87%) but afterwards cycles, the isolated yield remained almost constant at values above 80%. In each catalytic cycle, Ni-pol was easily recovered by centrifugation, washed and rinsed with solvents, dried under air for 2 hours at 60 °C, and then employed for a new run.

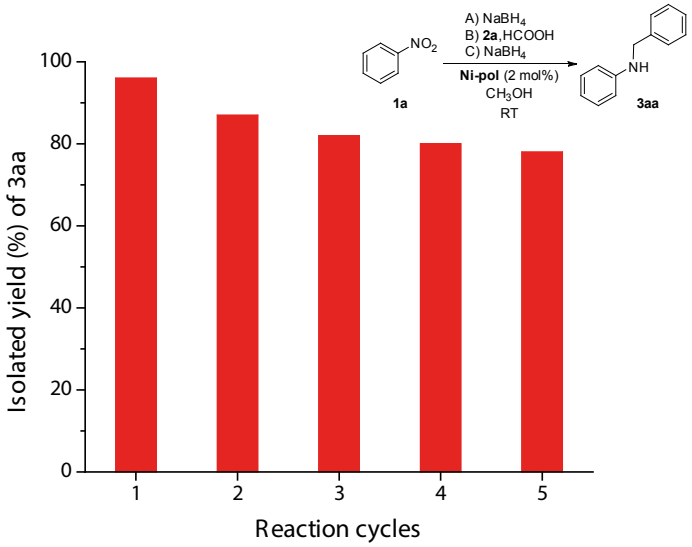

Figure II.10 - Recyclability of Ni-pol in the reductive amination of benzaldehyde (2a) with nitrobenzene (1a) to give N-benzylaniline (3aa).

These results demonstrated that a Ni-pol catalyst is recyclable and active for several cycles. The catalyst was recovered after first and fifth cycle in order to analyze it together with catalyst before and after thermal reduction.

2.6.2.1 Heterogeneity test

The heterogeneity of Ni-pol catalyst was studied by analysing the activity of mother liquor in the first step of reaction (step A). After 15 min from the start of the reaction, the catalyst was removed from the solution and the filtrate was left under stirring for 2 h and 45 min. Analysing the solution after 15 minutes by GC, results showed that conversion was about 85%, consisting in the chromatographic yield of 31% in aniline, 17% and 40% in diazobenzene e diazoxybenzene. The solution was taken at the end of the reaction time and GC analysis demonstrated that without catalyst the percentage of reaction conversion did not change. This proves that Ni-pol catalyst works as heterogeneous catalyst fact confirmed also by graphite furnace atomic absorption spectroscopy (GFAAS). The catalyst filtrated after 15 minutes and the catalyst after the last catalytic cycle were mineralized and analyzed by the same GFAAS. Results confirmed that the amount of Ni in the catalytic system is the same as before catalytic application.

The possibility to scale-up our catalytic system was also tested. The benchmark reaction was carried out on 6.0 mmol and the product recovered was about 1.02 g (93%). It confirms that our protocol is scalable for industrial application. Scheme II.10 reports the general accepted reaction pathways (direct and condensation routes) with relative intermediates for the reduction of nitrobenzene (1a) to aniline (I), explaining the presence of diazo- and diazoxy-products.

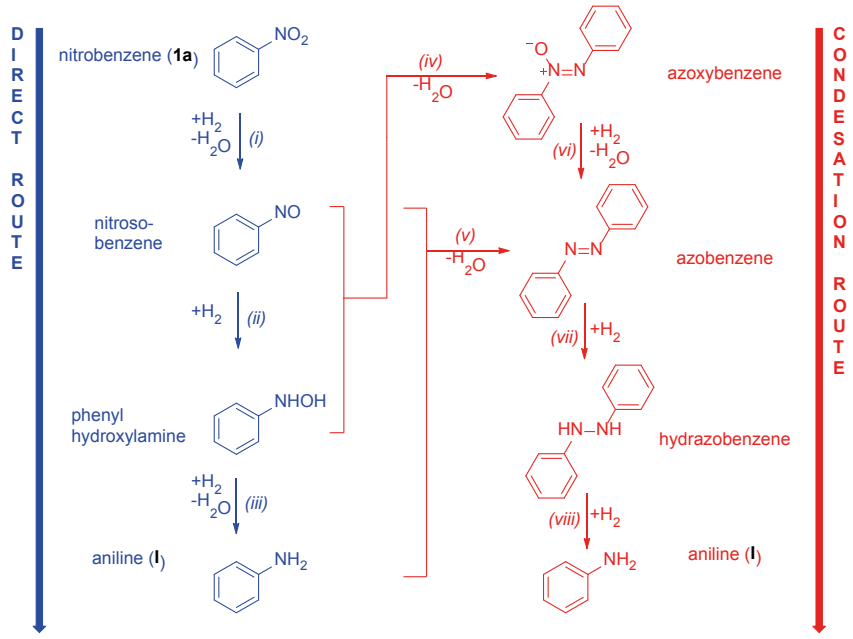

Scheme II.10 - Accepted reaction pathways for the reduction of nitrobenzene (1a) to aniline (I).

2.6.2.2 Characterization of Ni-pol: STEM analysis

As already discussed Ni(AAEMA)$_2$-pol and Ni-pol were investigated by STEM analysis. The first one was just characterised by an homogenous polymeric support on which the Ni(II) centres were deposited. Ni-pol, after thermal annealing, showed nanoparticles (NPs) with diameter comprising between 11 and 37 nm and a few quantity of Ni(0) nanocubes with a cube side of 85-200 nm. Since the catalyst is the same, in this study we analyzed just Ni-pol samples after first and fifth cycles. They were inspected by FESEM analyses with STEM mode, aiming at gaining insights into the morphology and the dispersion of the nickel active species on the polymeric support, checking if they change with the recycles.

FESEM picture of Ni-pol recovered after the first run (Figure II.11 a) shows a homogenously distributed cubic crystals of Ni in the average cross section value of 35 nm. The particle size distribution is quite narrow (25-45 nm) and monomodal (Figure II.11 b). The crystalline habitus is uniform and characteristic of cubic lattice. High degree of nanoparticles dispersion and the absence of aggregation suggest that the polymer matrix has a strong confinement effect and an efficient stabilizing feature towards Ni NPs.

The catalyst recovered after the fifth cycle (Figure II.11 c) did not show a significant difference from the sample after the first cycle. The only relevant aspect is that some of nanoparticles begin to aggregate at the surface of the polymer flake. This phenomenon can explain why the catalytic activity of the system slightly decreases with the re-cycles (see Figure II.10). FESEM analysis also revealed that the number of small nanoparticles (8-10 nm in diameter) in Ni-pol recovered after the last run is higher compared to the catalyst employed in the first one. NPs were smaller and with more irregular shape. These small Ni NPs are very uniformly distributed, as are the biggest ones, thus generating a bimodal NPs size distribution (Figure II.11 d). The amount of the smallest nanoparticles increases with the re-uses, presumably due to further formation of Ni NPs under reductive reaction conditions, as already observed by us.[281] In fact, during thermal calcination under inert atmosphere only a fraction of the whole amount of Ni(II) centres passes from +2 to 0 oxidation state giving rise to metal NPs. The reduction of the remaining quantity of Ni(II) centres to Ni NPs occurs during duty, thus explaining the broader distribution of Ni NPs compared to that of the catalyst before use.

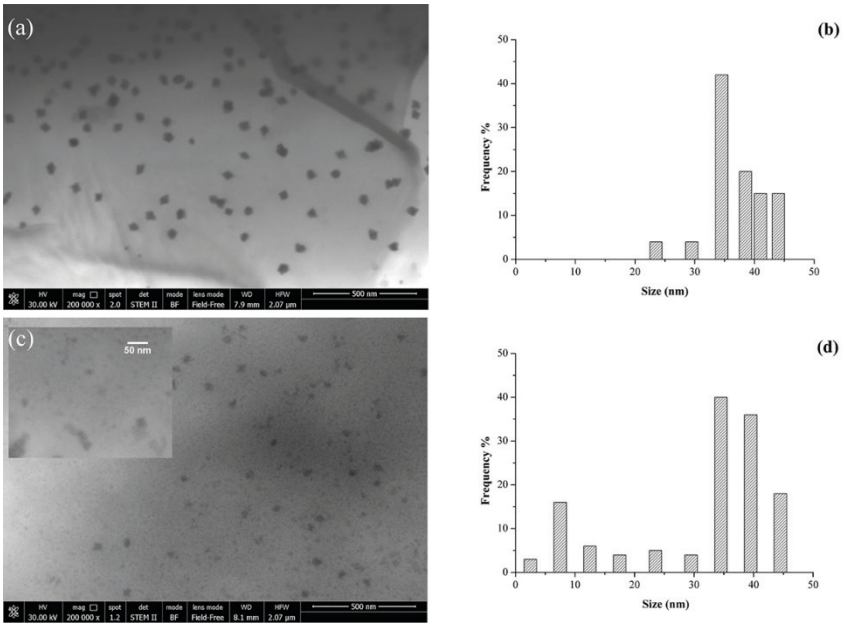

Figure II.11 - STEM micrographs and associated size distribution (on the right) of matrix polymer embedded Ni nanoparticles: (a) Ni-pol recovered after the first run of the model reaction and (b) its size distribution; (c) Ni-pol recovered after five subsequent runs of the model reaction and (d) its size distribution.

2.6.3 Final considerations

Ni-pol catalyst obtained as described in the first part of this chapter was found active, selective and recyclable catalyst in hydrogenation of nitroarenes and in one-pot stepwise reductive amination of arylaldehydes with nitroarenes. Ni-pol, as nanoparticles of Ni(0) was stabilized on insoluble acrylamide polymer (Ni-pol) as catalyst and $NaBH_4$ as mild, inexpensive, and safe reducing agent. The protocol used for the reductive amination is a one-pot indirect method having several advantages, such as the use of a no-precious metal catalyst, the facile separation of the catalyst by centrifugation, an excellent stability towards air and moisture, mild reaction conditions, good recyclability and scalability as well as broad substrate scope. Morphological analyses prove that the active species in Ni-pol are Ni NPs in the form of cubic crystals having an average cross section of 35 nm with a quite narrow (25-45 nm) and monomodal size distribution. Although such distribution becomes bimodal with the recycling reactions, no agglomeration of NPs was observed, and the catalytic activity of Ni-pol was preserved.

2.7 Study of Pd and Ni catalysts for biodiesel upgrading

2.7.1 Introduction

In 1900 Rudolf Diesel presented his own working creation using as the motor fuel the vegetable peanut oil, thus employing for the first time natural sources for industrial and mechanical applications. Subsequently, during the second World War there was an increased interest in using natural energy sources, because fossil fuel amount was inadequate. Starting from 1970 a new crisis in finding fossil oil led to a growth of the price of crude oil, inducing researchers at investigating the possibility of using vegetable oils and other alternative energy sources. In this framework, the most studied fuels can be divided mainly into two types: oily, derived from vegetable oil obtained by transesterification, used as Diesel, and alcohols, obtained by biomass treatment that produces bio-ethanol.

Several advantages are related to the strategy of using renewable sources as fuels, such as: reduction of carbon monoxide, unburned hydrocarbon emissions, no production of sulphur compounds and other substances which cause an increase of the smoke-screen. In addition, bio-fuel, obtained by treatment of natural sources has higher detergent power than hydrocarbons, and it is not subject to spontaneous combustion, parameter particularly important for the transport and storage phases. Furthermore, it is possible of obtain bio-fuel from raw materials which are easily available and from agri-food wastes, such as waste cooking oil (WCO). Biodiesel is a natural fuel extracted from oily plants and subsequently subjected to trans-esterification to obtain fatty acid mono-alkyl esters. Three different types of biodiesel can be considered.

- First generation Biodiesel: deriving from agricultural materials such as cereals and sugar canes;
- Second generation Biodiesel: deriving from inedible materials, such as waste cooking oil;
- Third generation biodiesel: deriving from algae.

In recent years, several efforts have been done aiming at obtaining fuels from animal fats, vegetable oils and biomass. In particular, biodiesel is made by fatty acids methyl esters (FAMEs). This fuel is recognized worldwide as the best substitute in automotive engines thanks to its chemical and physical characteristics that are very similar to those of petro-diesel. FAMEs can be obtained directly by processing plants having seeds containing oil (rapeseed, soybean, sunflower, palm and generally exhausted vegetable oils) by trans-esterification reactions that allow the replacement of glycerol using methanol (Scheme II.11).

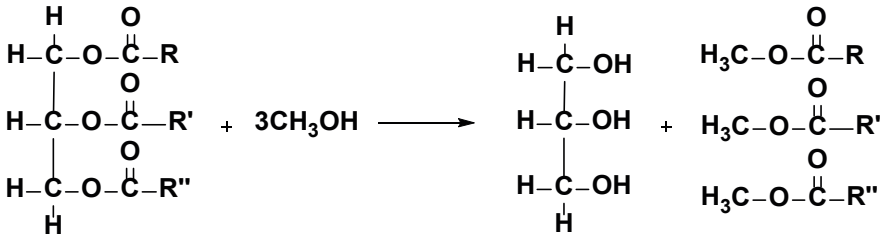

Scheme II.11 – Trans-esterification reaction for synthesis of FAMEs.

Trans-esterification reaction can occur with or without catalyst. The most commonly used catalysts are potassium hydroxide (KOH) and sodium hydroxide (NaOH), both very sensitive to water and free fatty acids. In the presence of water, the saponification of esters under alkaline conditions occurs. This causes the decrease of the catalyst activity and the formation of emulsions that compromise the separation and purification of the biodiesel. Using methanol and NaOH, yield about 94% can be obtained in range between 60 and 65 °C, with a catalyst concentration of 0.5% (w/w), and twice the stoichiometric proportion of methanol.

Biodiesel can be produced by the alkaline trans-esterification of sunflower oil with low acid value, with methanol at 65 °C for two hours, using a molar methanol/oil ratio of 6:1, using KOH as a catalyst (1%). By comparing NaOH and KOH activities, the reaction rate in the presence of KOH is higher than NaOH. Therefore, potassium hydroxide is currently considered the best catalyst for trans-esterification of food oils. Unfortunately, the obtained biodiesel cannot be used directly. Even if this type of fuel has several advantages compared to traditional diesel, it has different problems related to high corrosivity and viscosity, low cold flow properties and low powder density, due to high level of oxygen still present in the final product. In order to overcome these problems, FAMEs are commonly partially hydrogenated before use. Completely hydrogenation of polyunsatured methyl esters deriving from vegetable oils leads to solid soaps and surfactants. To enhance the combustible performances, biodiesel is often diluted with materials such as petrodiesel or solvents (ethanol). For example, adding 4% of ethanol to biodiesel increases its thermal efficiency. Moreover the boiling point of ethanol, lower than biodiesel, can promote the combustion process.

Biodiesel deriving from vegetable oils has important problems, such as high viscosity and the tendency to polymerize itself, due to high amount of insaturation, which makes it sensitive to oxidative processes and several. This limits its practical use as fuel. All these problems can be solved by partial hydrogenation of double bounds present in the alkyl chains of the corresponding esters

(Scheme II.12); partial hydrogenation that can be carried out using different catalysts under hydrogen flow.

The catalytic upgrading of FAMEs is considered a good method for the production of bio-fuel with high amount of C18:1 (oleic acid methyl ester).

The partial hydrogenation allows overcoming problems related to the oxidative decomposition, or to the formation of totally hydrogenated esters (margarine), that do not have chemical-physical properties useful for bio-fuel.

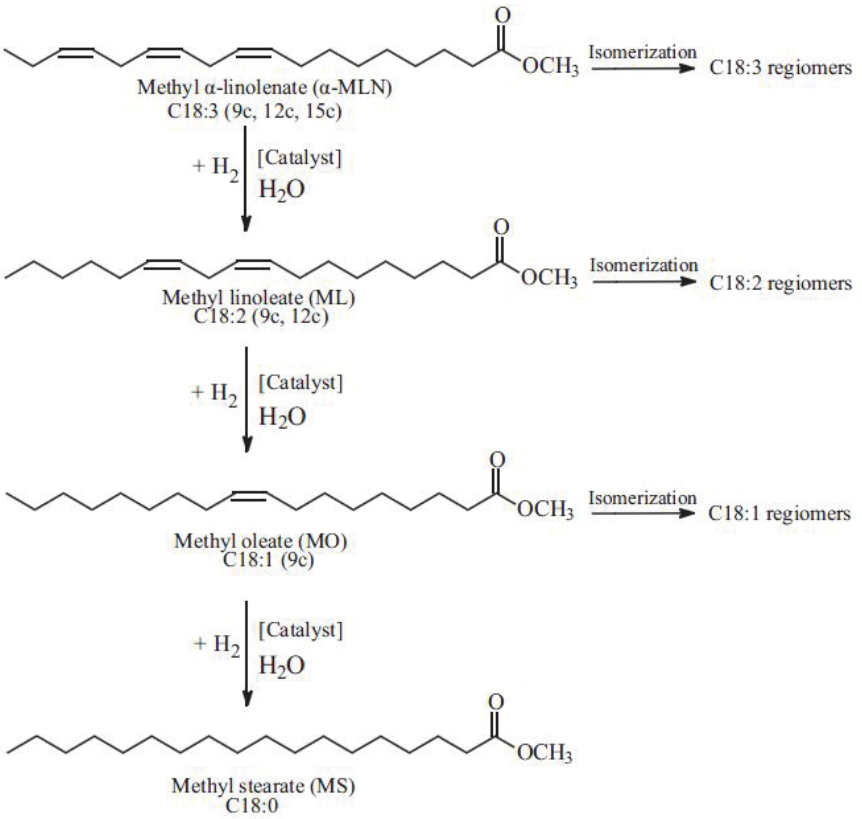

Scheme II.12 - Hydrogenation of FAMEs.

By using Cu/SiO_2 as catalyst for partial hydrogenation of different methyl esters, derived from different biomasses (soybean oil, fish oil), a decreasing of C18:3 (linolenic acid esters) was obtained, while the amount of C18:0 (stearic acid esters) remained almost the same. In the case of fish oil, the 23% of the poly-unsaturated amount was quantitative converted after 10 minutes at 160 °C and under 4 atmospheres of hydro-

gen gas. Also Cu/Al_2O_3 has been successfully tested in similar processes to implement the quality of methyl esters. Other metals were employed as catalysts, in particular Pd, Pt, and Ni were tested and their performances were compared. Palladium resulted to be the best catalyst in the hydrogenation reaction in very short time and under mild conditions. Products obtained with Pd catalyst show good oxidation stability and other favourable properties of cold flow. Palladium nanoparticles have also been used for upgrading biodiesel derived from fish oil with excellent hydrogenation results. The high cost of noble metals greatly reduces their practical use. Nickel, and other transition metals much abundant than Pd in nature, can be used as catalyst obtaining great advantage from the economic point of view.

In this framework we decided to test the catalytic activity and recyclability of Pd-pol and Ni-pol in the partial hydrogenation of FAMEs derived from soybean oil and waste cooking oil (WCO).

2.7.2 Synthesis of FAMEs

The trans-esterification reaction of soybean oil and WCO was carried out in the presence of KOH at 60 °C in methanol under nitrogen atmosphere. After two hours of reaction, the colour of the mixture turned from yellow to red-yellow. The final reaction mixture was left overnight in a separation funnel in order to recover glycerine (red one) and FAMEs (yellow one), as reported in Figure II.12. The FAMEs phase was washed with water and dried over Na_2SO_4. Figure II.13 reports the composition of FAMEs obtained from soybean oil and WCO, respectively.

Figure II.12 - Separation of glycerine (bottom part) and FAMEs (upper part).

FAMEs coming from both sources have very similar composition, being the amount of C18:2 the most relevant in both products. This suggests that they cannot be used before upgrading in order to decrease C18:2 and raise C18:1 amounts, letting C18:0 and C16:0 in the same quantity. In this study we carried out the upgrade of both bio-oils using Pd-pol and Ni-pol as catalysts.

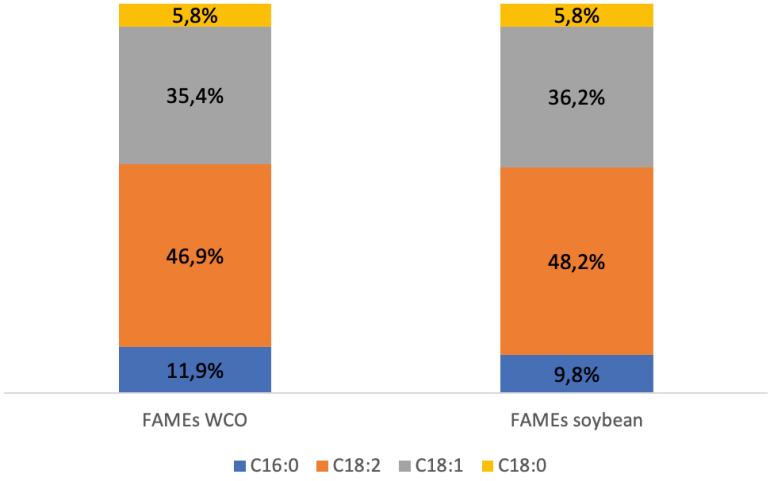

Figure II.13 - Composition of FAMEs obtained from WCO and from soybean oil.

2.7.3 Biodiesel-upgrade catalyzed by Pd-pol and Ni-pol: catalytic investigation

2.7.3.1 Pd-pol catalyzed upgrade of bio-oils

2.7.3.1.1 Synthesis of Pd-pol

The first catalyst employed in this study was Pd-pol. It was synthesized as reported in literature, using a low polymerization temperature, in order to prevent the thermal reduction of metal, which could decrease the catalytic performance of the insoluble material. $PdCl_2$ and NaCl were putted in reaction flask and then deionized water was added. A brown suspension was observed, and it was left under stirring for 30 minutes at 50 °C. The brown solution was converted into a brick red solution which was cooled to room temperature. HAAEMA was added to NaOH solution in water and the mixture was left under stirring for 5 minutes at room temperature. The resulting solution was added to Na_2PdCl_4 solution at room temperature causing the sudden precipitation of red oil. After 30 minutes under stirring the red oil was recovered and washed with water, extracted with CH_2Cl_2 and dried over Na_2SO_4. After filtration, the solvent was removed

and the oil was dissolved in THF in order to add cold pentane with formation of Pd(AAEMA)$_2$ as orange powder which was washed and dried. A copolymerization between the resulting Pd-complex, ethyl methacrylate and ethylene glycol methacrylate was carried out and the corresponding Pd-pol pre catalyst (Scheme II.13) was recovered at the end of polymerization as military green powder (Figure II.14). The percentage of Pd in the final catalyst is about 2.5%, as revealed by elemental analysis. Pd-pol pre catalyst was mainly constituted by Pd(II) centres, which were reduced into polymer supported Pd NPs (the real catalytically active species) during duty, giving rice to Pd-pol (Figure II.15).

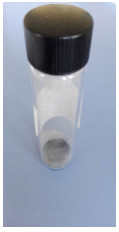

Figure II.14 - Pd-pol pre-catalyst.

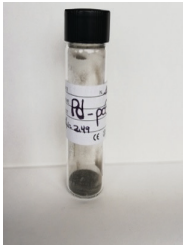

Figure II.15 – Pd-pol catalyst.

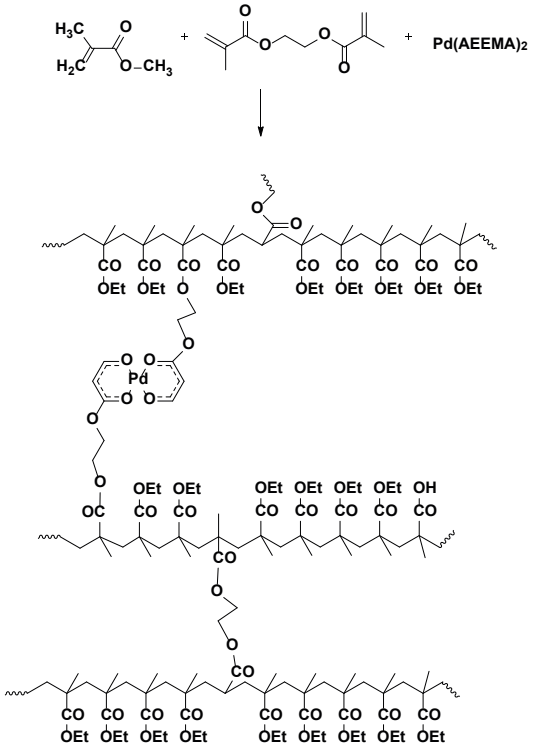

Scheme II.13 - Structure of Pd-pol pre catalyst.

2.7.3.1.2 Catalytic test

The partial hydrogenation of bio-oil was carried out at room temperature under 10 bar of H_2 in methanol in the presence of Pd-pol pre catalyst, using a steel autoclave as the reactor (Figure II.16). During duty, Pd-pol pre catalyst turned into Pd-pol under reaction conditions, due to in situ reduction of Pd(II) centres to Pd(0) (Scheme II.14).

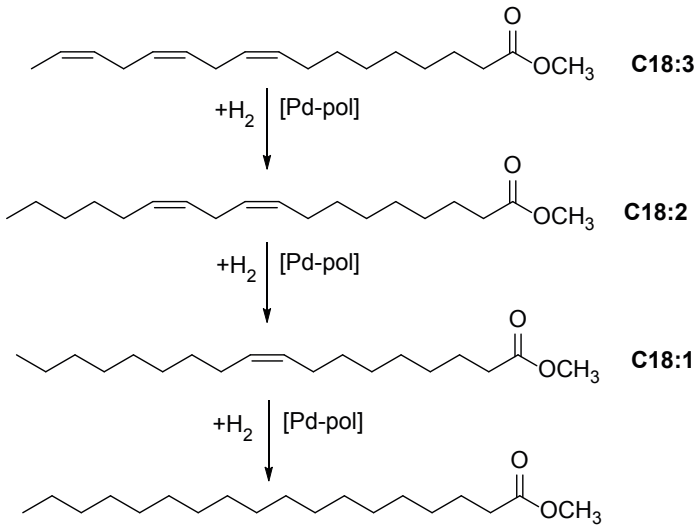

Scheme II.14 - Hydrogenation of poly-unsaturated FAMEs catalyzed by Pd-pol.

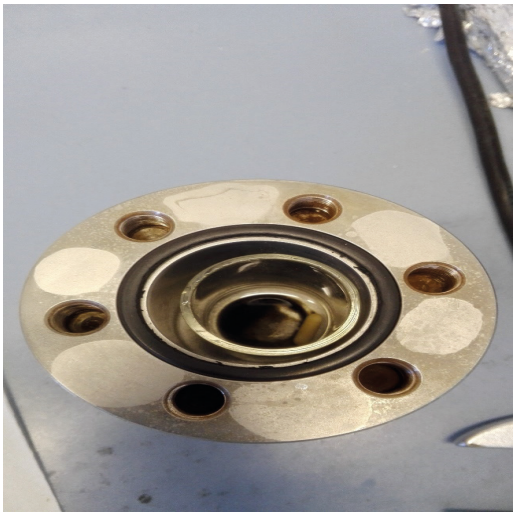

Figure II.16 - Steel autoclave.

The reaction mixture was analyses at time intervals of 5 minutes by GC-MS and GC-FID. Figure II.17 shows that soybean oil FAMEs were almost totally hydrogenated after 30 minutes, when the main product was methyl stereate. The highest concentration of the desired C18:1 methyl esters were obtained after 5 minutes reaction. Afterwards their amount became lower. Same trend was observed also for the hydrogenation of WCO FAMEs (Figure II.18).

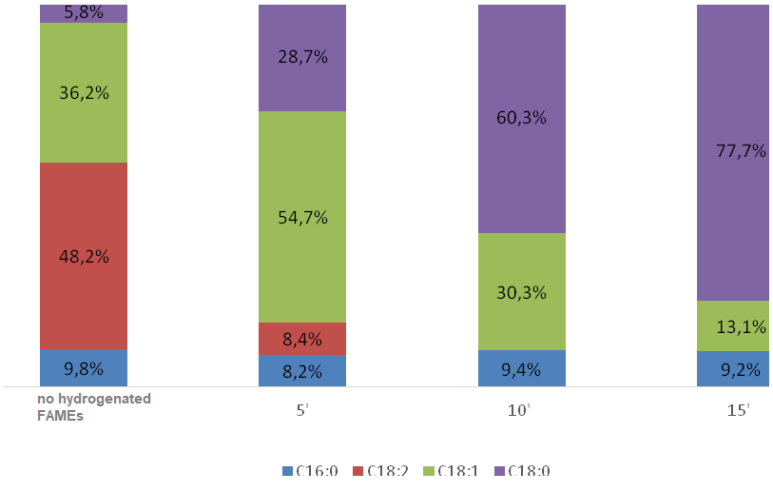

Figure II.17 - Soybean oil FAMEs composition with the time during hydrogenation reaction in the presence of Pd-pol, under 10 bar H_2 at RT in CH_3OH.

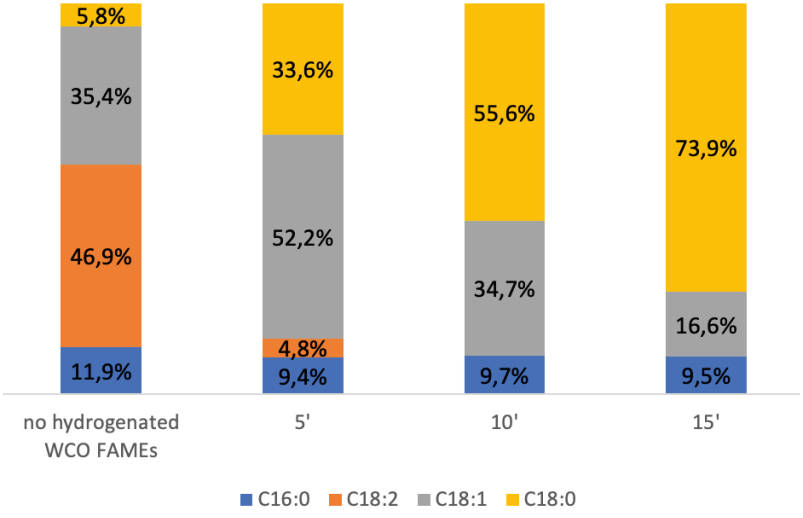

Figure II.18 - WCO FAMEs composition with the time during hydrogenation reaction in the presence of Pd-pol, under 10 bar H_2 at RT in CH_3OH.

2.7.3.1.3 Recyclability of Pd-pol catalyst

The recyclability of Pd-pol was studied for the hydrogenation of both soybean and WCO FAMEs, stopping the reaction after 5 minutes, i.e. when the concentration of the desired C18:1 isomers was as highest as possible (at least in the first run). The catalyst was removed from the reaction mixture, washed with methanol and hexane, and then dried overnight. The recovered catalyst was re-used six times. Figure II.19 shows that the catalyst activity increased with the re-cycles, and its selectivity towards C18:1 product decreased, favouring the formation of totally hydrogenated esters. In fact, the amount of C18:1 isomer passed from 54.7% after the first run to 37.4% after the sixth cycle (17.4% after 10 minutes reaction of the sixth run). As already demonstrated for other Pd-pol hydrogenation reaction,[63,65] the real catalytically active species are Pd NPs formed under reaction conditions for reduction of the polymer supported Pd(II) centres. The amount of these Pd NPs probably increased with the re-cycles, thus enhancing the overall catalytic activity.

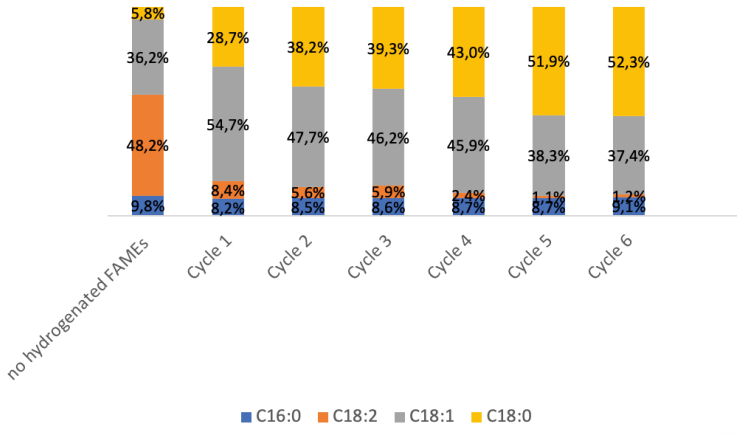

Figure II.19 - Soybean oil FAMEs composition with the re-cycles after hydrogenation reaction in the presence of Pd-pol, under 10 bar H_2 at RT in CH_3OH (t = 5 minutes for each cycle). In the last cycle, the mixture was analysed also after 10 minutes reaction.

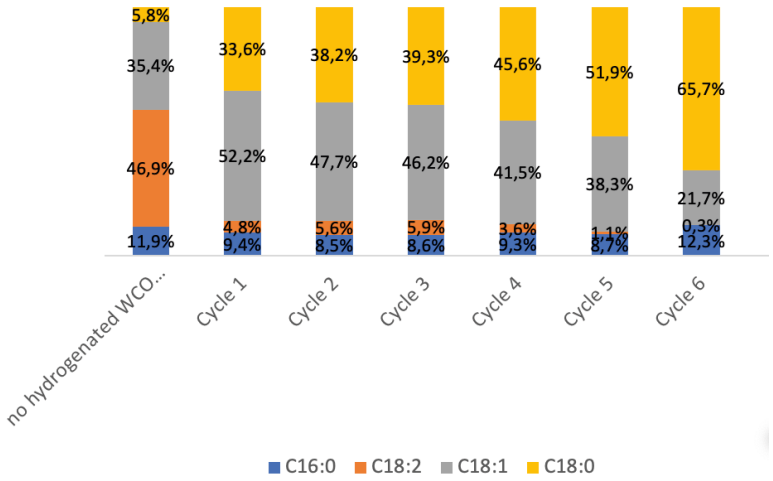

Figure II.20 - WCO FAMEs composition with the re-cycles after hydrogenation reaction in the presence of Pd-pol, under 10 bar H_2 at RT in CH_3OH (t = 5 minutes for each cycle). In the last cycle, the mixture was analysed also after 10 minutes reaction.

2.7.3.2 Ni-pol catalyzed upgrade of bio-oils

2.7.3.2.1 Synthesis of Ni-pol

This study was continued with Ni-pol catalyst, whose synthesis was widely described in the second chapter. Here we report the structure of the polymer supported Ni-complex (Figure II.21) As for the reduction of nitroarenes, the resulting pre-catalyst (green powder on the left in Figure II.22) was thermally reduced under nitrogen flow and a black solid was obtained. It was ground with a mortar and pestle, obtaining a black powder (Figure II.22 on the right). The percentage of Ni in the final catalyst is 5.35% (elemental analysis).

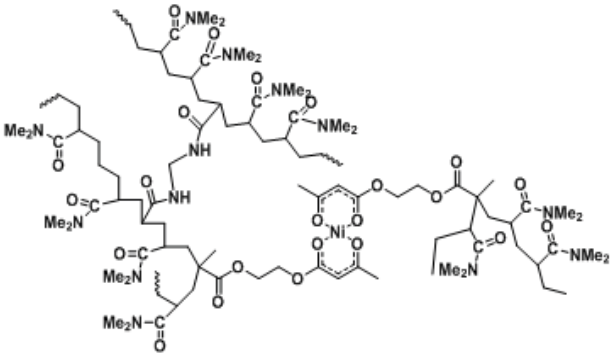

Figure II.21 - Structure of Ni-pol catalyst.

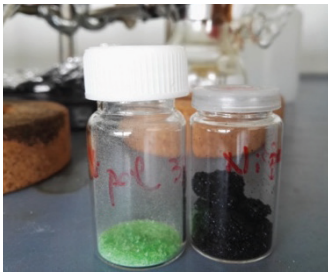

Figure II.22 - On the left: green powder related to polymer supported $Ni(AAEMA)_2$; on the right: black powder related to Ni-pol.

2.7.3.2.2 Catalytic test

Ni-pol was used as catalyst for the upgrade of bio-oils. In this experiment different reaction conditions were used in order to reach satisfactory results (Scheme II.15).

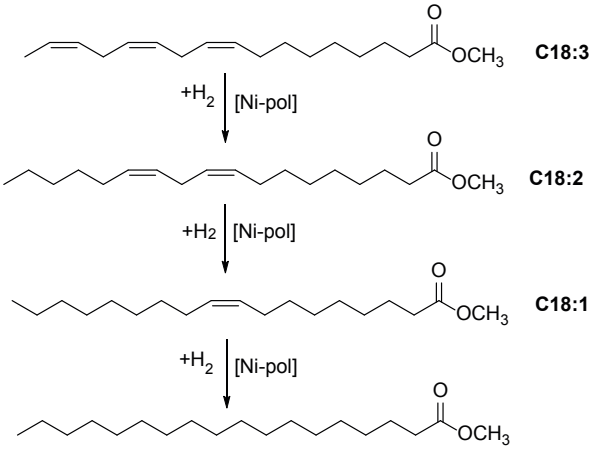

Scheme II.15 - Hydrogenation of poly-unsaturated FAMEs catalyzed by Ni-pol.

By using the same reaction conditions employed for Pd-pol, i.e. under 10 bar H_2, at room temperature and methanol as the solvent, the hydrogenation was negligible even after 16 h reaction. Only increasing the reaction temperature to 100 °C, the hydrogenation of poly-unsaturated FAMEs occurred. Figure II.23 shows that the best result in terms of selectivity towards the desired C18:1 isomers was reached after 10 h reaction (67.1% of C18:1), which is still better than the result obtained in the presence of Pd-pol after 5 minutes reaction in the first run.

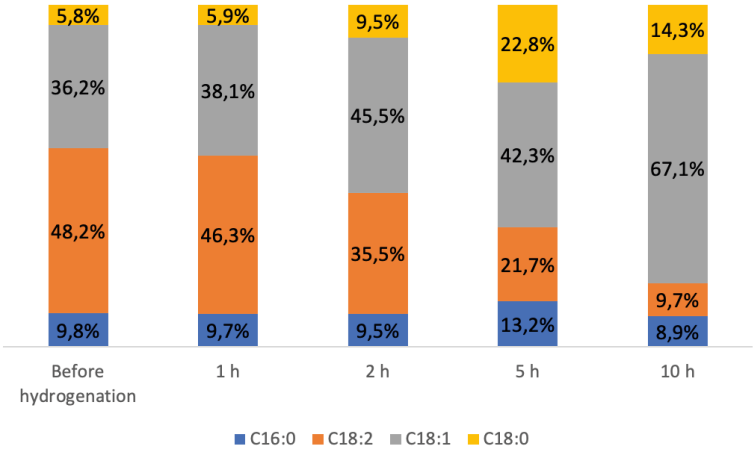

Figure II.23 - Soybean oil FAMEs composition with the time during hydrogenation reaction in the presence of Ni-pol, under 10 bar H_2 at 100 °C in CH_3OH.

2.7.3.2.3 Recycling of Ni-pol catalyst

Under the best catalytic reaction conditions the catalyst was recovered and reused for several times. The catalytic system showed the same activity and selectivity over six cycles (Figure II.24, Figure II.25). After reaction, bio-oil solution was pipetted out and the remaining black catalyst was washed three times with methanol and hexane. The recovered catalyst was used for six subsequent runs, showing an unaltered catalytic activity and selectivity (Figure II.24).

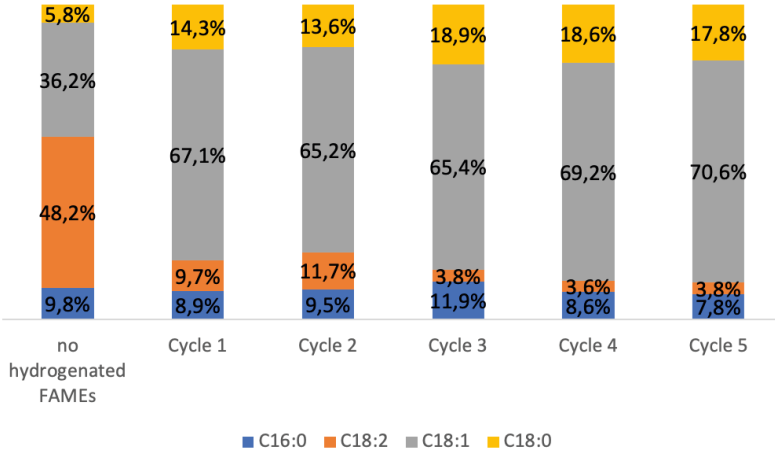

Figure II.24 - Soybean oil FAMEs composition with the re-cycles after hydrogenation reaction in the presence of Ni-pol, under 10 bar H_2 at 100 °**C in** CH_3OH (t = 10 hours for each cycle).

Figure II.25 shows the recyclability of Ni-pol catalytic system for partial hydrogenation of WCO FAMEs. Also for WCO FAMEs the selectivity towards C18:1 isomers is satisfactory.

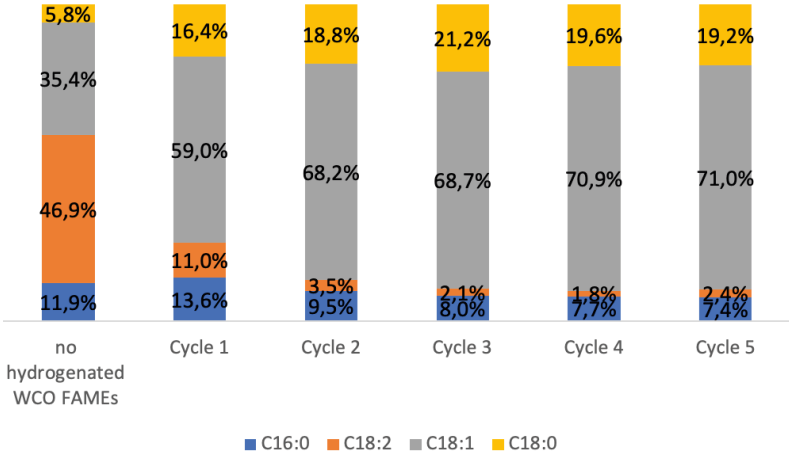

Figure II.25 - WCO FAMEs composition with the re-cycles after hydrogenation reaction in the presence of Ni-pol, under 10 bar H_2 at 100 °C in CH_3OH (t = 10 hours for each cycle).

The obtained results suggest that even if Ni-pol catalyst is less active than the analogues Pd-pol, it is more selective towards products with a single unsaturation, although it requires longer reaction times and higher temperatures compared to Pd-pol based system. Notably, no metal leaching was detected for both Ni-pol and Pd-pol catalytic system.

2.7.4 Conclusions

In conclusion, a new catalyst based on polymer supported Ni nanoparticles (Ni-pol) was synthesised and characterised. It efficiently catalysed the transfer hydrogenation reaction of aromatic nitro compounds with $NaBH_4$ under sustainable conditions (aqueous medium and room temperature), thus avoiding the use of the commonly employed noble metals (Pd, Pt). Similar reaction conditions can be applied also for the synthesis of secondary aromatic amines by one-pot stepwise reductive amination of arylaldehydes with nitroarenes. STEM analyses showed that the active species were metallic Ni nanoparticles ranging from 25 to 70 nm in diameter, stabilized by the polymeric support. Ni-pol was stable in aqueous medium and could be reused for at least five cycles keeping the same activity and selectivity. These occurrences are not trivial for catalysts supporting Ni nanoparticles, because the latter have been found water-sen-

sitive in similar catalytic systems. In addition, Ni-pol catalytic system was selective towards haloanilines, avoiding the hydro-dehalogenation side reaction. Finally, Ni-pol can be also used as active, selective and recyclable catalyst for the partial hydrogenation of poly-unsaturated fatty acid methyl esters for the upgrading of bio-fuels under mild conditions (10 bar of H_2, 60 °C). All the results collected for Ni-catalyst were compared with results reported for the analogous Pd-catalyst. The comparison demonstrated that Ni-catalyst was in any case more selective than the noble metal Pd, although the latter showed higher activity than Ni-pol.

CHAPTER III

Synthesis, characterization and catalytic applications of transition metal nanoparticles embedded in polymeric nanoreactors.

TABLE OF CONTENTS

CHAPTER III

Synthesis, characterization and catalytic applications of transition metal nanoparticles embedded in polymeric nanoreactors.

3.1 Introduction

The ability to construct functionalized polymers with precise architecture, topology, composition, and location of specific functional groups leads to an essentially limitless number of advanced materials with specific functions. In this area, giant steps have been made in recent times by the development of controlled radical polymerization techniques that combine the precision in macromolecular synthesis of living and/or controlled polymerization and the typical advantages of radical polymerization, namely the large choice of polymerizable monomers. [138] Among the functionalities that can be attached to a polymer backbone, phosphines have received little attention with respect to the controlled radical polymerization approach. However, phosphine functionalized polymers have been prepared and studied for quite some time by the catalysis community. For instance, polymer supported rhodium complexes were first described by Manassen and then developed by Grubbs, Capka and Pittman as hydrogenation, hydrosilylation and hydroformylation catalysts. Since then, many polymer supported phosphine ligands have been reported in the literature.

Many strategies have been used to access polymer supported phosphine ligands, mostly leading to materials with anchored triphenylphosphine. In 2013, the research group in which I spent six month during my PhD course described the first generation of triphenylphosphine ligands anchored on linear polystyrene chains by controlled radical polymerization. This synthesis method enables easy tailoring of polymer chain length, with a narrow molecular weight distribution, and phosphine incorporation. They applied these polymer-supported phosphines in Rh-catalyzed 1-octene hydroformylation which provides comparable results to those obtained with PPh_3-containing polymers obtained by other less-controlled methods, in terms of activity and selectivity. This study reveals a slight dependence of the hydroformylation linear/branched selectivity as a function of the amount of PPh_3 in the polymeric catalyst, which should not exceed the maximum quantity of 25%. In 2016 the same research group reported core–shell

structure of the polymers TPP@CCM (TTP = triphenyl phosphine; CCM = core cross-linked micelle) generated by using amphiphilic diblock arms cross-linked at the end of the hydrophobic segment, with anchored ligands in the hydrophobic core outside the cross-linked part. They demonstrated that the phenomenon of molecular migration from one polymer core to another one is very rapid and mostly occurs through direct contact between the particle cores during collisions.[143] In 2017 they reported that triphenylphosphine-functionalized core-shell polymers can be successfully used in the biphasic aqueous hydrogenation of simple alkenes (styrene and 1-octene). The catalytic aqueous phase can be recycled efficiently at least 6 times, but the activities and selectivities are slightly eroded in some cases.[147]

Following these studies on core-shell cross-linked polymer TPP@CCM, I synthesized metal nanoparticles embedded in polymeric nanoreactor and I evaluated their confinement in the polymer spheres. Moreover, I tested their catalytic activity in hydrogenation of acetophenone and styrene.

3.2 Synthesis of polymer TPP@CCM (5% of DPPS)

The controlled radical polymerization technique is a perfect tool to accurately regulate the chain length of each unit. Thus, combining the best attributes of reversible-deactivation radical polymerization (RDRP) in water and the use of polymerization in dispersed media, allows full control of the structure of the final nano-object from the extremity of the stabilizing layer to the very heart of the particle. To achieve spherical nanoparticles as nanoreactors, RAFT copolymerization of methacrylic acid (MAA) with poly(ethylene oxide) methyl ether methacrylate (PEOMA) to generate a P(MAAco-PEOMA) macromolecular RAFT agent (macroRAFT) in water, was accomplished. In a second step and in the same reactor, styrene (S) and 4-diphenylphosphinostyrene (DPPS) were added to generate P(MAA-co-PEOMA)-b-P(S-co-DPPS) amphiphilic block copolymers that self-assembled into nanometric micellar particles. Finally, subsequent addition of a cross-linker, namely, diethylene glycol dimethacrylate (DEGDMA) allowed the generation of stable and core-cross-linked particles that incorporate the triphenylphosphine ligand, referred to as TPP@CCM (Scheme III.1). These particles were evaluated in terms of mass transport of organic molecules across the hydrophilic barrier, coordination chemistry with a typical hydroformylation precatalyst, namely, $[Rh(acac)(CO)_2]$ (acac=acetylacetonate), and efficiency as catalytic nanoreactors.[138]

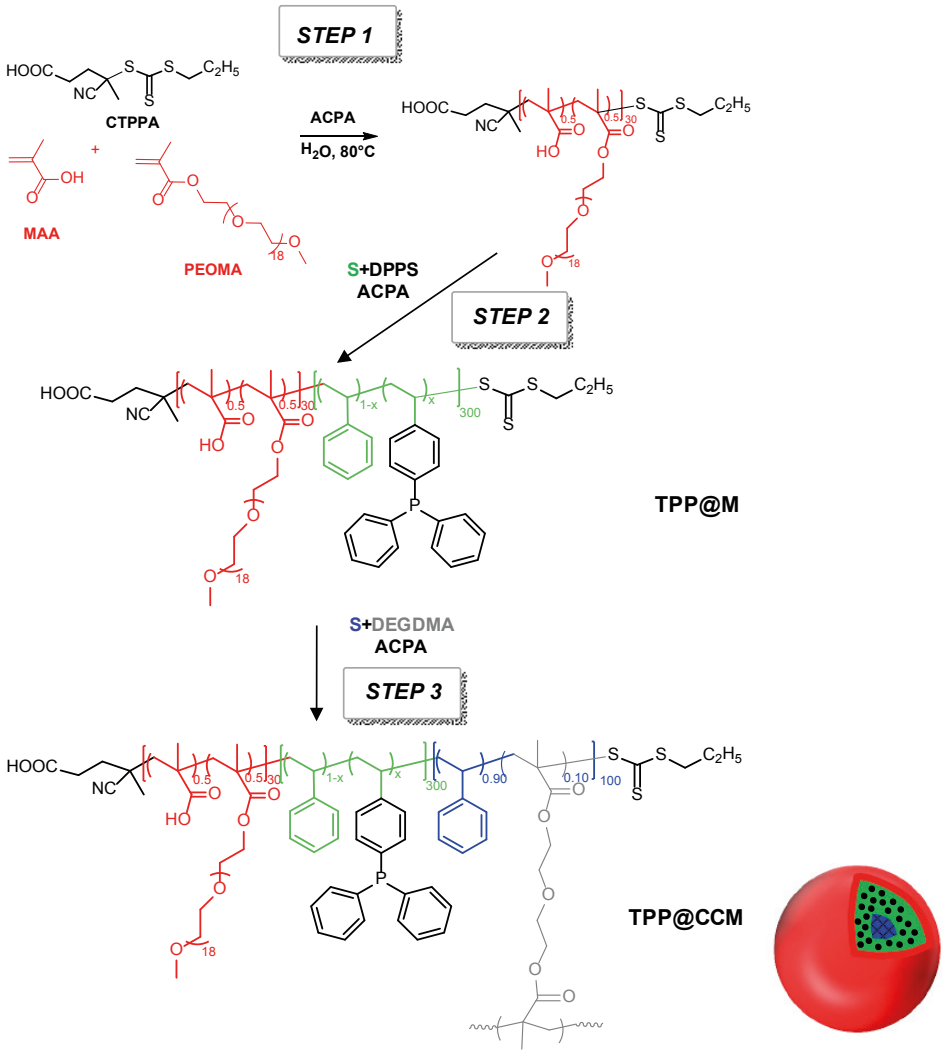

Scheme III.1- Synthesis of the core-cross-linked micelles functionalized with triphenylphosphine (TPP@CCM).

The polymeric nanoreactor TPP@CCM was characterized by ^{1}H NMR, TEM and DLS analysis. The ^{1}H NMR spectrum of the product is reported in Figure III.1. It shows a small resonance at $\delta = 3.5$ (starred resonance in Figure III.1) related to the methylene protons of the PEO side chains. The core proton resonances are not visible in this spectrum because the core is not solvated by DMSO. The incorporation of DPPS was confirmed by ^{31}P{^{1}H} NMR analyses in $CDCl_3/D_2O$ which is a good solvent for the core swelling (Figure III.2). The phosphorus resonance at -5.9 ppm belonging to the free DPPS monomer is missing and it is replaced by a broadened and shifted-resonance

in the polymer structure (δ = -7). The displacement of the $^{31}P\{^{1}H\}$ NMR resonance upon incorporation of the DPPS monomer in the polymer was a convenient probe for monitoring the DPPS consumption during the polymerization. The TPP@CCM latex was synthesized with 5% of DPPS monomers in step 2, which is the most important parameter influencing the metal coordination and the nanoparticles stabilization.

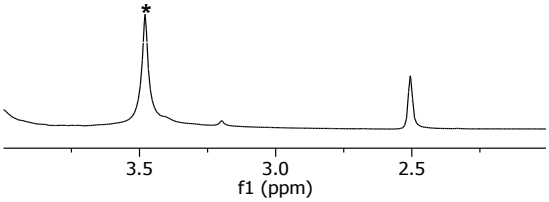

Figure III.1 - ^{1}H NMR of TPP@CCM in DMSO at 298 K.

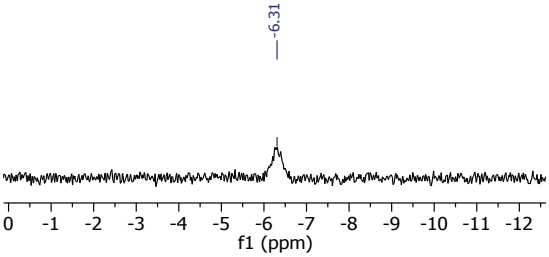

Figure III.2 - $^{31}P\{^{1}H\}$ NMR of TPP@CCM in $CDCl_3/D_2O$ at 298 K.

The particle size of the final dispersion of the cross-linked particles was measured by dynamic light scattering (DLS) in water as well as in THF. The z-average particle sizes Dz are in the range of 70–80 nm in water (Figure III.3). The CCM swell by a factor of about 2 in diameter (8 in volume). The spherical morphology was confirmed by TEM observations (Figure III.4). In all cases the results were conform to those already described in the literature[142].

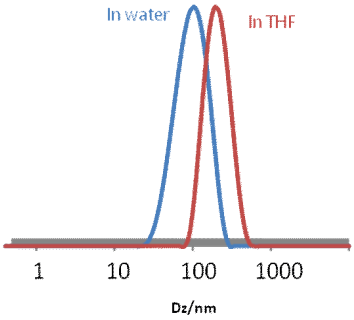

Figure III.3 - DLS in water and THF for the final TPP@CCM.

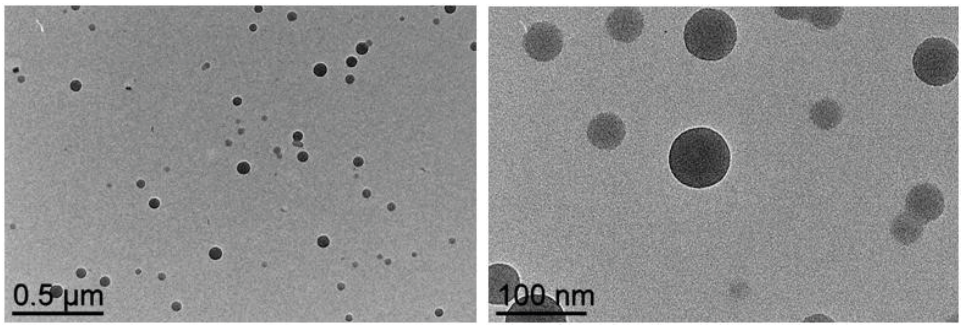

Figure III.4 - TEM micrographs about TPP@CCM with 5% of DPPS.

The phenomena concerning unimolecular core-shell polymers in stable aqueous dispersions were well studied in literature.[138, 317,142]

With the aim at synthesizing metal nanoparticles embedded in the polymer core, the TPP@CCM sample (Figure III.5) was charged with seven metals pre-catalyst.

Figure III.5 - Latex as TPP@CCM synthesized by three step one-pot using RAFT copolymerization.

3.3 Metalation of TPP@CCM (5% of TPP)

3.3.1 Rh coordination inside the nanoreactor (P/Rh= 1)

In order to transfer the precatalyst to the polymer core for the purpose of the NMR investigations, it was necessary to pre-swell the core with toluene. In fact, it was demonstrated that when the pristine unswollen latex was treated with a concentrated precursor's solution, a rapid crystallization of the complex occurs, while the organic phase disappeared due to migration into the polymer core. This revealed that the migration of organic solvent into the core of polymer is faster than that of the metal complex.

The swollen latex was treated with the precursor solution of $[Rh(COD)Cl]_2$, showing a complete transfer of the yellow precursor from the organic phase to the aqueous phase upon stirring for one hour at room temperature. The $^{31}P\{^1H\}$ NMR analysis confirmed that the phosphine functions coordinated to the metal centres in the polymer core to yield [Rh(COD)Cl(TPP@CCM)] (Figure III.6) (broad doublet at 29.58 ppm, d, $J_{Rh,P} = 145.2$ Hz, PPh_3, see Figure III.7) and with complete disappearance of the free phosphine resonance. This was observed using a stoichiometric amount of Rh complex, (Rh/P = 1). In fact, it had already been demonstrated that when half the amount of Rh complex was used (Rh/P = 0.5), neither the free phosphine nor the coordinated phosphine resonance was visible.[317] This is related to a resonance coalescence phenomenon because of rapid phosphine exchange, like for the molecular complex.

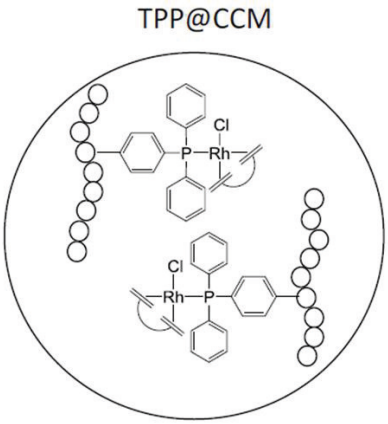

Figure III.6 - Metal coordination by tryphenylphoshine (TPP).

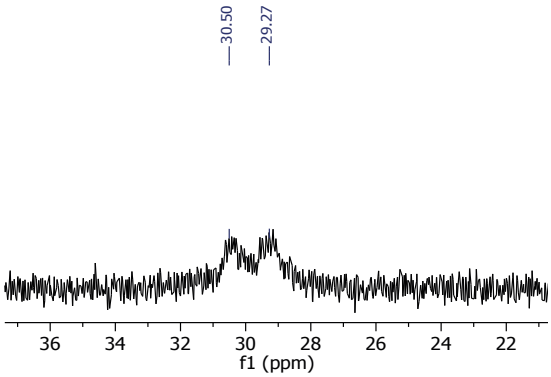

Figure III.7 - $^{31}P\{^{1}H\}$ NMR spectra related to [Rh(COD)Cl(TPP@CCM)] in $CDCl_3$.

DLS measurements of the diluted, toluene-swollen TPP@CCM latex before and after charging with $[Rh(COD)Cl]_2$ show similar Dz value within experimental error, suggesting that metal coordination has a negligible structuring effect on the particle core (Figure III.8).

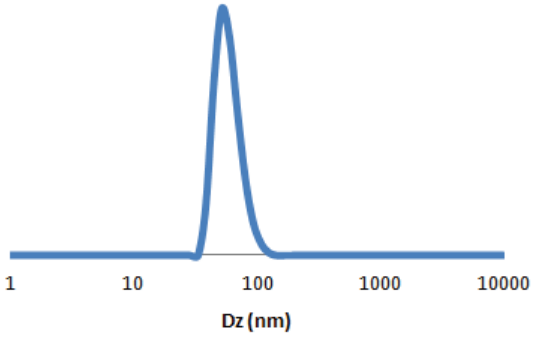

Figure III.8 - DLS in water of [Rh(COD)Cl(TPP@CCM)].

3.3.2 Pd coordination inside the nanoreactor (P/Pd = 1)

The latex loading with the Pd precursor, $[Pd(Cl)(C_3H_5)]_2$ was faster than with the $[Rh(COD)Cl]_2$ complex. The reaction was monitored by $^{31}P\{^{1}H\}$ NMR analysis which showed a coordination peak at 21.1 ppm, *i.e* in the chemical shift range expected for phosphine Pd complexes (Figure III.9, a). DLS analysis suggested that the dimension of the nanocore was not affected by the metal coordination (Figure III.9, b).

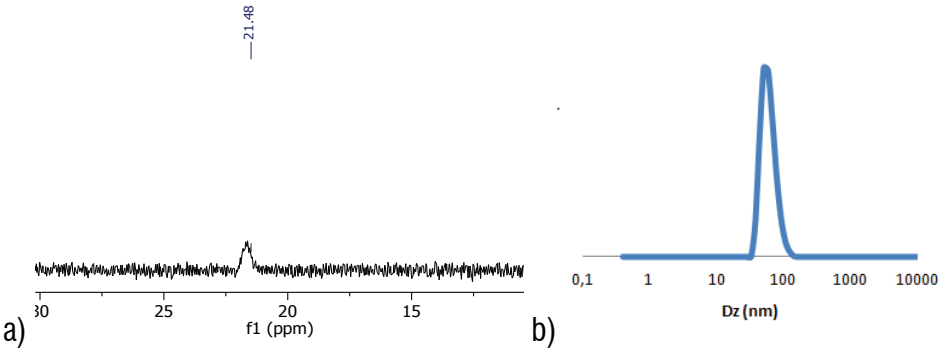

Figure III.9 - a) $^{31}P\{^{1}H\}$ NMR spectra related to [Pd(C_3H_5)Cl(TPP@CCM)] in $CDCl_3$; b) DLS in water of [Pd(C_3H_5)Cl(TPP@CCM)].

3.3.3 Ru coordination inside the nanoreactor (P/Ru= 1)

In the case of Ru loading, [Ru(p-cymene)Cl_2]$_2$ was used as precursor. The coordination of Ru metal was observed by colour change of the latex from white to pink. The $^{31}P\{^{1}H\}$ NMR spectrum showed a broad signal at 23.1 ppm related to phosphine coordinated to Ru, consistent with what reported in the literature for soluble phosphine Ru complexes (Figure III.10, a). DLS analysis confirmed what was observed for the Rh and Pd-latexes (Figure III.10, b).

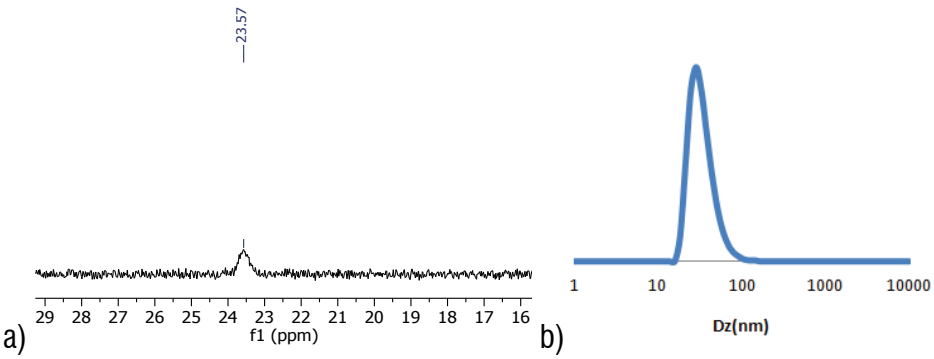

Figure III.10 - a) $^{31}P\{^{1}H\}$ NMR spectra related to [Ru(p-cymene)Cl_2(TPP@CCM)] in $CDCl_3$; b) DLS in water of [Ru(p-cymene)Cl_2(TPP@CCM)].

3.3.4 Ir coordination inside the nanoreactor (P/Ir = 1)

The loading with Ir was achieved using $[Ir(Cl)(COD)]_2$. After 4 h reaction between the Ir solution and the latex occurred, the signal detected by $^{31}P\{^1H\}$ NMR at 21.1 ppm (Figure III.11, a), confirmed the metal loading. The particle diameter size distribution was not affected by the metal loading (Figure III.11, b).

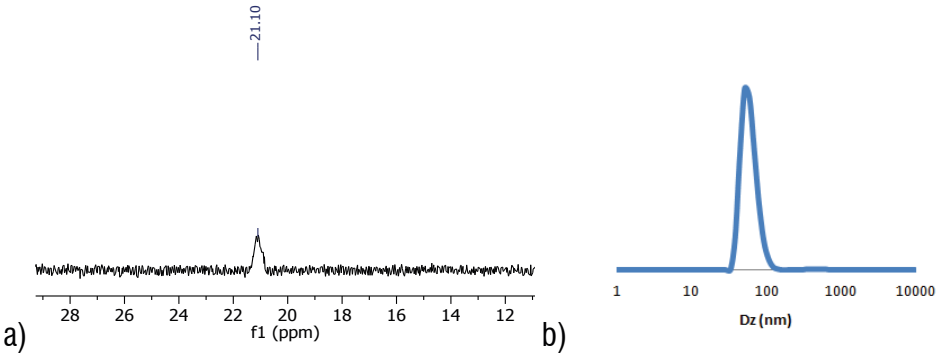

Figure III.11 - a) $^{31}P\{^1H\}$ NMR spectra related to [Ir(Cl)(COD)(TPP@CCM)] in $CDCl_3$; b) DLS in water of [Ir(Cl)(COD)(TPP@CCM)].

3.3.5 Pt coordination inside the nanoreactor (P/Pt = 1)

For Pt loading, a solution of $[Pt(COD)Br_2]$ was left under stirring with the latex, causing the change of the polymer colour from white to green-yellow. The $^{31}P\{^1H\}$ NMR spectrum did not show any signal even at low temperature (Figure III.12, a) presumably due to fluxional behaviour. The DLS results are consistent with unchanged nanocore size distribution after Pt loading (Figure III.12, b).

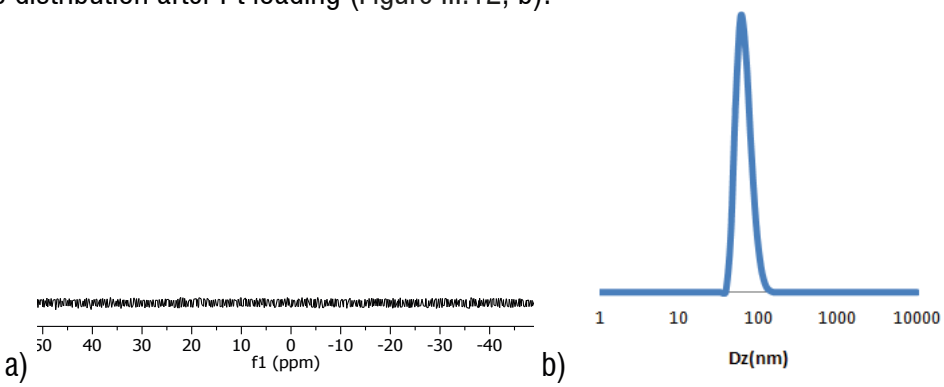

Figure III.12 - a) $^{31}P\{^1H\}$ NMR spectra related to $[Pt(COD)Br_2(TPP@CCM)]$; b) DLS in water of $[Pt(COD)Br_2(TPP@CCM)]$.

A different Pt-precursor, $(C_6H_5CN)_2PtCl_2$, was also used in the platination of the nanoreactor. The same results as for $[Pt(COD)Br_2]$ were obtained (Figure III.13, a). The particles size remains unchanged, as shown in Figure III.13, b.

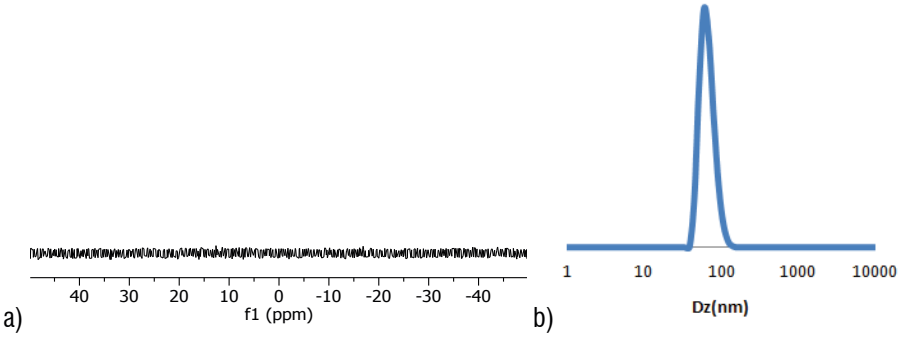

Figure III.13 - a) $^{31}P\{^1H\}$ NMR spectra related to $[(C_6H_5CN)_2PtCl_2(TPP@CCM)]$; b) DLS in water of $[(C_6H_5CN)_2PtCl_2(TPP@CCM)]$.

3.3.6 Au coordination inside the nanoreactor (P/Au = 1)

For gold loading, $(CH_3)_2SAuCl$ solution was reacted for 3 h with the latex. The $^{31}P\{^1H\}$ NMR spectrum (Figure III.14, a) shows the coordination peak at 32.4 ppm, consistent with similar phosphine gold complexes. The DLS is reported in Figure III.14, b.

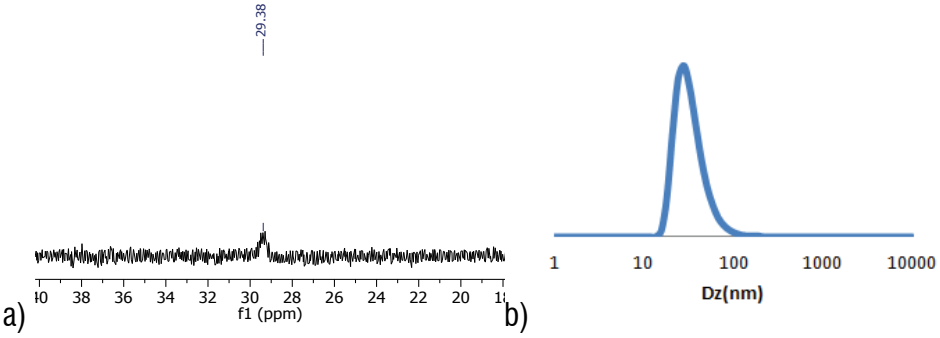

Figure III.14 - $^{31}P\{^1H\}$ NMR spectra related to $[(CH_3)_2SAuCl(TPP@CCM)]$; on the right: DLS in water of $[(CH_3)_2SAuCl(TPP@CCM)]$.

3.4 Confinement study of nanoparticles in the nanoreactor

3.4.1 Synthesis and characterization of metal nanoparticles in TPP@CCM (5% DPPS)

In order to synthesize metal nanoparticles embedded in the polymeric nanoreactors, several tests were carried out under different reaction conditions. The results demonstrated that metal reduction occurs only under hydrogen pressure. Using $NaBH_4$ as reducing agent, the nanoparticles formation was not observed, due to the acid functions of the polymer located on the shell, which react with the reductant before it reaches the metal centres in the polymer core. The metal reduction to produce NPs was carried out in a steel autoclave under 20 bar hydrogen pressure, for 20 h at different temperature depending on the metal (Scheme III.2, Scheme III.3). The addition of toluene solution of triethylamine (NEt_3) promotes the nanoparticles formation.

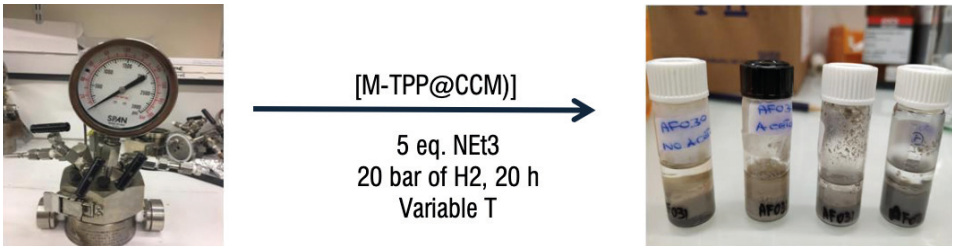

Scheme III.2 - Synthesis of metal nanoparticles under H_2 in autoclave.

$$[Rh(COD)Cl(TPP@CCM)] \xrightarrow[NEt_3,\ 25°C]{H_2\ (20\ bar)} [Rh\text{-}NPs(TPP@CCM)]$$

$$[Pd(COD)Cl(TPP@CCM)] \xrightarrow[25°C \text{ or } 60°C \text{ or } 90°C]{H_2\ (20\ bar)} [Pd\text{-}NPs(TPP@CCM)]$$

$$[Ru(p\text{-}cymene)(Cl)_2(TPP@CCM)] \xrightarrow[25°C]{H_2\ (20\ bar)} [Ru\text{-}NPs(TPP@CCM)]$$

$$[Ir(COD)Cl(TPP@CCM)] \xrightarrow[25°C]{H_2\ (20\ bar)} [Ir\text{-}NPs(TPP@CCM)]$$

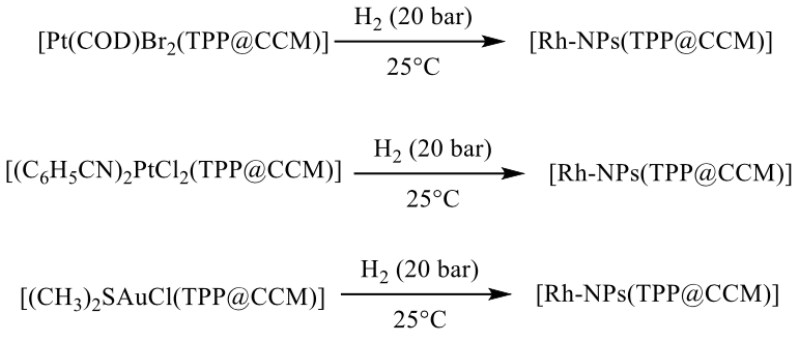

Scheme III.3 - Formation of metal nanoparticles in TPP@CCM.

At the end of the reduction two different phases were observed. The upper phase was the organic phase as a toluene solution; the bottom phase was the water phase, in which the NPs, embedded into the nanoreactors, are confined. The upper organic phase was colourless in all cases, suggesting that no metal leaching occurred and that NPs were confined in the core of the nanoreactors. The upper phase was removed by pipette and the water phase containing the nanoreactor-embedded NPs were directly tested as catalyst for the hydrogenation reactions. All new catalysts were characterized by TEM and DLS analyses, before and after the catalytic application. The DLS analyses demonstrated that the core size distribution of CCMs did not change after metal reduction and catalytic tests.

The TEM analyses showed that unfortunately the NPs synthesised will each metal were never confined in the core of the micelle core (from Figure III.15 to Figure III.34). In some cases, migration of the metal NPs from a core to another was observed and NPs agglomeration was always found.

3.5 TEM analyses

3.5.1 [Rh-NPs(TPP@CCM)]

The CCM-stabilized rhodium nanoparticles [Rh-NPs(TPP@CCM)], were synthesized by hydrogen reduction of [Rh(COD)Cl(TPP@CCM)] at 25 °C. After the reduction the colour of the latex changed from yellow (phosphine rhodium complex) to black (Rh NPs). The [Rh-NPs(TPP@CCM)] TEM images show that the NPs are agglomerated together; indicating that the Rh complex had migrated from a core to another one (Figure III.15).[146] In fact, the TEM images show that several nanocores are completely empty. Moreover, the Rh NPs were not confined inside the polymer sphere but seem to be localised on the shell.

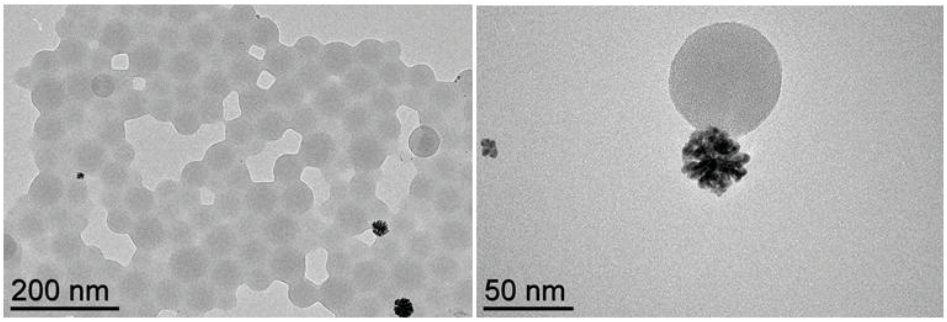

Figure III.15 - TEM micrographs of [Rh-NPs(TPP@CCM)] synthesized at 25 °C under 20 bar of H_2 for 20 h.

3.5.2 [Pd-NPs(TPP@CCM)]

The reduction of Pd centres was optimized at 60 °C because at 25 °C the metal reduction was not quantitative (the latex colour was grey instead of black). The TEM analyses showed that nanoparticles synthesized at 25 °C (Figure III.16) are similar to those obtained 60 °C (Figure III.17). In both cases, the formation of aggregates was evident, even if only at 25 °C they were formed outside of the latex.

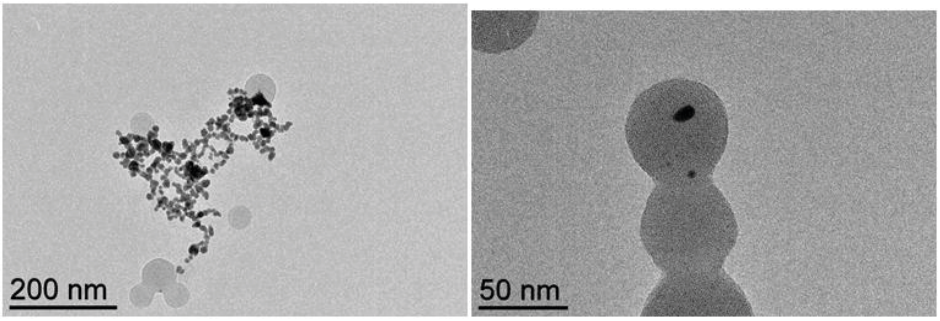

Figure III.16 - TEM micrographs of [Pd-NPs(TPP@CCM)] synthesized at 25 °C under 20 bar of H_2 for 20 h.

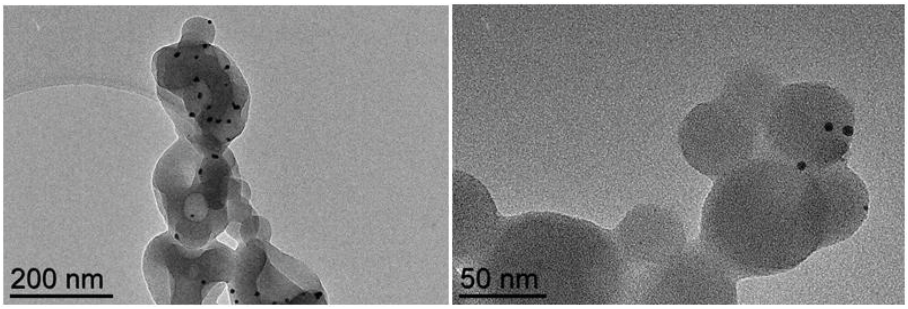

Figure III.17 - TEM micrographs of [Pd-NPs(TPP@CCM)] synthesized at 60 °C under 20 bar of H_2 for 20 h.

The reduction was also carried out in the absence of hydrogen, in air, at 80 °C by using an excess of organic base NEt_3, overnight. Black latex was obtained. The TEM pictures of the obtained NPs in CCMs (Figure III.18) show smaller Pd NPs than those obtained under H_2. In this case, however, the Pd NPs distribution within the polymer seems more uniform than the in the previous ones.

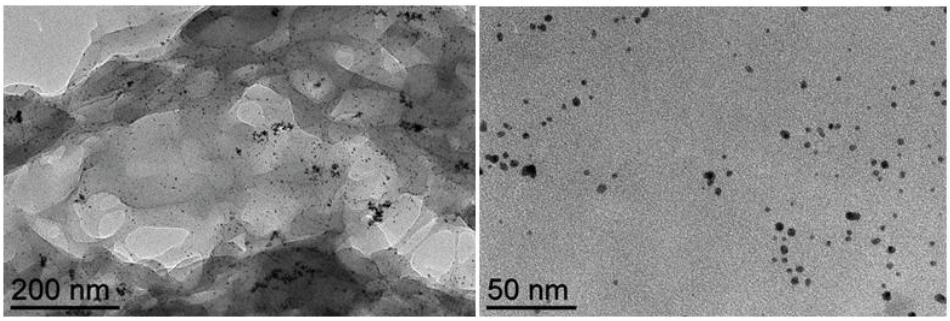

Figure III.18 - TEM micrographs of [Pd-NPs(TPP@CCM)] synthesized at 80 °C in air with excess of NEt_3, over night.

3.5.3 [Ru-NPs(TPP@CCM)]

The reduction reaction of the Ru(p-cymene)$(Cl)_2$(TPP@CCM)] was carried out at 40, 60 and 90 °C. At 25 °C and 40 °C the Ru reduction did not occur (the latex pink colour did not change). The TEM images of the black CCMs obtained at 60 °C and 90 °C revealed that the Ru NPs formed at 60 °C (Figure III.19) are better dispersed than those obtained at 90 °C (Figure III.20). The latter one, in fact, show again quite clearly the phenomenon of metal migration and aggregation like those Rh and Pd (see above).

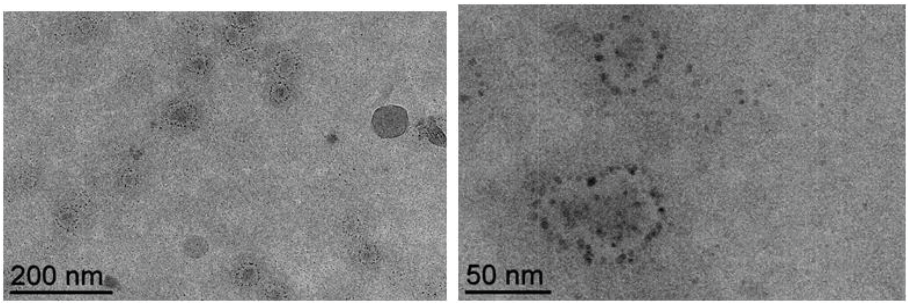

Figure III.19 - TEM micrographs of [Ru-NPs(TPP@CCM)] synthesized at 60 °C under 20 bar of H_2 for 20 h.

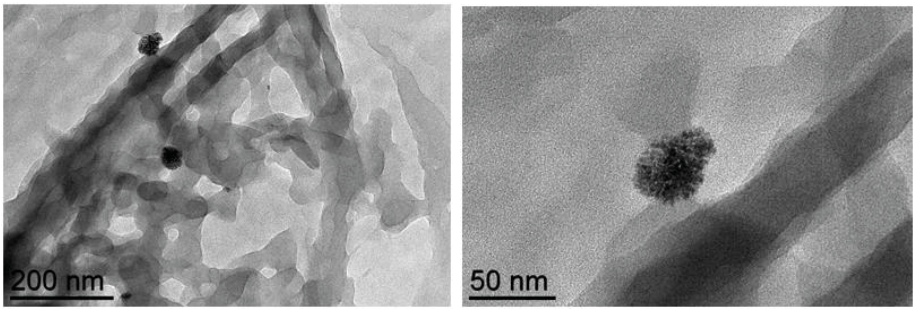

Figure III.20 - TEM micrographs of [Ru-NPs(TPP@CCM)] synthesized at 90°C under 20 bar of H_2 for 20 h.

3.5.4 [Ir-NPs(TPP@CCM)]

At 25 °C the reduction of the Ir centres did not occur. Like for the Ru NPs, the Ir NPs were synthesised at 40, 60 and 90 °C. The TEM pictures (Figure III.21, Figure III.22, Figure III.23) suggested that the Ir NPs were not confined inside the CCMs core.

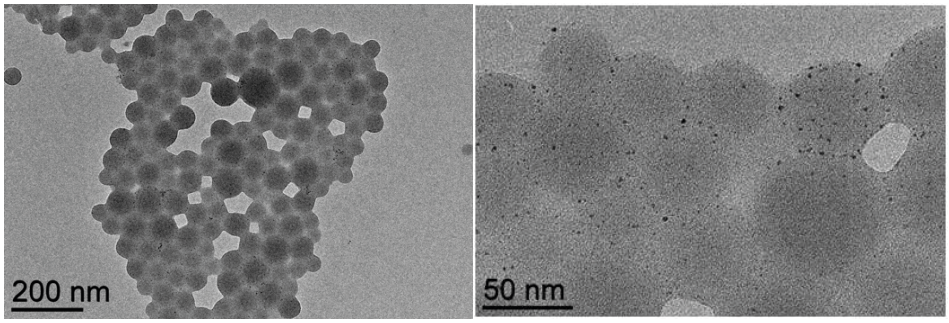

Figure III.21 - TEM micrographs of [Ir-NPs(TPP@CCM)] synthesized at 40 °C under 20 bar of H_2 for 20 h.

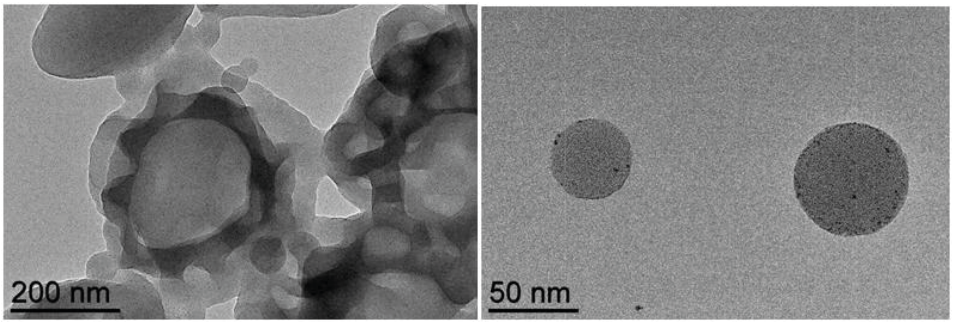

Figure III.22 - TEM micrographs of [Ir-NPs(TPP@CCM)] synthesized at 60 °C under 20 bar of H_2 for 20 h.

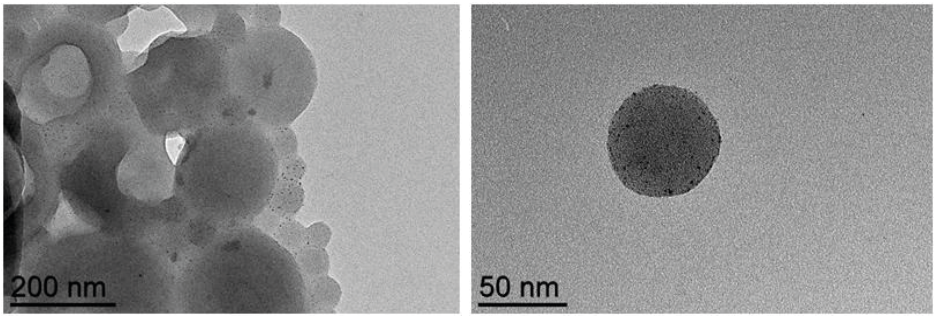

Figure III.23 - TEM micrographs of [Ir-NPs(TPP@CCM)] synthesized at 90 °C under 20 bar of H_2 for 20 h.

3.5.5 [Pt-NPs(TPP@CCM)]

The reduction of the yellowish [Pt(COD)Br_2(TPP@CCM)] latex yielded a completely black product after 20 h under 20 bar of H_2 at room temperature. The TEM images of the obtained NPs showed the formation of agglomerated Pt NPs, in addition to uniformly distributed small size metal NPs (Figure III.24).

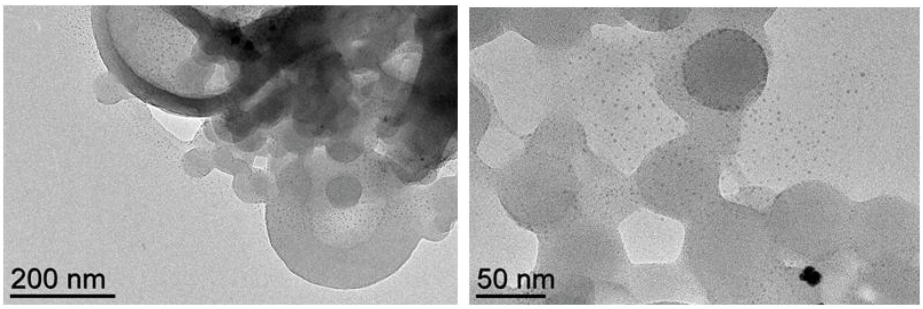

Figure III.24 - TEM micrographs of [Pt-NPs(TPP@CCM)] synthesized at 25 °C under 20 bar of H_2 for 20 h.

The $[(C_6H_5CN)_2PtCl_2$(TPP@CCM)] platinum complex was also treated at 25 °C under 20 bar of hydrogen, but no reduction occurred in this case. Treatment at 40 and 60 °C, however, led to the formation of big metal nanoparticles at 40 °C (Figure III.25) and smaller ones at 60 °C (Figure III.26).

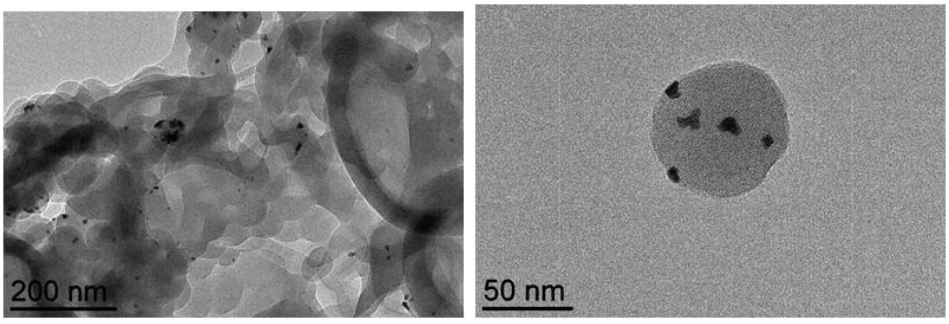

Figure III.25 - TEM micrographs of [Pt-NPs(TPP@CCM)] synthesized at 40 °C under 20 bar of H_2 for 20 h.

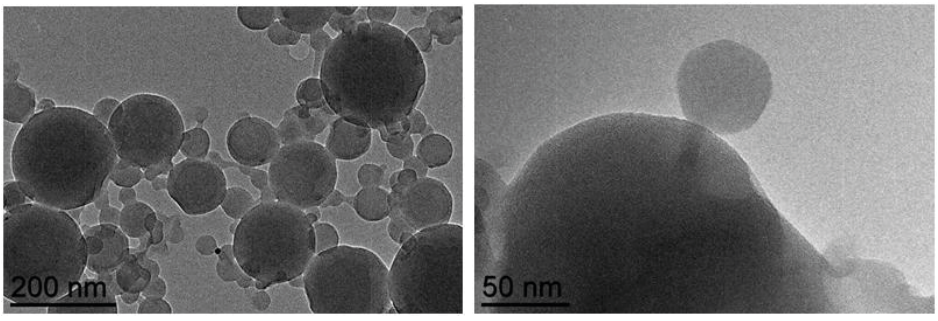

Figure III.26 - TEM micrographs of [Pt-NPs(TPP@CCM)] synthesized at 60 °C under 20 bar of H_2 for 20 h.

3.5.6 [Au-NPs(TPP@CCM)]

Attempts to synthesise Au NPs were carried out at 25 °C and 40 °C, but in neither cases did Au reduction occur (as suggested by the latex colour). The reduction tem-

perature was then increased to 60 and 90 °C. At 90 °C a macroscopic agglomeration was observed, so the NPs were not used in the catalytic hydrogenations. The colour of the latex of the CCM-supported Au NPs obtained at 90 °C and at 60 °C was similar, suggesting that the reduction was complete also at the lower temperature. The NPs formed at 60 °C appeared as large size nanoparticles (Figure III.27).

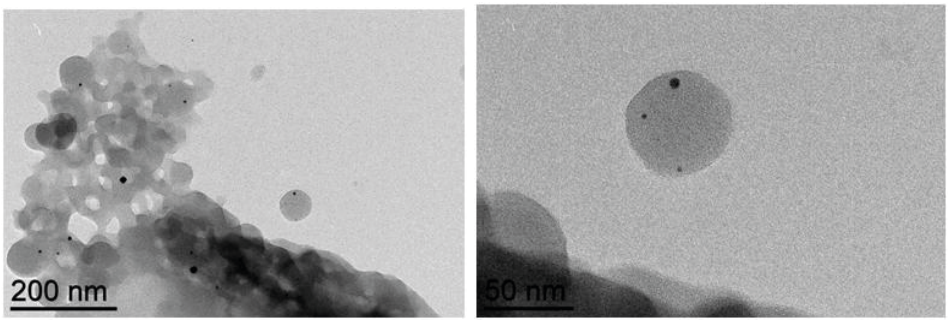

Figure III.27 - TEM micrographs of [Au-NPs(TPP@CCM)] synthesized at 60 °C under 20 bar of H_2 for 20 h.

All the metal nanoparticles synthesized showed same tendency to form agglomerates. This is due to the interpenetration phenomenon between the polymer cores. This provides some polymer sphere completely empty, so the homogeneous distribution of metal nanoparticles is not guaranteed.

3.5.7 TEM analysis after catalysis

All the synthesised [M-NPs(TPP@CCM)], obtained as black latexes, were applied in the hydrogenation reaction of acetophenone under 20 bar of hydrogen, for 20 h at 25, 40 and 90 °C in order to investigate if and how the NPs change their morphology and distribution. Less black aqueous polymer solution containing NPs were applied directly under critical reaction condition (90 °C). All the NPs were characterized by TEM analysis. Images show two relevant phenomena: the aggregation of metal NPs, already observed before catalysis, (some examples are reported in Figure III.28 and Figure III.29) and the migration on the shell of CCMs (some examples are reported in Figure III.31, Figure III.32, Figure III.33). In few cases big NPs were formed, localized on the shell (Figure III.34). With the aim to avoid both phenomena and to obtain metal NPs homogenously distributed and confined in all the spheres of polymer, we adopted different strategies. First was considered that the ratio P/M should influence the NPs confinement; this suggests to synthesized metal complex with an excess of phosphine, such as P/M = 4. Second strategy consists of synthesized new polymer with 20% of DPPS in the core.

An increasing amount of DPPS in the polymer core can better stabilized NPs in the core, avoiding migration on the polymer shell. Thirst strategy provides to synthesise metal NPs in nanoreactor containing cationic outer shell. All the strategies developed were done on the Rh NPs due to a well-known chemistry of this metal in the polymeric nanoreactor TPP@CCM. Moreover the strategy should apply to other metals without trouble.

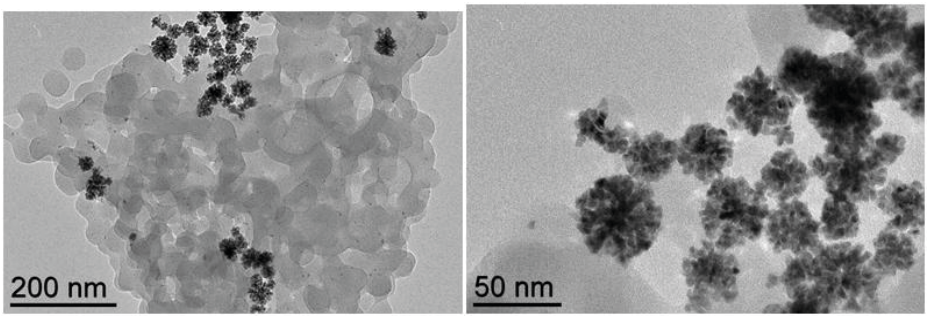

Figure III.28 - TEM micrographs of [Rh-NPs(TPP@CCM)] synthesized at 25 °C; applied at 90 °C, under 20 bar of H_2 for 20 h.

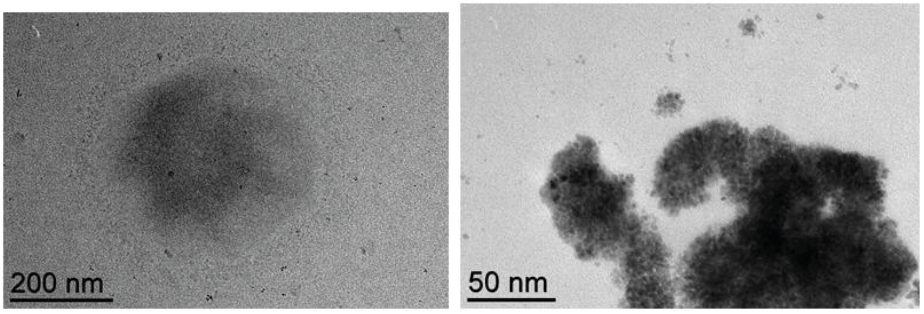

Figure III.29 - TEM micrographs of [Ru-NPs(TPP@CCM)] synthesized at 60 °C, applied at 90 °C, under 20 bar of H_2 for 20 h.

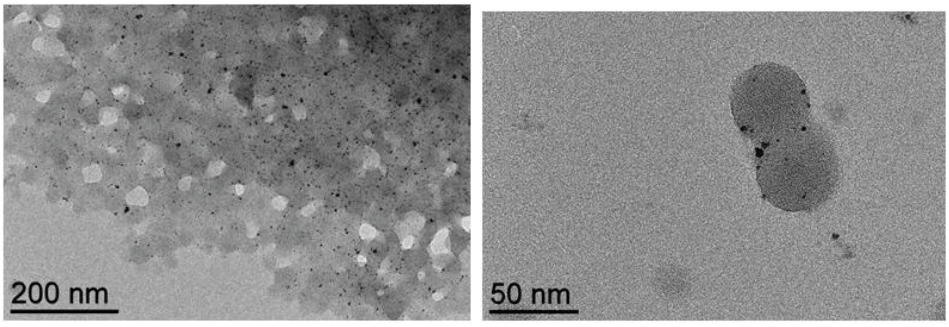

Figure III.30 - TEM micrographs of [Ru-NPs(TPP@CCM)] synthesized at 40 °C, applied at 90 °C, under 20 bar of H_2 for 20 h.

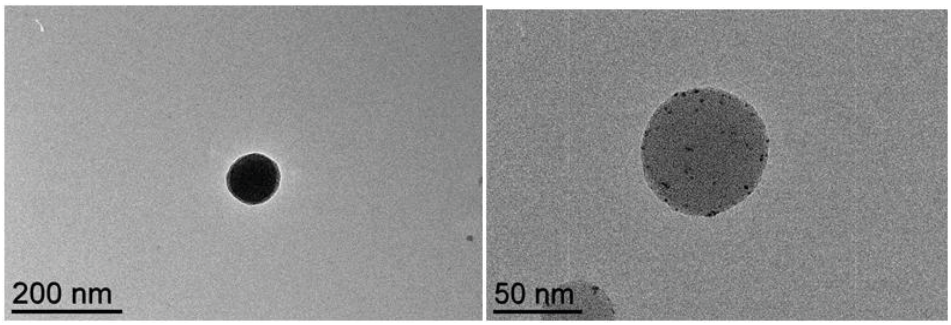

Figure III.31 - TEM micrographs of [Ir-NPs(TPP@CCM)] synthesized at 40 °C, applied at 90 °C, under 20 bar of H_2 for 20 h.

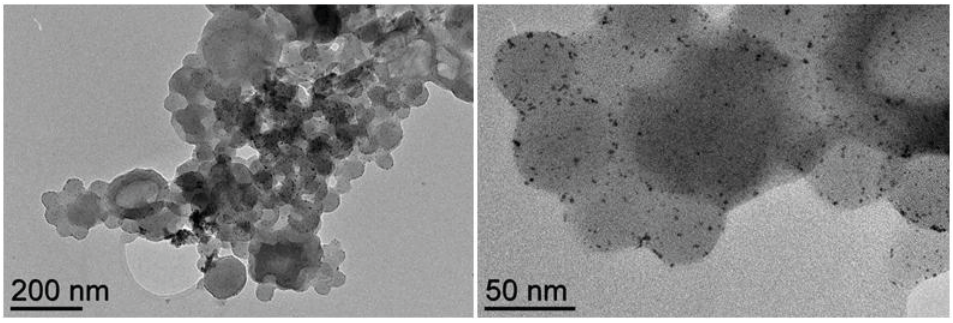

Figure III.32 - TEM micrographs of [Ir-NPs(TPP@CCM)] synthesized at 90 °C, applied at 90 °C, under 20 bar of H_2 for 20 h.

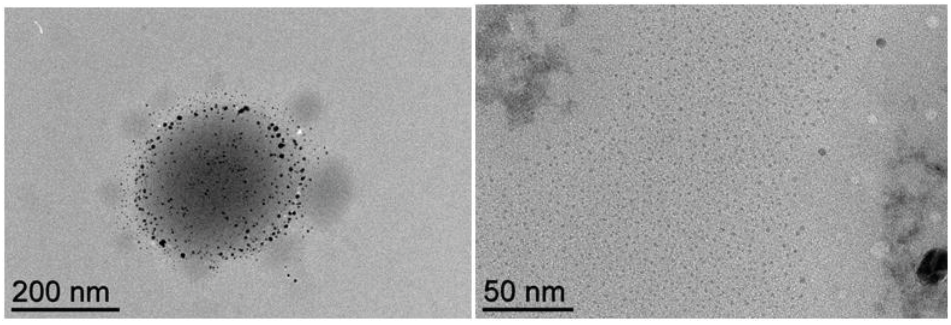

Figure III.33 - TEM micrographs of [Pt-NPs(TPP@CCM)] ([Pt(COD)Br_2(TTP@CCM)] complex) synthesized at 25 °C, applied at 90 °C, under 20 bar of H_2 for 20 h.

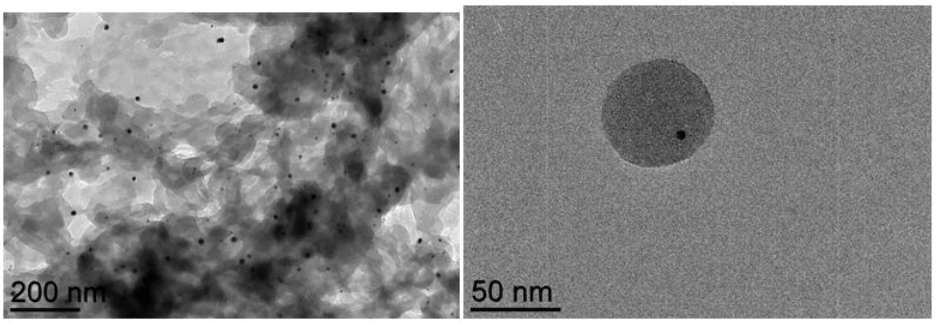

Figure III.34 - TEM micrographs about Au-NPs synthesized at 60 °C, applied at 40 °C, under 20 bar of H_2 for 20h.

3.6 Strategy for embedded metal nanoparticles in polymeric nanoreactor

The following strategies applied aiming at obtaining metal NPs confined in the nanoreactor cores were employed using Rh-TPP@CCM, as model catalyst.

3.6.1 First strategy: Change of ratio P/M

The rhodium polymeric complex was synthesized using the same procedure described in paragraph 3.3.1, except for decreasing the amount of $[Rh(COD)Cl]_2$ employed for the loading of the polymeric ligand, i.e. in the P/Rh molar ratio = 4. The $^{31}P\{^1H\}$ NMR spectrum did not show the resonance related to the metal coordination (Figure III.35).This might be due to a rapid exchange between metal and phosphine which did not allow the signal to be detected. The coordination was confirmed by the change in colour of both the organic phase and the aqueous phases. The colourless organic solution was removed, and the CCM latex was directly used for the nanoparticles synthesis (Scheme III.4), as previously reported.

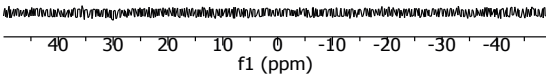

Figure III.35 - $^{31}P\{^1H\}$ NMR spectra related to [(Rh(COD)Cl)TPP@CCM] (5% DPPS).

The reduction occurred at 60 °C, as indicated by the black colour of the CCM latex. The synthesized NPs were analyzed by TEM analysis, which confirm the formation of a high number of metal nanoparticles, better dispersed than NPs having P/Rh = 1 but not confined in the polymer sphere (Figure III.36). After the catalytic applications, in hydrogenation reaction of acetophenone at 25 °C, the NPs show the same distributions as before catalysis (Figure III.37). In both samples the polymer spheres are not well visible maybe because of a spontaneous reorganization of the polymer.

Scheme III.4 - Process for synthesis of Rh NPs inside TPP@CCM in ratio P/Rh = 4, starting from latex.

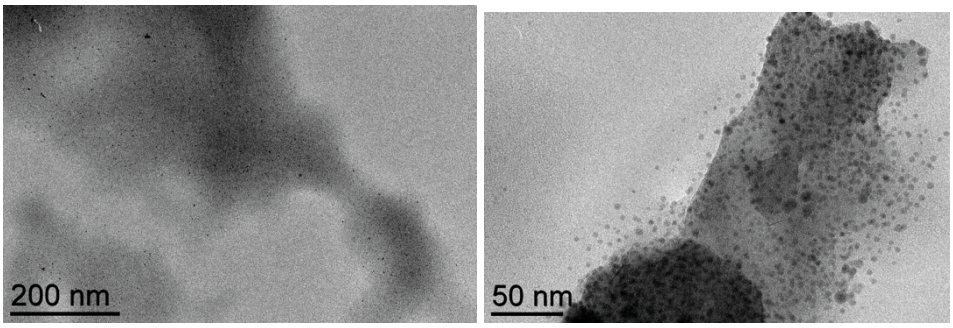

Figure III.36 - TEM micrographs of [Rh-NPs(TPP@CCM)] (P/Rh = 4 in TPP@CCM with 5% DPPS) synthesized at 60 °C.

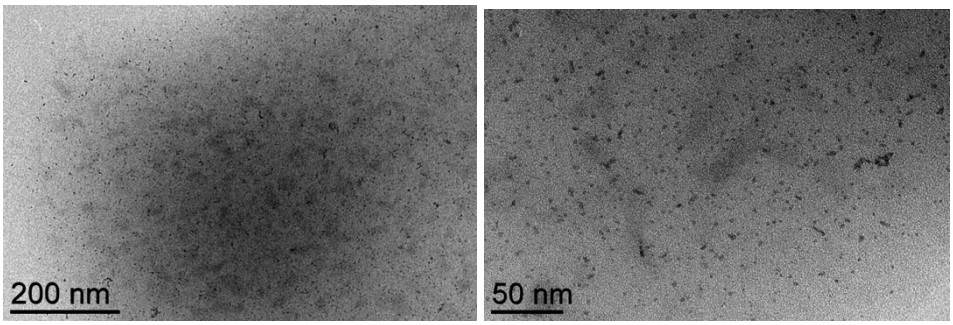

Figure III.37 - TEM micrographs of [Rh-NPs(TPP@CCM)] (P/Rh = 4 in TPP@CCM with 5% DPPS) synthesized at 60 °C, applied at 25 °C, under 20 bar of H_2 for 20 h.

The strategy of using a higher P/Rh molar ratio was not successful for the confinement of the metal NPs in the core of the CCM. We tried to overcome this problem by synthesizing a new polymer having 20% DPPS in the core (instead of 5% DPPS).

3.6.2 Second strategy: TPP@CCM with 20% of DPPS

3.6.2.1 Polymer synthesis

The TPP@CCM latex was synthesized using the same procedure reported in par-

agraph 3.2, increasing the amount of phosphine in the second step of the synthesis (Scheme III.1), using this time 20% of DPPS. The synthesis of the hydrophobic part of the polymer was completed after 3 h and the cross-linking step after 6 h. The resulting polymer particles were well dispersed (not agglomerated) and the final latex was characterized by ^{1}H NMR, $^{31}P\{^{1}H\}$ NMR, TEM and DLS analysis. The NMR results were similar to those reported in paragraph 3.2 (Figure III.38).

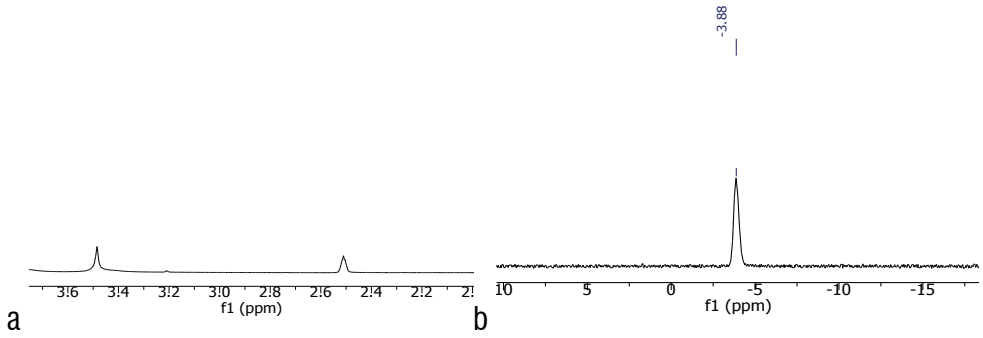

Figure III.38 - a) ^{1}H NMR, b) $^{31}P\{^{1}H\}$ NMR about TPP@CCM 20% DPPS.

The DLS analysis (Figure III.39) and the TEM micrographs are very similar to those of the TPP@CCM with 5% of DPPS. The nanoparticles size did not change with the variation of DPPS amount. The TEM images show a very good dispersion of polymer sphere (Figure III.40).

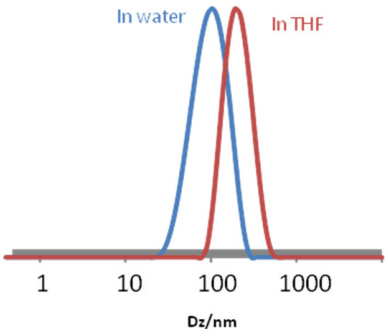

Figure III.39 - DLS in water and THF of the latex TPP@CCM with 20% DPPS.

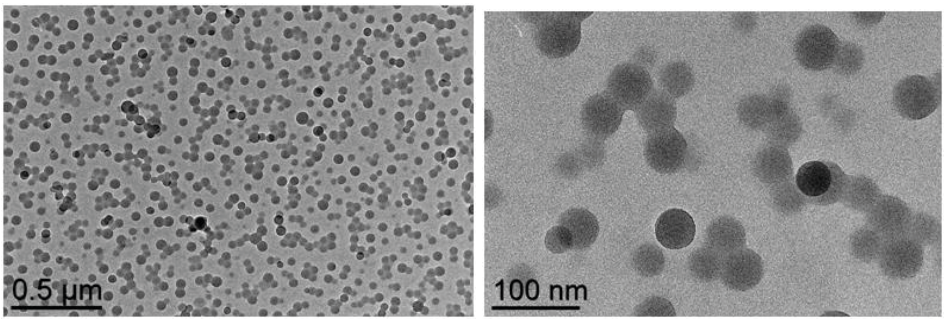

Figure III.40 - TEM micrographs about TPP@CCM with 20% of DPPS.

3.6.2.2 Rh coordination inside the TPP@CCM nanoreactors with 20% DPPS (P/Rh = 1)

The final latex was charged with rhodium, using as precursor $[Rh(COD)(Cl)]_2$ in molar ratio = 1:1 with respect to the phosphine ligand. The procedure was not changed and the occurrence of Rh loading complex was confirmed by the $^{31}P\{^1H\}$ NMR spectrum, which showed a doublet at 29.8 ppm, like the previously detected one (Figure III.41).

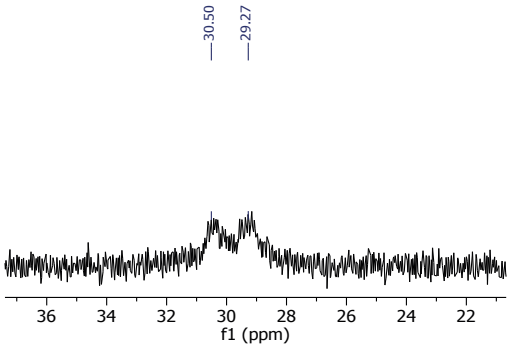

Figure III.41 - ^{31}P-NMR spectra related to [Rh(COD)Cl(TPP@CCM)], with 20% of DPPS in the hydrophobic core, in P/Rh=1.

3.6.2.3 Rh coordination inside the TPP@CCM nanoreactors with 20% DPPS (P/Rh = 4)

The coordination to Rh was carried out also in molar ratio P/Rh = 4. The $^{31}P\{^1H\}$ NMR spectrum of the polymeric metal complex shows a signal at -6.22 ppm, belonging to free phosphine, and a broad doublet at 29.22 ppm related to the PPh_3 coordinated to Rh (Figure III.42). The metalation was also confirmed by the changed colour of the polymer latex, from white to yellow.

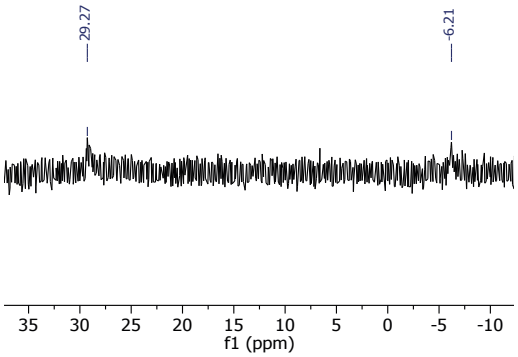

Figure III.42 - $^{31}P\{^{1}H\}$ NMR spectra related to [Rh(COD)Cl(TPP@CCM)] with 20% of DPPS in the core, in P/Rh = 4.

3.6.2.4 Synthesis of NPs and catalytic application

All the new synthesized CCM Rh-complexes with 20% of DPPS and P/Rh molar ratio equal to 1 or 4 were reduced under 20 bar of hydrogen, at 25 °C for 20 h. The TEM pictures of the obtained NPs-TPP@CCMs show in all cases the formation of big agglomerates of small nanoparticles and unfortunately the absence of the confinement of the Rh NPs into the CCM cores as a homogeneous distribution (Figure III.43, Figure III.44, Figure III.45). The NPs were directly used in the reduction of acetophenone at 25 °C (vide infra). After the catalytic application, the NPs were characterized by TEM analysis. The micrographs show smaller NPs than before catalysis. They are more localized in the shell than in the core (Figure III.46).

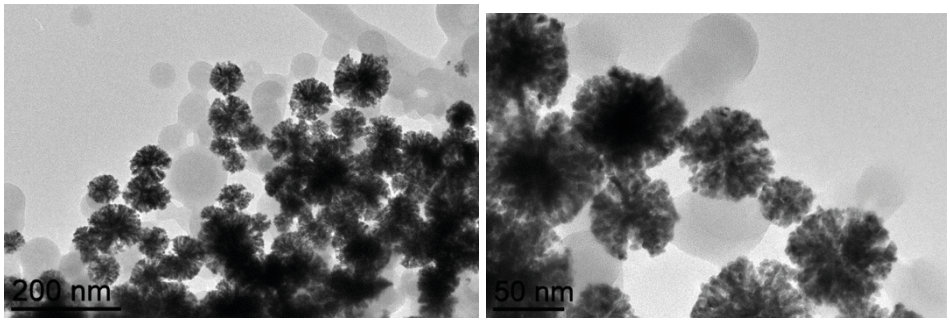

Figure III.43 - TEM micrographs about [Rh-NPs(TPP@CCM)] (P/Rh = 1_TPP@CCM(20%)) synthesized at 25 °C.

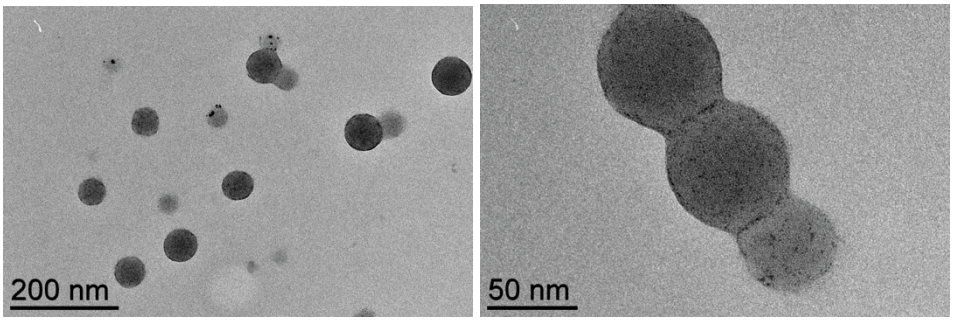

Figure III.44 - TEM micrographs about [Rh-NPs(TPP@CCM)] P/Rh = 1_TPP@CCM(20%)), synthesized at 25 °C, applied at 25 °C.

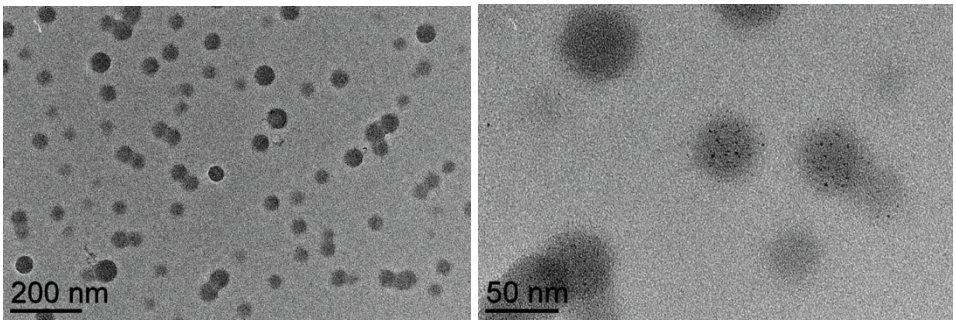

Figure III.45 - TEM micrographs about [Rh-NPs(TPP@CCM)] (P/Rh = 4_TPP@CCM (20%)) synthesized at 25 °C.

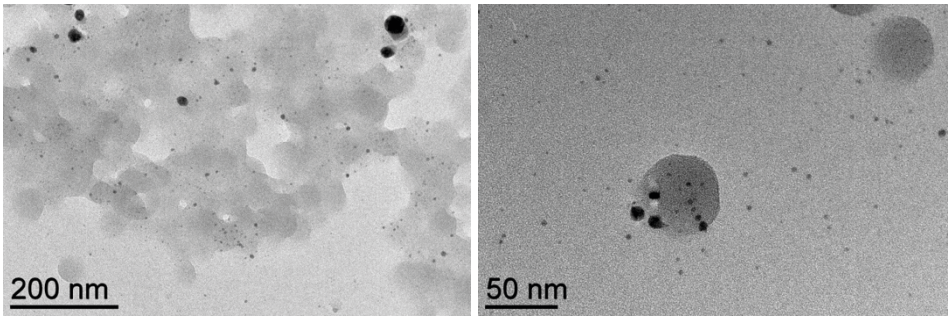

Figure III.46 - TEM micrographs about [Rh-NPs(TPP@CCM)] (P/Rh = 4_TPP@CCM(20%), synthesized at 25 °C, applied at 25 °C.

3.6.3 Comparison between Rh-NPs TPP@MCC and Rh NPs stabilized by PEG in neat solvent

Recently, poly(ethylene glycol) (PEG), inexpensive, an easily available and environ-

mentally benign polymer, has attracted great attention as stabilizing agent for transition-metal nanoparticles. The resulting Pd or Co nanoparticles have been investigated as catalyst in the oxidation,[279] Heck reaction,[280] and hydrogenation reaction.[281,282] In 2010 Lu et al. demonstrated that PEG-substituted triphenylphosphine can be use as a stabilizer for rhodium nanoparticles. They were used in aqueous biphasic hydrogenation of benzene showing high activity and good recyclability.[283] In 2012, PEG-stabilized Rh nanoparticles, prepared in the presence of PEG_{4000}, were efficient and recyclable catalysts for the hydroformylation of olefins in a thermoregulated biphasic system. The Rh NP catalyst could be separated from products by simple phase separation and recycled for twenty times without evident loss of activity.[284] Moreover, it was reported in 2015 that PEG-stabilized rhodium nanoparticles catalyse the hydrogenation of quinoline and their derivatives. The Rh NPs exhibited high activity, selectivity and recyclability.[285]

On the basis of the above literature references and considering that in our CCMs, PEG chains are on the micelle shell, we can conclude that the Rh NPs are likely to be better stabilized by the shell PEG chains than by the core phosphine functions, therefore the Rh atoms migrate from the core to the shell before or after nucleation. Therefore, Rh NPs were also synthesised in toluene solution in the presence of PEG, in order to compare their morphologies with those of [Rh-NPs(TPP@CCM)]. PEG_{1000} and $[Rh(COD)(Cl)]_2$, in molar ratios identical to those present for the Rh-NPs(TPP@CCM) when P/Rh = 1 and P/Rh = 4, were dissolved in toluene and left under stirring for few minutes. Both homogeneous solutions obtained were reduced under 20 bar of hydrogen for 20 h, at 25 °C.

TEM analyses of the obtained Rh NPs, dispersed into toluene and stabilized by PEG, show large agglomeration of small NPs (Figure III.47 and Figure III.49), even after use in catalysis (Figure III.48 and Figure III.50).

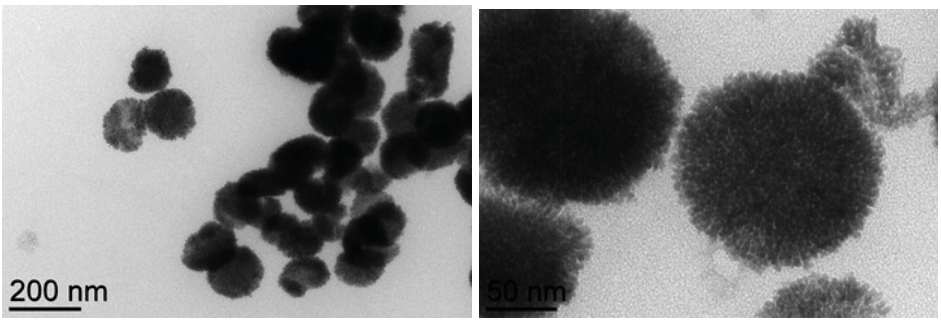

Figure III.47 - TEM micrographs about [Rh-NPs(PEG)] stabilized by PEG in ratio PEG/Rh = 1 synthesized at 25 °C.

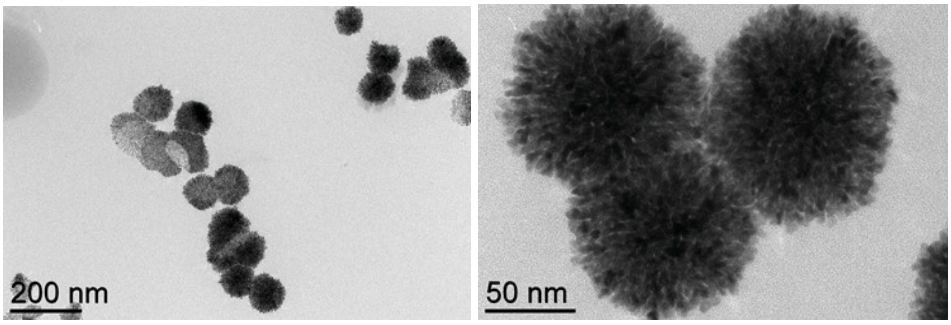

Figure III.48 - TEM micrographs about [Rh-NPs(PEG)] stabilized by PEG in ratio PEG/Rh = 1, synthesized at 25 °C, applied at 25 °C.

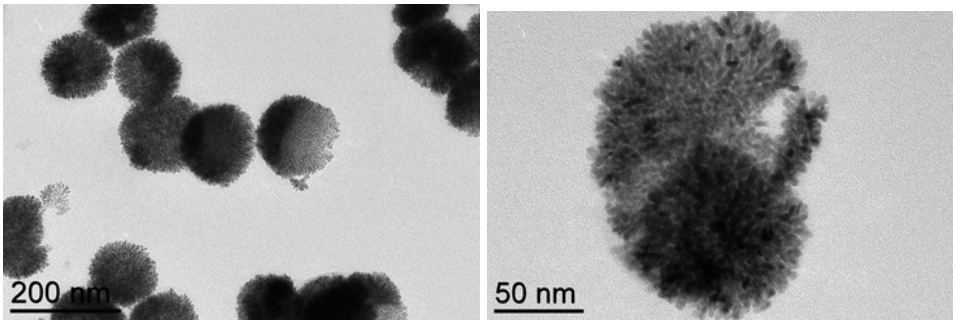

Figure III.49 - TEM micrographs about [Rh-NPs(PEG)] stabilized by PEG in ratio PEG/Rh = 4 synthesized at 25 °C.

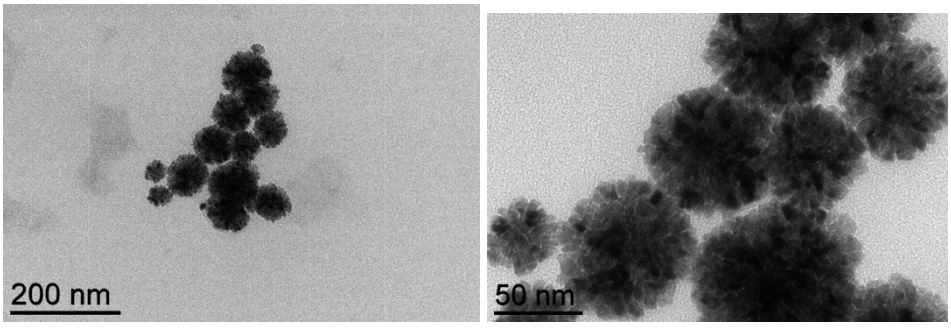

Figure III.50 - In the upper part: TEM micrographs about [Rh-NPs(PEG)] stabilized by PEG in ratio PEG/Rh = 4, synthesized at 25 °C, applied at 25 °C.

The PEG-stabilized NPs revealed that the phenomenon of metal NPs agglomeration observed mainly on the shell in [Rh-NPs(TPP@CCM)] is due to the presence of PEG on the neutral micelle shell. Moreover the presence of PEG stabilizes the metal NPs on the polymer shell; this explains the NPs stabilization in TPP@CCM on the outer

shell. This problem can be overcome by using CCMs with PEG-free shell. Furthermore the problem of metal migration, which is favour by the particle interpenetration, was avoided by rendering the shell polycationic. Preliminary results in this field revealed that the NPs distribution was more uniform than the one by using neutral shell, due to the presence of Coulombic repulsion.

3.6.4 Fourth strategy: Polymeric nanoreactor with a cationic shell

3.6.4.1 Rh coordination inside polymer core with cationic shell

The polymer used (polymer structure reported in Figure III.51) was prepared by Hui Wang in the laboratory of equipe G in LCC-CNRS (Toulouse). The polymer was synthesized using 1-methylpyridinium iodide during the synthesis of hydrophilic shell. By using this new polymer, the migration of the Rh complex could be blocked since the Coulombic repulsion between the cationic shells avoids the nanoreactor interpenetration, which is the established mechanism of Rh migration.

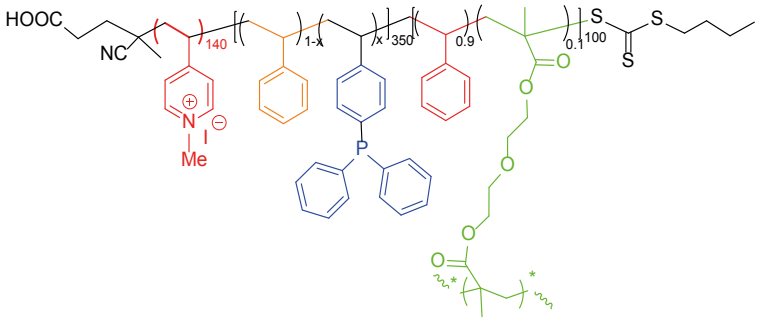

Figure III.51 - Polymer with cationic shell.

The final latex containing the polycationic outer shell was charged with rhodium, using $[Rh(COD)(Cl)]_2$ as precursor in molar ratio P/Rh = 1 and P/Rh = 4. The procedure was the same one described before and the Rh loading was confirmed by the colour change of both the organic and aqueous phases. The $^{31}P\{^1H\}$ NMR spectrum did not show the resonance related to the metal coordination. This might be due to the same phenomenon described in the neutral outer shell polymer (paragraph 3.6.1). The cationic shell CCM latex was directly used for the nanoparticles synthesis.

[Rh-NPs(TPP@CCM)], obtained from [Rh(COD)Cl(TTP@CCM)] in cationic shell, were synthesized at 25 and 60 °C in both molar ratio (P/Rh = 1 and P/Rh = 4). TEM micrographs of [Rh-NPs(TPP@CCM)] show that the Rh NPs synthesized at 25 °C, before and after catalysis, are mixture of NPs and large agglomerates (Figure III.52). The

polymer particles seem to be heavily agglomerated on top of each other and the contrast does not allow to show their shape in all TEM images (Figure III.53). Upon increasing the temperature (Rh NPs synthesized at 60 °C), the images show that each polymer particle contains uniformly distributed small Rh NPs (Figure III.54 and Figure III.55). The NPs are well dispersed and located more or less in every polymer particle (Figure III.59).

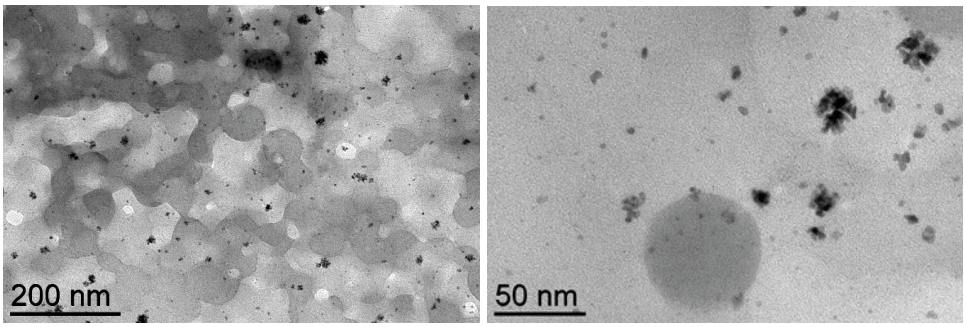

Figure III.52 - TEM micrographs of [Rh-NPs(TPP@CCM)] (P/Rh =1_TPP@CCM (cationic shell)) synthesized at 25 °C.

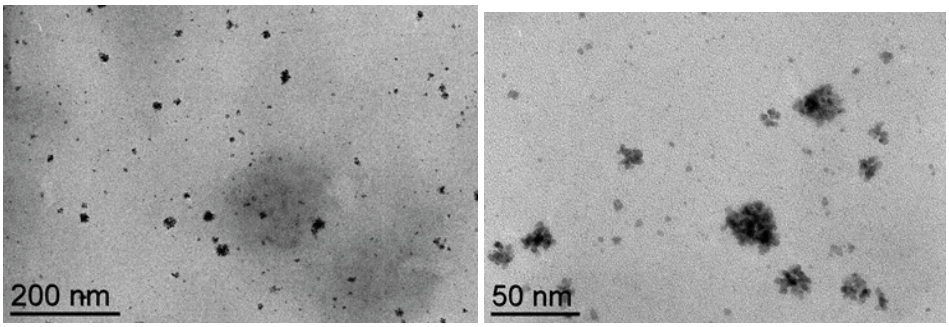

Figure III.53 - TEM micrographs of [Rh-NPs(TPP@CCM)] (P/Rh = 1_TPP@CCM (cationic shell)), synthesized at 25 °C, applied at 25 °C.

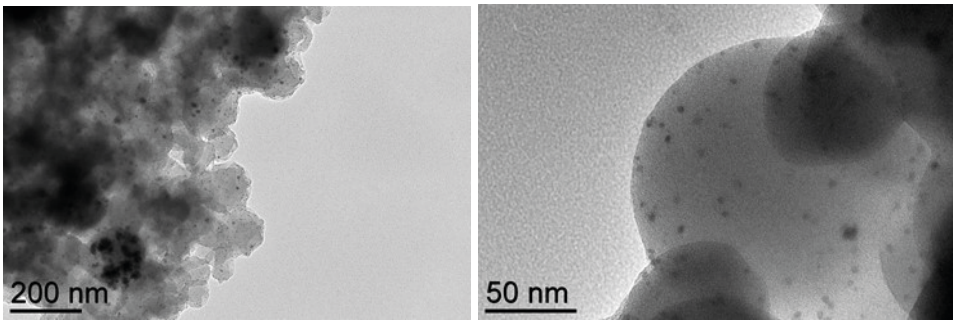

Figure III.54 - TEM micrographs of [Rh-NPs(TPP@CCM)] (P/Rh = 1_TPP@CCM (cationic shell)) synthesized at 60 °C.

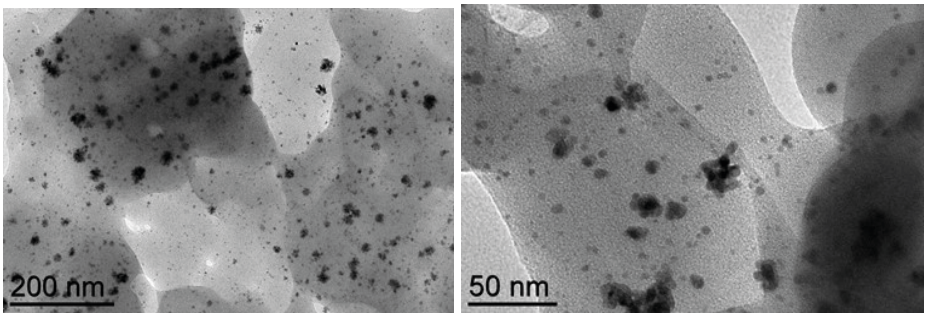

Figure III.55 - TEM micrographs of [Rh-NPs(TPP@CCM)] (P/Rh = 1_TPP@CCM (cationic shell)), synthesized at 60 °C, applied at 25 °C.

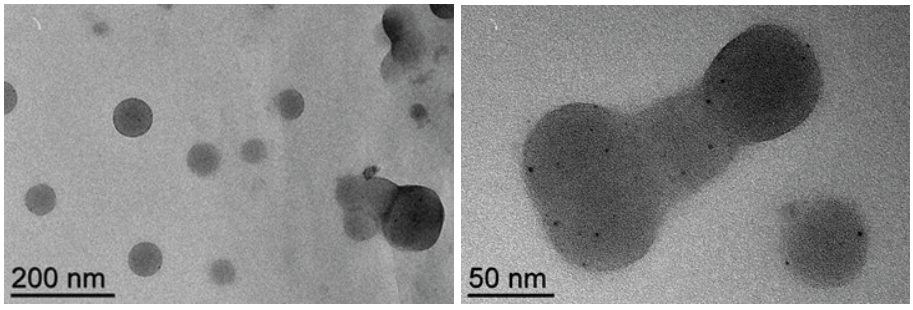

Figure III.56 - TEM micrographs of [Rh-NPs(TPP@CCM)] (P/Rh = 4_TPP@CCM (cationic shell)) synthesized at 25 °C.

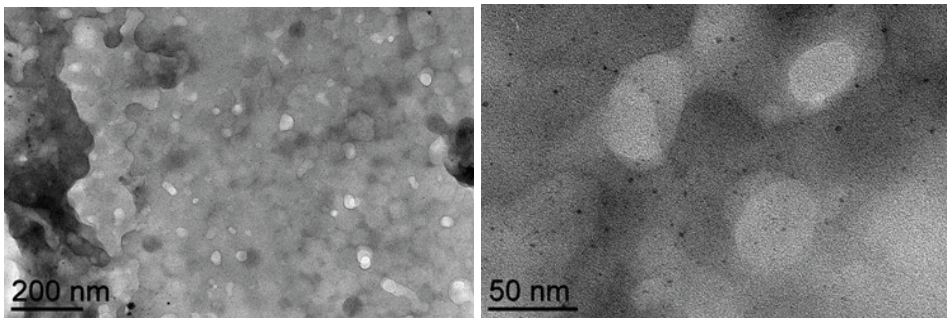

Figure III.57 - TEM micrographs of [Rh-NPs(TPP@CCM)] (P/Rh = 4_TPP@CCM (cationic shell)), synthesized at 25 °C, applied at 25 °C.

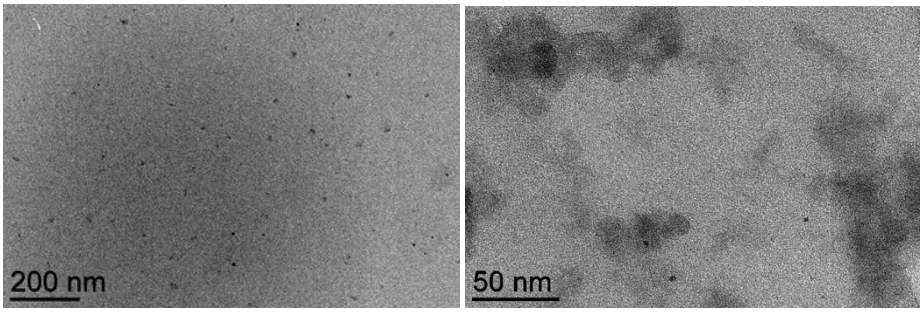

Figure III.58 - TEM micrographs of [Rh-NPs(TPP@CCM)] (P/Rh = 4_TPP@CCM (cationic shell)) synthesized at 60 °C.

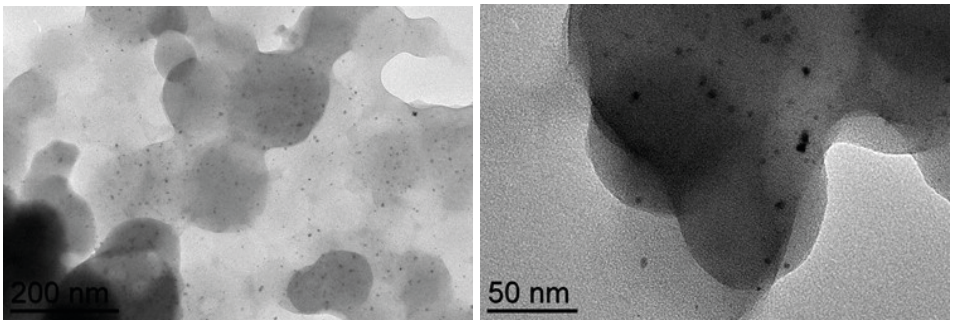

Figure III.59 - TEM micrographs of [Rh-NPs(TPP@CCM)] (P/Rh = 4_TPP@CCM (cationic shell)), synthesized at 60 °C, applied at 25 °C.

3.7 Catalytic activity of metal nanoparticles embedded in polymeric nanoreactor

3.7.1 [M-NPs(TPP@CCM)] containing neutral outer shell

With the aim to evaluate the catalytic activity of the metal NPs embedded in CCMs, they were used for the acetophenone (ACP) hydrogenation reaction of under 20 bar of hydrogen, for 20 h at different temperatures.

The ACP reduction can follow two different paths (Scheme III.5). In the first the double bond is firstly reduced forming phenylethanone, followed by the reduction of the benzene ring forming phenylethanol (Scheme III.5, path A). In the second one the reduction of benzene ring occurs firstly, followed by reduction of the double bond (Scheme III.5, path B). Employing these catalysts, we also investigated the selectivity of different metal NPs on the hydrogenation of acetophenone.

The catalytic application was simple and rapid. In the autoclave were introduced the NPs latex, the organic substrate dissolved in toluene and dodecane as an internal standard. At the end of the experiment, the hydrogen excess was vented off and the organic phase was easy recovered thanks to fast decantation of the biphasic mixture. The organic solution was diluted and analyzed with GC instrument.

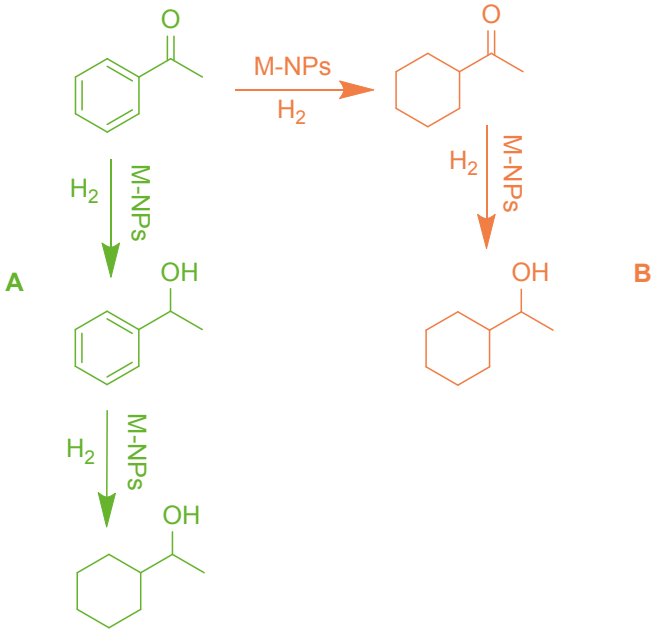

Scheme III.5 - Two possible pathways for the acetophenone hydrogenation reaction.

The results reported in Table III.1 demonstrated that increasing the temperature the NPs activity increases (entry 1, 2, 3, 6, 7 etc.). Moreover when the temperature for the NPs synthesis was increased the conversion did not increase for all the NPs, such as for Ir-NPs (entry 11, 12, 13).

Table III.1 - Catalytic results of the metal NPs embedded in nanoreactors (TPP@CCM) activity and selectivity in acetophenone hydrogenation.

				Conversion%	**Selectivity%**		
Entry	**M-NPs**	**Synt. NPs (T °C)**	**T (°C)**		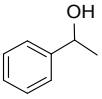	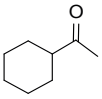	
1	Rh NPs	25	25	97%	58%	16%	26%
2	Rh NPs	25	40	95%	61%	16%	23%
3	Rh NPs	25	90	>99%	11.5%	31.2%	57.3%
4	Pd NPs	60	90	63%	>99%	trace	trace
5	*Pd NPs	80	90	75%	99.3%	0.5%	/
6	Ru NPs	60	40	75%	53%	trace	47%
7	Ru NPs	60	90	97%	43%	trace	57%
8	Ru NPs	40	90	97%	75%	4%	22%
9	Ir NPs	60	25	55%	55%	trace	trace
10	Ir NPs	60	40	64%	>99%	trace	trace
11	Ir NPs	60	90	96%	98%	2%	/
12	Ir NPs	40	90	>99%	96%	/	4%
13	Ir NPs	90	90	>99%	82%	/	18%
14	**Pt NPs	25	90	>99%	/	9%	90%

* NPs synthesized under air at 80 °C

** [Pt(COD)Br_2(TPP@CCM)] complex

The TPP@CCM role in the hydrogenation reaction was also evaluated by estimation of the NPs activity in homogeneous solutions for the reduction of acetophenone.

NPs were synthesized by reduction of a homogeneous solution containing PPh_3 and all metal precursor used in TPP@CCM. All the homogeneous metal nanoparticles were synthesized in molar ratio as P/M = 1, at 25 °C and applied in catalysis at the same temperature.

Before and after catalytic application the metal NPs were analysed by TEM. The images show a uniform distribution of small metal nanoparticles without formation of

aggregates (see for instance the images in Figure III.60 before a) and after b) catalysis for the Pd NPs). This suggests that phosphine well stabilized metal nanoparticles. Therefore the phenomenon of NP aggregation and stabilization on the outer shell, observed in polymeric nanoreactors containing the neutral shell, is due to the molecules present on the shell. Moreover the catalytic results demonstrated that the NP activity is low (Table III.2 entry 3-4) or completely absent for each metals (Table III.2 entry 6-7). This result suggests that the NPs activity is provided by the confinement in the polymeric nanoreactor TPP@CCM.

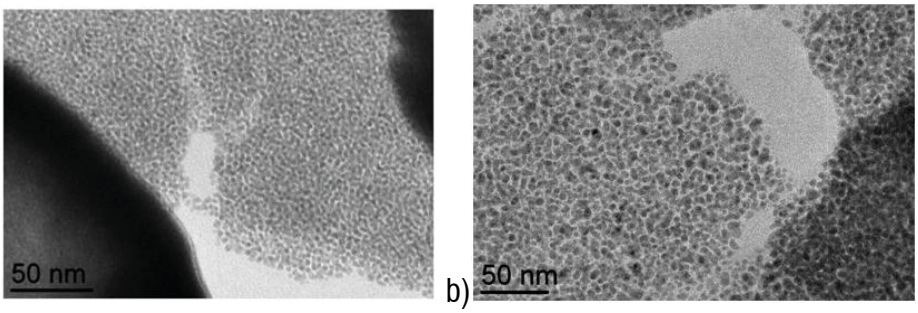

Figure III.60 - TEM micrographs about Pd NPs in homogenous solution in ratio P/Rh = 1: a) NPs synthesized at 25 °C before catalysis; b) NPs applied at 25 °C.

Table III.2 – Catalytic results of the metal NPs, synthesised in homogeneous solution, applied in the acetophenone hydrogenation reaction at 25 °C, for 20 h under 20 bar of H_2.

				Conversion%	**Selectivity%**		
Entry	**M-NPs**	**P/M**	**T NPs synt. (°C)**		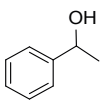	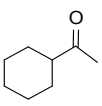	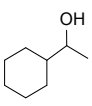
1	Rh NPs	1:1	25	>99%	71%	3%	26%
2	Rh NPs	4:1	60	84%	74%	17%	10%
3	Pd NPs	1:1	25	9%	>99%	trace	trace
4	Ru NPs	1:1	25	15%	>99%	trace	trace
5	Ir NPs	1:1	25	6%	>99%	/	/
6	Pt NPs	1:1	25	0%	/	/	/
7	Au NPs	1:1	25	0%	/	/	/

3.7.2 Catalytic activity of Rh-NPs stabilized by PEG

Rh-nanoparticles stabilized by PEG, in both ratio P/Rh = 1 and P/Rh = 4, were applied at 25 and 60 °C. The results demonstrated that the Rh-NPs stabilized by PEG

are active and selective in the reduction of acetophenone (Table III.2). With the NPs obtained using

Rh/PEG = 4 the substrate conversion was complete after 20 h with formation of 1-cycloehylethanol as the major product (86.40% at 25 °C and 73.46 at 60 °C; Table III.2 entry 3,4). This suggests that increasing the amount of PEG the catalytic activity of NPs increases.

Table III.3 - Catalytic results about the hydrogenation of acetophenone catalyzed by Rh NPs synthesized in ratio 1:1 and 4:1 at 25 °C and applied at 25 and 60 °C, 20 bar H_2, 20 h.

			Conver (%)	**Selectivity (%)**	
Entry	**P/Rh**	**T NPs application (°C)**		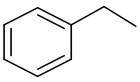	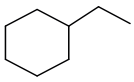
1	1:1	25	/	trace	trace
2		60	75%	19%	44%
3	4:1	25	>99%	8%	89%
4		60	>99%	20%	79%

3.7.3 Catalytic activity of [Rh-NPs(TPP@CCM)] cationic shell

Catalytic investigations using the Rh-NPs embedded in the TPP@CCM with the cationic shell were conducted by Hui Wang within the framework of her ongoing Ph.D. thesis and therefore will not be presented here in all details. However, a few relevant results are of interest in comparison with those shown above with the TPP@CCM with the neutral shell. The catalytic results in acetophenone hydrogenation for the [Rh-NPs(TPP@CCM)] latex with polycationic outer shell demonstrated that the substrate reduction did not occur also upon increasing the reaction temperatures. This suggested that the mass transport into the polymer core is limited due to a less compatibility between acetophenone and polystyrene (PS) hydrophobic core. Therefore the same [Rh-NPs(TPP@CCM)] latex was applied in hydrogenation of styrene (Scheme III.6), which is a more compatible substrate with the PS core, using both P/Rh molar ratios and at 25 and 60 °C. The formation of vinylcyclohexane intermediate was never observed, while the ethylbenzene was formed as major product. The results revealed that the NPs were highly active and selective in the synthesis of ethylbenzene at 60 °C (Table III.4, entry 2, 4).

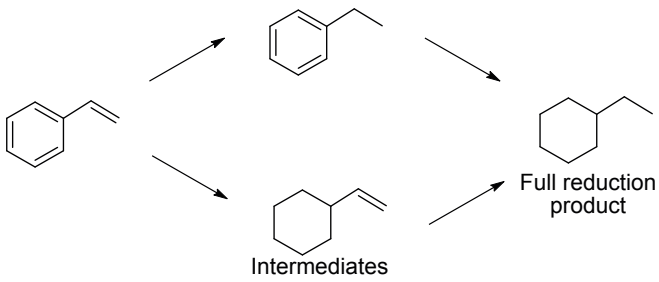

Scheme III.6 - Two possible pathways for the hydrogenation reaction of styrene.

Table III.4 - Catalytic results about the hydrogenation of styrene catalyzed by: Rh-NPs embedded in polymer with cationic shell in ratio P/Rh = 1 and 4.

				Conver (%)	**Selectivity (%)**	
Entry	**Stabilizer**	**P/Rh**	**T NPs application (°C)**		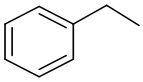	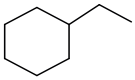
1	PPh_3	1:1	25	28%	>99%	trace
2			60	100%	97%	3%
3		4:1	25	41%	98%	2%
4			60	100%	>99%	/

3.8 Conclusions

We have introduced the synthesis of metal nanoparticles embedded in polymeric nanoreactor TPP@CCM. The investigation revealed that a uniform distribution of metal nanoparticles, confined in polymeric nanoreactor, can be obtained only upon removing PEG chains from the hydrophilic shell and introducing Coulombic repulsion with polycationic shell.

Increasing the amount of ligand PPh_3 in the synthesis of the hydrophobic core or decreasing the quantity of metal loading in the preparation of the polymer metal complexes, the confinement in the CCM core of the metal NPs, obtained by subsequent reduction, was not guaranteed. The metal NPs migrate from a CCM particle to another one leaving several particles completely empty. The polymeric nanoreactors with cationic shell avoid this problem and cause a homogeneous distribution of metal nanoparticles thanks to the Coulombic repulsion, which blocks the particle interpenetration and the metal migration. In addition, the PEG stabilizer promotes the agglomeration of small metal nanoparticles. This is in agreement with what was observed in the polymeric nanoreactor. The results demonstrated that the phenomena observed with the polymer containing the neutral outer shell (stabilisation of the NPs on the shell and NPs agglomeration) are due to the presence of PEG on the shell of TPP@CCM. The NPs confinement was successful in the CCMs with the cationic shell, which allows obtaining a homogenous distribution of metal nanoparticles within all particles, avoiding the presence of empty CCMs.

Several parameters can influence the nanoparticles size and morphology. This study demonstrates that the NPs size in TPP@CCM increases by increasing the temperature. The temperature influences neither the position of the metal NPs nor the formation of agglomerates. In fact, the NPs were localized on the neutral shell of the polymer. The catalytic activity of all metal nanoparticles was evaluated on the acetophenone hydrogenation reaction, demonstrating that it is less compatible with the hydrophobic polystyrene core. In fact, the same NPs (tested in TPP@CCM cationic shell) were active in hydrogenation of styrene and selective in the synthesis of ethylbenzene. The results demonstrated that the activity increased by increasing the reaction temperature.

CHAPTER IV
Experimental section

TABLE OF CONTENTS

CHAPTER IV

Experimental section

4.1 Ni-pol catalyst

4.1.1 Materials for the synthesis of Ni-pol and related catalytic tests

Nitrobenzene was distilled under inert atmosphere before use, while all other reagents/reactants and solvents were used as received. All manipulations belonging to nitroarene reductions (including reductive alkylations) were carried out under inert dinitrogen atmosphere using standard schlenk techniques unless otherwise specified.

Commercial soybean oil was used as received. Waste cooking oil was recovered after several used and was employed as received. Transesterification reactions of oils were carried out under air. Partial hydrogenation of FAMEs was conducted in a steel autoclave under H_2 pressure as described below.

Tap water was de-ionized before use by ionic exchange resins (Millipore). All other chemicals were purchased from commercial sources and used as received. Nickel content in Ni-pol catalyst was evaluated after sample mineralization by atomic absorption spectrometry using a Perkin–Elmer 3110 instrument. The experimental error on the nickel percentage was $\pm$ 0.3. Before Ni-pol analyses, mineralization of Ni-pol was carried by microwave irradiation with an ETHOS E-TOUCH Milestone applicator, after addition of HCl/HNO_3 (3:1 v/v) solution (12 mL) to each weighted sample. Microwave irradiation was used up to 1000 W, the temperature being ramped from room temperature to 220 °C in 10 minutes and the sample being held at this temperature for 10 min. After cooling to room temperature, the digested Ni-pol was diluted to 1000 mL before submitting to Graphite Furnace Atomic Absorption Spectrometric nickel determination. The products were identified by comparison of their GC–MS features with those of authentic samples.

Gas chromatography (GC) data were acquired on a HP 6890 instrument equipped with a FID detector and a HP-1 (Crosslinked Methyl Siloxane) capillary column (60.0 m x 0.25 mm x 1.0 μm). GC–MS data (EI, 70 eV) were acquired on a HP 6890 instrument using a HP-5MS cross-linked 5% phenyl methyl siloxane (30.0 m $\times$ 0.25 mm $\times$ 0.25 m) capillary column coupled with a mass spectrometer HP 5973.

GLC analysis of the products was performed using a HP 6890 instrument equipped with a FID detector and a HP-1 (Crosslinked Methyl Siloxane) capillary column (60.0

m × 0.25 mm × 1.0 m). Conversions and yields were calculated by GLC analysis by using biphenyl as internal standard, or by column chromatography using silica gel and n-hexane/ethyl acetate as the eluent.

FT-IR spectra (in KBr pellets) were recorded on a Jasco FT/IR 4200 spectrophotometer. Elemental analyses were obtained on a Euro Vector CHNS EA3000 elemental analyser using acetanilide as analytical standard material.

The high-resolution mass spectrometry (HRMS) analysis was performed using a Bruker micro TOF QII mass spectrometer equipped with an electrospray ion source operated in positive ion mode. The sample solutions (CH_3OH) were introduced by continuous infusion with a syringe pump at a flow rate of 180 μL min^{-1}. The instrument was operated with end-plate off set and capillary voltages set to −500 V and −4500 V respectively. The nebulizer pressure was 0.4 bar (N_2), and the drying gas (N_2) flow rate was 4.0 L min^{-1}. Capillary exit and skimmer voltages were 90 V and 30 V, respectively. The drying gas temperature was set at 180 °C. The calibration was carried out with a sodium formate solution (10 mM NaOH in isopropanol/water 1:1 (+0.2% HCOOH)) and the software used for the simulations was Bruker Daltonics Data Analysis (version 4.0).

Thermogravimetric analyses (TGA) were performed in a nitrogen flow (40 mL min^{-1}) with a Perkin-Elmer Pyris 6 TGA in the range from 30 to 800 °C with a heating rate of 10 °C min^{-1}. Triplicate TGA runs have been performed to ensure reproducibility.

Column chromatography was performed using Merck® Kiesel gel 60 (230–400 mesh) silica gel. ^{1}H NMR and ^{13}C{^{1}H} NMR were recorded on a Bruker Avance 400 MHz and are reported in ppm relative to tetramethylsilane.

Surface morphology was investigated on a selected piece of Ni-supported catalyst considered to be representative of the material. Nova Nano SEM 450 manufactured by FEI Company, USA, was used to perform FESEM analysis on the selected samples, equipped with Energy Dispersive X-ray Spectroscopy (X-EDS; Bruker QUANTAX-200) and Electron Backscatter Diffraction (EBSD) detectors (Nordlys with Channel 5 software). Tinyplate-like of the powdered catalyst were mounted on TEM copper grids, and gold-palladium sputtered (K550, Emitech Ltd, United Kingdom). Scanning Transmission Electron Microscopy (STEM) Detector allowed transmission images to be taken at 30 keV, lower energy level with respect to commonly used TEM, beam voltage 100–200 keV. Resolution limits of this microscope are remarkable: 1.4 nm @ 1 kV in high vacuum mode. The particle sizes were analyzed by STEM image analysis using the Image J software (free ware software: http://rsb.info.nih.gov/ij/).

4.1.2 Ni(AAEMA)$_2$

To a solution of KOH (579 mg, 10.3 mmol) in ethanol (10 mL), 2-(acetoacetoxy) ethyl methacrylate (HAAEMA) (2.211 g, 10.3 mmol) was added and left under stirring at room temperature for 5 min. The resulting solution was added to a solution of $Ni(NO_3)_2 \cdot 6\ H_2O$ (1.5 g, 5.16 mmol) in ethanol (15 mL), causing the sudden precipitation of Ni(AAEMA)$_2$ as a pale green solid. After 1 h stirring, the solid was filtrated and washed with water (3 × 5 mL), ethanol (3 × 5 mL) and pentane (3 × 5 mL), and dried overnight under vacuum.

Anal. Calc. for $NiC_{20}H_{26}O_{10}$: C, 45.00; H, 4.92; Ni, 19.97. Found: C, 44.50; H, 4.99; Ni, 19.76. HRMS: (ESI, CH_3OH, positive ion mode) m/z: calc. for $NiC_{20}H_{27}O_{10}$ $[M + H]^+$ 485.0952; found 485.0954. IR (cm^{-1}): 1720 (s), 1635 (s), 1623 (s), 1521 (s), 1385 (vs), 1259 (vs), 1161 (vs), 977 (m), 785 (m). UV-vis (CH_2Cl_2): 280 nm ($\varepsilon = 10660$ mol $L^{-1}cm^{-1}$), 227 nm ($\varepsilon = 4800$ mol $L^{-1}cm^{-1}$). m.p. = 120.3±0.4 °C. Yield: 2.01 g, 80%.

4.1.3 Ni(AAEMA)$_2$-pol

Ni(AAEMA)$_2$ (4.0 mmol, 2.0 g) [$AAEMA^-$ = deprotonated formof 2-(acetoacetoxy) ethyl methacrylate] was dissolved in N,N−dimethylformamide (DMF, 5 mL) and the resulting solution was added of a mixture of N,N'-methylenebisacrylamide (1.2 mmol, 0.186 g) and N,N −dimethylacrylamide (43.2 mmol, 4.434 g) in DMF (6 mL) and heated at 120 °C under vigorous stirring. After 1 h from the addition of azaisobutyronitrile (5 mg), the green jelly solid, which formed in the reaction vessel, was filtered off, washed with acetone and diethyl ether, dried under vacuum, kept overnight in oven at 95 °C and grinded with a mortar to give a pale green powder. Yield: 4.04 g of polymer supported Ni(AAEMA)$_2$ [Ni(AAEMA)$_2$-pol].

Elemental Analysis (found): Ni 3.69; C 57.06; H 7.94; N 9.91%. IR(cm^{-1}): 3477 (bs), 2923 (bs), 1720 (s), 1622 (s), 1527 (s), 1256 (vs),1144 (vs), 1355 (s), 780 (m).

4.1.4 Ni-pol catalyst

The as obtained Ni(AAEMA)$_2$-pol was put in a tube furnace, ramped at 10 °C min^{-1} in flowing N_2 to 300 °C, and kept at the final temperature for 30 min, yielding a black powder referred to as Ni-pol. Yield: 3.83 g.

Elemental Analysis (found): Ni 5.35; C 56.66; H 9.20; N 11.54%. IR (cm^{-1}): 3482 (bs), 2930 (bs), 1720 (s), 1631 (s), 1495 (m), 1402 (m), 1258 (m), 1144 (s), 1053 (m).

4.1.5 General experimental procedure for the reduction of nitroarenes

0.5 mmol of nitroarene, 10.2 mg of Ni-pol (Ni%w = 5.35, $9.3 \cdot 10^{-3}$ mmol of Ni) and 10.0 mmol of sodium borohydride were stirred under nitrogen at room temperature in 2.5 mL of double deionized water and 2.5 mL of diethyl ether for the appropriate amount of time, using a three-necked flask equipped by a gas bubbler to discharge the hydrogen excess produced during reaction. The progress of the reaction was monitored by GLC. After completion of the reaction, the reaction mixture was centrifuged to separate the catalyst. The solid residue was first washed with deionized water and then with acetone and diethyl ether to remove any traces of organic material. The filtrate containing the reaction mixture was extracted with ethyl acetate (3 × 5 mL) and then dried over anhydrous Na_2SO_4. The solvent was evaporated under reduced pressure to yield the crude product, which was then purified by column chromatography using silica gel and n-hexane/ethyl acetate as an eluent to afford the pure product. The products were characterized by GC–MS by comparison with authentic samples. For the assessment of the chromatographic yields, biphenyl (50.0 mg) was used as the internal standard.

4.1.5.1 Recycling procedure

At the end of reaction, the organic layer was removed with a syringe and the aqueous phase suspending the supported catalyst was washed with diethyl ether (3 × 5 mL), and, then, added of fresh reagents. Iteration of this procedure was repeated for five reuses of the catalytic system.

4.1.6 General experimental procedure for one-pot stepwise reductive amination of aromatic aldehydes with nitroarenes

Ni-pol (11.0 mg, Ni%w = 5.35, 10.0 μmol of Ni), the desired nitroarene (0.50 mmol), methanol (5.0 mL) and $NaBH_4$ (1.5 mmol) were introduced in a 25 mL three-necked round flask (equipped with a magnetic stirrer and a gas bubbler to discharge the di-hydrogen excess produced during reaction), and the mixture was stirred under magnetic stirring at 25 °C for the time necessary to form the corresponding anilines (step A, monitoring by TLC and/or GC and GC–MS). Then, 40 μL (ca. 1.0 mmol) of formic acid and the desired arylaldehyde (0.70 mmol) were introduced in the vessel and the reaction mixture was stirred for further 40 min (step B). Then, 3.0 mmol of $NaBH_4$ was added under stirring, leaving the system to react for two times (step C). The reaction mixture was then diluted with 5.0 mL of methanol and filtered. The solid (Ni-pol) was washed with methanol (3×5.0 mL) and the combined organic layers were dried (Na_2SO_4) and concentrated under reduced pressure to get the crude product,

which was then purified by column chromatography using a short plug of silica gel and eluted with the appropriate solvent mixture. Evaporation of solvents afforded the desired secondary amines.

All secondary amines, except for 3al and 3am, are compounds already known in the literature and were characterized by comparison with their ^{1}H-NMR and MS (EI, 70 eV) data. Amines 3al and 3am were characterized by ^{1}H and ^{13}C{^{1}H} NMR, MS (EI, 70 eV), and elemental analysis. N-(thiophen-3 ylmethyl)aniline (3al) was eluted from silica gel using petroleum ether 40-60 °C/dichloromethane in a volume ratio of 7:4 (Rf = 0.36) affording the title compound as a yellow oil.

^{1}H-NMR (400 MHz, $CDCl_3$, δ): 7.32 (m, 1 H), 7.24-7.16 (m, 3 H), 7.09 (d, J=5.0 Hz, 1 H), 6.75 (t, J=7.3 Hz, 1 H), 6.67 (d, J=7.3 Hz, 2 H), 4.35 (s, 2 H), 3.52 (br s, 1H, NH). ^{13}C{^{1}H} NMR (100.6 MHz, $CDCl_3$, δ): 148.2, 140.6, 129.4, 127.3, 126.3, 121.9, 117.9, 113.1, 43.9. EI/MS m/z (%): 189 (63) [M^+], 97 (100), 77 (21), 65 (14). Anal. Calc for $C_{11}H_{11}NS$: C, 69.80; H, 5.86; N, 7.40; S, 16.94; found: C, 69.44; H, 5.63; N, 7.37. N-((5-bromothiophen-2-yl)methyl)aniline (3am) was eluted from silica gel using petroleum ether bp 40–60 °C/dichloromethane in a volume ratio of 7:3 (Rf = 0.30) affording the title compound as a pale yellow oil.

^{1}H-NMR (400 MHz, $CDCl_3$, δ): 7.20 (t, J=8.0 Hz, 2 H), 6.91 (d, J=3.6 Hz, 1 H), 6.80-6.74 (m, 2 H), 6.66 (d, J=8.0 Hz, 1 H), 4.45 (s, 2 H), 4.06 (br s, 1H, NH). ^{13}C{^{1}H} NMR (100.6 MHz, $CDCl_3$, δ): 147.3, 145.2, 129.7, 129.3, 125.2, 118.5, 113.3, 111.1, 43.9. EIMS m/z (%): 267 (37) [M^+], 175 (100), 96 (33), 77 (21), 65 (15). Anal. Calc. for $C_{11}H_{10}BrNS$: C, 49.27; H, 3.76; Br, 29.80; N, 5.22; S, 11.96; found: C, 49.11; H 3.69; N, 5.30.

4.1.6.1 Recycling of catalyst

Ni-pol (66.0 mg, Ni%w = 5.35, 60.0 μmol of Ni), nitrobenzene 3a (3.0 mmol), methanol (30.0 mL) and $NaBH_4$ (9.0 mmol) were introduced in a 100 ml three-necked round flask (equipped with a magnetic stirrer and a gas bubbler), and the mixture was stirred under magnetic stirring at 25 °C until aniline I quantitatively formed (2 h, step A). Then, 240 μL (ca. 6.0 mmol) of formic acid and benzaldehyde 2a (4.2 mmol) were introduced in the vessel and the reaction mixture was stirred for futher 40 min (step B). Then, maintaining the stirring, $NaBH_4$ (18.0 mmol) was added leaving the system to react for 3 h (step C). The reaction mixture was then diluted with 20.0 mL of methanol and centrifugated for separating Ni-pol, which was washed with methanol (3 × 25.0 mL), water (2 x 25.0 mL) and rinsed in n-hexane (20 mL). The methanol phase was dried (Na_2SO_4) and concentrated under reduced pressure to get the crude product, which was then purified by column chromatography using a short plug of silica gel

and eluted with petroleum ether 40–60 °C/dichloromethane in a volume ratio of 7:3 and evaporation of solvents afforded the desired amine 3aa. The recovered Ni-pol was dried in air at 60 °C for 2 h, and then brought to room temperature, re-weighed and used for the subsequent catalytic cycle. Iteration of this procedure was repeated for five reuses of the catalyst.

4.1.7 Trans-esterification reaction of vegetable oil

A solution of methanol (16.9 g) and potassium hydroxide (0.5 g) was added to 50 g of soybean or WCO oil, previously heated at 60 °C, and left under stirring at 600 rpm for 2h under refluxing conditions. The reaction was completed when the mixture colour changed from yellow to orange. Then, the mixture was placed into a separating funnel overnight, in order to obtain two phases (FAMEs and glycerine). The FAMEs phase was separated from glycerine, washed with hot water (5 x 5.0 mL) and dried over Na_2SO_4. The obtained FAMEs were stored at -22 °C.

4.1.7.1 Partial hydrogenation of bio-oil

FAMEs (125 mg) and Ni-pol (60.3 mg, Ni%w = 5.35) were putted in stainless steel reactor in 5 mL of methanol. The catalytic system was purged three times with hydrogen and left under stirring for 10 h at 100 °C under 10 bar of H_2. The progress of the reaction was monitored by GLC (internal standard method).

4.1.7.2 Recycling catalyst

At the end of the reaction, the solid catalyst was filtrated, washed with methanol (3 x 5.0 mL) and hexane (3 x 5.0 mL) and dried overnight before re-use.

4.2 Metal nanoparticles in TPP@CCM

4.2.1 Materials for the synthesis of M-NPs and related catalytic tests

All manipulations were performed under an inert atmosphere of dry argon by using schlenk line techniques. 4,4-azobis(4-cyanopentanoic acid) (ACPA, ≥97%, Aldrich), methacrylic acid (MAA, 99.5%, Acros), poly(ethylene oxide) methyl ether methacrylate (PEOMA, Mn = 950 g mol^{-1}, Aldrich), di(ethylene glycol) dimethacrylate (DEGDMA, 95%, Aldrich), 4-diphenylphosphinostyrene (DPPS, 97%, Aldrich), acetylacetonato-dicarbonyl rhodium(I), ([Rh(acac)$(CO)_2$], 99% Strem), chloro(1,5-cyclooctadiene) rhodium(I) dimer ([Rh(COD)Cl]$_2$, 98%, Strem), chloro(1,5-cyclooctadiene) iridium(I)

dimer, $[Ir(COD)Cl]_2$ (99%, Strem), triphenylphosphine (PPh_3 or TPP, >98.5%, Fluka), allylpalladium(II) chloride dimer ($[Pd(Cl)(C_3H_5)]_2$ 98% Strem), dichloro (p-cymene) ruthenium(II) dimer $[Ru(p\text{-cymene})Cl_2]_2$ (98% Strem), dibromo (1,5-cyclooctadiene) platinum(II) ($C_8H_{12}Br_2Pt$, 98% Strem), bis(benzonitrile)dichloropalladium(II) ($(C_6H_5C\text{-}N)_2PtCl_2$, 99% Strem), Chloro(dimethylsulfide)gold(I) ($(CH_3)_2SAuCl$, 97% Strem), were used as received.

The deuterium solvents ($CDCl_3$, CD_2Cl_2, toluene-*d8*, THF-*d8*, DMSO-*d6* and D_2O) provided by Eurisotop were used as received. Styrene (S, 99%, Acros) was purified by passing through a column of active basic aluminium oxide to remove the stabilizer.

All the 1D NMR spectra ^{1}H-NMR spectra were recorded in 5 mm diameter tubes at 297 K on a Bruker Avance 400 spectrometer. The ^{1}H shifts were determined using the residual peak of deuterated solvent as internal standard and are reported in ppm (δ) relative to tetramethylsilane. ^{31}P chemical shifts are reported relative to external 85% H_3PO_4. For the CCM characterization, the chemical shift scale was calibrated on the basis of the solvent peak (δ 2.50 for DMSO, 3.58 and 1.73 for THF), and 1, 3, 5-trioxane was used as an integration reference (δ 5.20). The NMR tubes were prepared in $CDCl_3$, D_2O and DMSO.

The intensity-average diameters of the latex particles (*D*z) and the dispersity factor (PDI, poly dispersity index) were obtained from measurements carried out at 25 °C on a Malvern Zetasizer Nano ZS. After filtration through a 0.45 μm pore-size membrane, deionized water or THF were used to dilute the latex sample. The solutions were analysed without further filtration to ensure that undesired populations were not removed. Data were analysed by the general-purpose non-negative least squares (NNLS) method. The typical accuracy for these measurements was 10-15%.

The morphological analysis of the copolymer nano-objects and of nanoparticles, before and after catalysis, was performed with a JEOL JEM 1011 transmission electron microscope equipped with 100 kV voltage acceleration and tungsten filament (Service Commun de Microscopie Electronique TEMSCAN, Centre de Microcaractérisation Raimond Castaing, Toulouse, France). Diluted latex samples were dropped on a formar/carbon-coated copper grid and dried under vacuum.

Samples were prepared dissolving one drop of the final product in 5 mL of ethanol. The resulting solution was sonicated for several minutes' prior analyses.

The intensity-average diameters of the latex particles (Dz) and the polydispersity index (PDI) were measured at 258 °C on a Malvern Zetasizer NanoZS. After filtration through a membrane (pore size= 0.45 mm) of regenerated cellulose, deionized water or THF was used to dilute the latex sample. The solutions were analyzed without further filtration to ensure that undesired populations were not removed. The data were ana-

lyzed by using the general-purpose non-negative least squares (NNLS) method. The typical accuracy for these measurements was 10–15%.

4.2.2 Synthesis of TPP@CCM by one pot RAFT polymerization in water

4.2.2.1 Step 1: Preparation of the P(MAA-co-PEOMA) macromolecular RAFT agent (macroRAFT) in water

A stock solution containing ACPA (40 mg) and $NaHCO_3$ (40 mg) in deionised water (5 mL) was prepared. 1 mL of this stock solution (8 mg ACPA, 0.029 mmol), CTPPA (40 mg, 0.14 mmol), MAA (0.19 g, 2.2 mmol), PEOMA (2 g, 2 mmol) and 7.8 g of additional deionized water were placed into a 50 mL flask equipped with a magnetic stirrer bar, which was then sealed with a rubber septum. 1,3,5-Trioxane was also added to the mixture as an internal reference for the determination of the monomer conversion by ^1H NMR. The solution was purged for 45 min with argon and then heated to 80 °C in a thermostated oil bath under stirring. After 120 min, 0.15 mL of solution was taken to determine the monomer conversion and the molar mass of the macroRAFT product. The overall monomer molar conversion was 98% as determined by ^1H NMR spectroscopy in DMSO-d6. The molar mass was analyzed by size exclusion chromatography (SEC) in THF (experimental Mn = 12100 g mol^{-1}; Đ = 1.2).

4.2.2.2 Step 2: RAFT copolymerization of S and DPPS in water

A stock solution containing ACPA (60 mg) and $NaHCO_3$ (60 mg) in deionised water (2 mL) was prepared. 14.83 mg of macroRAFT agent were placed into a 50 mL flask equipped with 17.2 mL of H_2O, with a magnetic stirrer bar, which was then sealed with rubber septum. The solution was left under stirring for several minutes and then purged for 30 minutes with argon. Homogeneous solution of styrene (6.84 mL) and DPPS (0.9 g) was added to the water solution prepared and then heated to 80 °C in a thermostated oil bath under stirring, ACPA solution was added before heat the solution. After 180 minutes, 0.1 mL of solution was taken to determine the monomer conversion. The overall monomer molar conversion was 98% as determined by ^1H NMR spectroscopy in DMSO-d6. The molar mass was analyzed by size exclusion chromatography (SEC) in THF (experimental Mn = 12100 g mol^{-1}; Đ = 1.2).

4.2.2.3 Step 3: Micelle core-cross-linking by RAFT chain extension with S and DEGDMA

New stock solution was prepared. In the same flask 1.09 mL of styrene, 0.23 mL

of DEGDMA, 1.22 mL of H_2O with 0.2 mL of ACPA, were added. The resulting solution was heated at 80 °C. After 120 minutes 0.1 mL of solution was taken to determine the monomer conversion. The overall monomer molar conversion was 98% as determined by ^1H NMR spectroscopy in DMSO-d6. The molar mass was analyzed by size exclusion chromatography (SEC) in THF (experimental Mn = 12100 g mol^{-1}; Đ = 1.2).

4.2.3 Loading of TPP@CCM with several metal precursors

Latexes metalated with the [RhCl(COD)] fragment were obtained by bridge-splitting of the corresponding dimer $[RhCl(COD)]_2$. A sample of TPP@CCM (5% or 20% DPPS) latex (1 mL, 0.06 mmol of TPP) was diluted with H_2O (3 mL), purged with Ar for 1 h, and swollen by addition of toluene (1 mL). The swelling was rapid as confirmed by visual partial disappearance of the toluene phase. To this sample was added $[RhCl(COD)]_2$ (14.8 mg, 0.03 mmol in ratio P/Rh = 1) in toluene (3 mL) and the resulting mixture was stirred at room temperature for 1 h, during which time the latex colour changed to yellow while the supernatant toluene phase became colourless. The aqueous phase was washed with toluene (3x2 mL) under argon to remove any excess of the Rh complex; both toluene washings were colourless. The resulting [RhCl(COD)(TPP@CCM)] latex was collected after decantation for further NMR studies. $^{31}P\{^1H\}$ NMR (162 MHz, $CDCl_3$, 298 K): δ 29.4 (d, J = 147 Hz). The same procedure was also used to load the latexes (5% or 20% DPPS) with the other metal precursors. Moreover, the same procedure was also used to load the latexes in different ratio, as P/Rh = 1 or P/Rh = 4, adjusting the amount of rhodium complex to the desired fraction. The ^{31}P NMR spectra of all metal precursors-loaded latexes were independent on the type of latex, depending only on the ratio of P/M.

4.2.4 Synthesis of metal nanoparticles M-NPs embedded in TPP@CCM

In the steel autoclave were putted five vials (about 5mL) containing different metal complex nano-objects, as M-TPP@CCM, (1 mL, 0.06 mmol) and NEt_3 (5 eq.) with addition of 1 mL of toluene. All the procedures were conducted under Ar, and the resulting closed system was left under stirring for 20 h under 20 bar of H_2, at desired temperature depending on the metal. At the end of the reaction the hydrogen pressure was removed and all vials containing M-TPP@CCM showed a black latex solution, confirming the metal reduction in polymeric nanoreactors. The toluene solution, in the upper part of the vial, was removed and the resulting nanoparticles were directly used in catalytic hydrogenation reaction.

4.2.4.1 Catalytic hydrogenation reaction

In the same steel autoclave where putted 5 vials containing: M NPs (1 mL), acetophenone (200 eq., 237.7 mg, $0.5 \cdot 10^{-3}$) and dodecane as internal standard, with the addition of 1 mL of toluene solution. All procedures were carried out under Ar and the closed system was left under stirring for 20 h under 20 bar of H_2 at different temperature depending on the used metal. At the end of the reaction the hydrogen pressure was removed and fast decantation of latex, embedding metal NPs, was observed. The organic phase was removed and recovered by a syringe. 0.1 mL of the resulting solution was diluted with 2 mL of toluene fresh solvent obtaining a suitable concentration for GC analysis.

4.2.5 Synthesis of metal nanoparticles M-NPs_HS in homogeneous solution

The procedure used for the synthesis of metal NPs embedded in polymeric nanoreactor was used also for the synthesis of metal nanoparticles in homogeneous solution. In fact, in the same steel autoclave were putted five vials (about 5 mL) containing PPh_3 (0.1 mmol) and metal precursor adjusting the amount to the desired fraction, and 1 mL of fresh toluene. In homogeneous solution, as for TPP@CCM, all the operations were carried out under Ar. The closed system was left under stirring for 20 h under 20 bar of H_2, at 25 °C. At the end of the reaction the colours of the homogenous solutions turned into black.

4.2.5.1 Catalytic hydrogenation reaction of homogenous metal NPs

The same procedure used for the application metal NPs embedded in TPP@CCM was employed for the homogenous metal nanoparticles. The ratios and amount of each reagent was always respected. All the metal NPs were applied only at 25 °C and analyzed by GC analysis using the same concentration of the recovered organic solution after catalysis.

CONCLUSIONS

The first goal of this work was the development of new synthetic strategies for the synthesis of active and recyclable cheap metal catalysts. In our approach, polymer supported Ni-nanoparticles (Ni-pol) were synthesized starting from a polymerisable β-ketoesterate Ni(II) complex, $Ni(AAEMA)_2$ [$AAEMA^-$ = deprotonated form of 2-acetoacetoxy ethyl methacrylate], which was co-polymerized with a suitable co-monomer (*N,N*-dimethylacrylamide) and cross-linker (*N,N*-methylenebisacrylamide) to give an insoluble organic resin supporting Ni(II) centres [$Ni(AAEMA)_2$-pol]. $Ni(AAEMA)_2$-pol was subsequently calcined at 300 °C giving rise to Ni-pol, which was fully characterized by IR, STEM and elemental analyses.

Ni-pol resulted air and moisture stable, swelling in water, acetone and halogenated solvents and shrinking in diethyl and petroleum ethers. Because of these features, we decided to test its catalytic activity in reactions carried out in an aqueous medium. In fact, it efficiently catalysed the transfer hydrogenation reaction of aromatic nitro compounds with $NaBH_4$ under sustainable conditions, in aqueous medium and room temperature. The new synthesized catalyst allows avoiding the use of the commonly employed noble metals. The same catalyst resulted active in the synthesis of secondary aromatic amines by a one-pot stepwise reductive amination of arylaldehydes with nitroarenes. STEM analyses showed that the active species were metallic Ni(0) nanoparticles ranging from 25 to 70 nm in diameter, stabilized by the polymeric support. Ni-pol was stable under reaction conditions and could be reused for at least five cycles keeping the same activity and selectivity. These occurrences are not trivial for catalysts supporting Ni nanoparticles, because the latter were found water-sensitive for similar catalytic systems. Moreover, Ni-pol catalyst was highly selective towards haloanilines, avoiding the hydro-dehalogenation side reaction. Finally, Ni-pol was also used as an active, selective and recyclable catalyst for the partial hydrogenation of poly-unsaturated fatty acid methyl esters for the upgrading of biofuels under mild conditions (10 bar of H_2, 60° C). All the results obtained for the Ni-catalyst were compared with results reported for the analogous Pd-catalyst. The comparison demonstrated that the Ni-catalyst was in all cases more selective than the noble metal Pd, although the latter showed higher activity than Ni-pol.

The second goal of this work was the synthesis of metal nanoparticles embedded in polymeric nanoreactors TPP@CCM (TPP = Triphenylphosphine; CCM = Core-Cross linked micelles) in collaboration with LCC-CNRS in Toulouse. In our strategy, a stable latex of unimolecular polymeric nanoreactors containing either a neutral or a cationic outer shell was used for the synthesis of metal nanoparticles (NPs), which were em-

bedded in TPP@CCM. By fine-tuning a few parameters in the syntheses of the TPP@CCM-embedded NPs, we were able to obtain a uniform distribution without formation of the agglomerates. The investigated metals were Rh, Pd, Ru, Ir, Pt and Au. These studies demonstrate that different metal nanoparticles can be obtained inside of polymeric nanoreactor as aqueous biphasic catalysts.

For all metals and type of TPP@CCM (containing either a neutral or a cationic shell), the NPs size increases by increasing the temperature. The catalytic activity of metal NPs-TPP@CCM, containing neutral or cationic outer shell, was investigated in the hydrogenation reaction of acetophenone under aqueous biphasic conditions. In all cases, the metal NPs remained confined in the latex phase during catalysis. The Rh and Pt-based system were the most active and selective catalysts among the investigated metals. The application of the NPs embedded in the polymeric nanoreactor containing the cationic shell revealed a limited mass transport, caused by the low compatibility of the acetophenone substrate with the polystyrene (PS) core. The activity of the Rh NPs was also tested in the hydrogenation of styrene, resulting in high activity and selectivity for the synthesis of ethylbenzene, which demonstrates a greater compatibility of styrene than acetophenone with the CCM core. Further studies are on-going to gain insight into the new developed nano-catalysts.

ACKNOWLEDGEMENTS

Ringrazio il mio tutor Piero Mastrorilli per avermi seguito con attenzione, per tutto quello che mi ha insegnato, per la sua disponibilità e per momenti piacevoli che abbiamo condiviso.

Ringrazio il mio tutor francese Rinaldo Poli, per avermi fatta sentire a casa quando ero spaesata e sola a Tolosa, per avermi insegnato la curiosità ed avermi permesso di scoprire quanto amore ci possa essere per la ricerca.

Ringrazio la mia co-tutor Maria Michela Dell'Anna, per avermi seguita in laboratorio con attenzione e dedizione, per tutta l'estrema disponibilità che ha mostrato e per essere sempre stata un punto di riferimento.

Ringrazio tutto il mio gruppo italiano per questi anni trascorsi insieme, per l'affetto e per i tanti caffe condivisi insieme. Un particolare ringraziamento va alle mie amiche, più che college, Stefania e Valentina. Sono state per me una spalla sia nei momenti difficili che nei momenti felici. La nostra complicità é stata per me una forza.

I'm grateful to team G in the LCC-CNRS of Toulouse. In particular to the polymer team which become my family for six month. I felt at home from the first days. A special thank is for Sandrine and Boss Christophe which teach me several things; to Lucas, for the coffee and hot water in the early morning; to Hui for the laughs in the office; to my Boss Eric for all the discussions. Thanks to all, Kevin also, for let me cry before leave, for all the presents, for their friendship. Toulouse became my second house, I cried when I arrived and I cried before leave. Merci a tout le monde!

One of the most big thank is for my best friend Jirong. For her there are no words that can really explain what she was and is for me. Thank you for shops, shopping, coffe,w wine and all the moments spent together. We are the evidence that friendship did not have nationality and distance. The life in Toulouse was the best period of my life, thanks forever.

Ringrazio con tanto amore mamma e papà. Per tutto il supporto che non mi hanno mai fatto mancare in questi anni. Per il tempo trascorso a Tolosa insieme. Per le chiamate infinite e per aver ascoltato e sopportato tutti i miei sfoghi. Sono stati, sono e saranno sempre per me la mia prima, meravigliosa e stupenda famiglia. Non c'é stato giorno in cui mi abbiano fatta sentire sola, per questo ve ne sono e ne sarò eternamente grata.

Ringrazio Giuseppe, Maria e i miei amati nipotini Paco e Gabri per i momenti passati insieme e tutto l'affetto che ci siamo dati negli anni. Un particolare grazie di cuore va al mio sempre Pippo, per aver trascorso con me un weekend a Tolosa. È stato un momento bellissimo che non dimenticherò mai.

Ringrazio la mia nonnina, per essere ancora qui a guadare i miei traguardi e a festeg-

giare insieme. Ringrazio anche i miei nonni che non ci sono più perchè so che non hanno smesso un momento di guardarmi da lassù. Un immenso ed eterno grazie va alla mia luce, sempre presente, che mi ha indicato la via nelle notti più buie. Il mio faro, la persona che dopo quasi 20 anni mi manca sempre nello stesso profondissimo modo.

Ringrazio con tantissimo affetto il mio, ormai amico, Enzo. In questo caso, non é necessario dire nulla, solo grazie mille per tutto.

Ringrazio i colleghi del dottorato, e in particolare Vincenzo per esserci sempre supportati e spalleggiati in questi tre anni.

Ringrazio le mie amiche, Milvia e Silvia per essere per me sempre le ragazze delle scale, nonostante le distanze.

Ringrazio i miei migliori amici Prugno e Vurro per essere sempre li stessi e sempre i migliori.

Ringrazio il moi cagnolino Milo, per avermi fatto tanta compagnia quando scrivevo la tesi e per il suo essere sempre così immensamente felice.

Ringrazio Andrea. Lo ringrazio per tutto, per il sostegno, per le attenzioni, per le coccole. Per essere per me da 5 anni una spalla, per sentirci sempre vicini anche se lontani. Lo ringrazio per tutte le volte che non ho avuto bisogno di parlare e lui già sapeva, per avermi incoraggiata e spronata quando ero stanca e pensavo di non farcela. Per essere stato il mio migliore amico prima e poi per essere diventato l'uomo della mia vita. Il futuro é meraviglioso ogni volta che lo guardiamo insieme. Grazie per tutto l'amore del mondo.

CURRICULUM

Name	FIORE, Ambra Maria
Place and date of birth	Bari, Italy; September, 10, 1991
Structure	Polytechnic University of Bari – Department of Civil, Environmental, Land, Building Engineering and Chemistry
Address	Via E. Orabona 4, 70125, Bari (Italy)
Phone	+39 3471282628
e-mail	ambramaria.fiore@poliba.it ambrafiore@gmail.com
Education	From October 2005 to July 2010 : Classic high school "Socrate" – Bari. From October 2010 to July 2014: Degree in Materials Science, University of Bari "Aldo Moro" Inter-university Department of Physics "M. Merlin", discussing a thesis on "Solid state transformation of iron-bearing hydrated sulfate to α-Fe_2O_3". Supervisor: Emanuela Schingaro, Department of Earth and Geo-environmental Science. From October 2014 to July 2016: Master degree in Science and Materials Technology, University of Bari "Aldo Moro" Department of Chemistry, discussing a thesis on "Emicroconaine: Synthesis of new multifunctional dyes as π-conjugated structure." Supervisor: Gianluca Farinola, Department of Chemistry.
Positions	From November 2016 until today: Ph.D. student in the XXXII cycle of the PhD course in Risk and environmental, territorial and building development in Polytechnic University of Bari. Supervisors: Piero Mastrorilli, Rinaldo Poli. Co-supervisor: Maria Michela Dell'Anna. From September 2018 to march 2019: visiting Ph.D. student at the Laboratoire de Chimie de Coordination (LCC) CNRS (Toulouse), under the supervision of Prof. Rinaldo Poli (Equipe G: Ligands, complex architectures and catalysis).
Scientific Interest	My research activities focus on Chemistry, with specific interest on: synthesis of metal nanoparticles, polymer and catalyst; synthesis of molecules for industrial applications.

Scientific production	Peer-Reviewed Publications • Polymer supported Nickel nanoparticles as recyclable catalyst for reduction of nitroarenes to aniline in aqueous medium,. G. Romanazzi, **A.M. Fiore**, M. Mali, A. Rizzuti, C. Leonelli, A. Nacci, P.Mastrorilli, 2018, Molecular Catalysis, 446, 31-38, Elsevier. • Mild and efficient synthesis of secondary aromatic amines by one-pot stepwise reductive amination of arylaldehydes with nitroarenes promoted by reusable nickel nanoparticles. **A.M. Fiore**, G. Romanazzi, M. Latronico, C. Leonelli, M. Mali, A. Rizzuti, P. Mastrorilli, 2019, Molecular Catalysis, 476, 110507, Elsevier. In preparation for international Journals • Partial hydrogenation of FAMEs catalyzed by recyclable polymer supported Ni nanoparticles. **A.M. Fiore**, M.M. Dell'Anna, P. Mastrorilli, 2020. • Synthesis, characterization and catalytic applications of transition metal nanoparticles embedded in polymeric nanoreactors. **A.M. Fiore**, H. Wang, C. Friedel, K. Philippot, M.M. Dell'Anna, P. Mastrorilli, R. Poli, 2020. Proceedings • Solid state transformation of iron-bearing hydrated sulfate to α-Fe2O3. **A.M. Fiore**, G. Ventruti, E. Schingaro, 2015, Proscience, 2, 26-30, Digilabs (ISSN: 2283-5954; DOI:10.14644/amam.2015.005). • Nickel catalyst: The new face of catalysis in green chemistry. **A.M. Fiore**, M.M. Dell'Anna, M. Mali, G. Romanazzi, P. Mastrorilli, 2017, Scientific Research Abstracts, 6, 30, Digilabs (ISSN online: 2424-9147). • One-pot synthesis of aromatic secondary amines from nitroarenes under mild conditions in the presence of a recyclable polymer-supported nickel catalyst. **A.M. Fiore**, M.M. Dell'Anna, M. Mali, G. Romanazzi, P. Mastrorilli, 2018, Scientific Research Abstracts, 9, 26, Digilabs (ISSN online: 2424-9147). • Ni-nanoparticles: promising catalyst for synthesis of organic molecole. **A.M. Fiore**, M.M. Dell'Anna, C. Leonelli, M. Mali, G. Romanazzi, P. Mastrorilli, 2019, Atti VIII Workshop Nazionale Associazione Italiana di Chimica per Ingegneria, Università degli Studi di Messina (ISBN: 978-88-3319-047-1). • Synthesis, characterization and catalytic applications of transition metal nanoparticles embedded in polymeric nanoreactors. **A.M. Fiore**, H. Wang, C. Friedel, M. M. Dell'Anna, P. Mastrorilli, E. Manoury, R. Poli. 2019, Consiglio Nazionale delle Ricerche - Istituto di Cristallografia, Cnr Edizioni, (ISBN 978-88-8080-352-2).

Meetings-Participation	• 7th Euro-Mediterranean Symposium on Laser Induced Breakdown Spectroscopy, Bari, Italy, 16-20 September 2013. • 1st workshop of Poliba PhD students research (PhDays 2017), Bari, Italy, 11-12 December 2017. Poster presentation. • Q-NMR Day, Bari, Italy, 12 February 2017. • L'esperimento flessibile. Studi di diffrazione in condizioni non ambientali, Bari, Italy, 22 February 2017. • Analisi quantitativa di fasi cristalline: Metodi tradizionali e Chemiometria a confronto, Bologna, Italy, 6 February 2018. • Jours de Science, Toulouse, France, 11-14 December 2018.
Conferences	Oral Presentations • 2nd International Conference on Applied Mineralogy & Advanced Materials - 13th International Conference on Applied Mineralogy (AMAM-ICAM 2017), Castellaneta Marina (TA), Italy, 5-9 June 2017. • 3rd International Conference on Applied Mineralogy & Advanced Materials (AMAM 2018), Bari, Italy, 24-26 July 2018. • VIII AICIng Workshop: Advanced materials for sustainable energy, environmental and sensing applications, Lipari, Italy, 27-29 June 2019. • XLVII Congresso Nazionale della Divisione di Chimica Inorganica, Bari, Italy, 9-12 September 2019. Oral presentation. Poster Presentation • 1st International Conference on Atmospheric Dust (DUST 2014), Castellaneta Marina (TA), Italy, 1-6 June 2014. • 1st International Conference on Applied Mineralogy & Advanced Materials (AMAM 2015), Castellaneta Marina (TA), Italy, 7-12 June 2015. • 13th European Congress on Catalysis (EUROPACAT 2017), Florence, Italy, 27-31 August 2017. • 28th International Conference on Organometallic Chemistry (ICOMC 2018), Florence, Italy, 15-20 July 2018. Organizing Committees • 2nd International Conference on Applied Mineralogy & Advanced Materials - 13th International Conference on Applied Mineralogy (AMAM-ICAM 2017), Castellaneta Marina (TA), Italy, 5-9 June 2017. • 3rd International Conference on Applied Mineralogy & Advanced Materials (AMAM 2018), Bari, Italy, 24-26 July 2018. Invited Lecture • Materials SUMer ScHool (MESH 2019), Bari, Italy, 23-25 September 2019.

Schools	• 1st European Crystallography School, Erasmus Intensive Programme (EU Lifelong Learning Programme), Pavia, Italy, 28 August - 6 September 2014. • Sils School of Nanomedicine, Bari, Italy, 11-13 October 2017. • Italian Crystallographic Association (AIC) International Crystallography School (AICS2018), Bari, Italy, 28 August - 2 September 2018.
Prizes	• Best Oral Presentation Prize at the VII AICIng Workshop: Advanced materials for sustainable energy, environmental and sensing applications, Lipari, Italy, 27-29 June 2019.
Professional Society Memberships	• Società Chimica Italiana (SCI) • Associazione Italiana Cristallografia (AIC) • Associazione Italiana per lo Studio delle Argille (AISA) • International Association for the Study of Clays (AIPEA)
Responsibilities	Scientific Research Project related to the University Research Found (FRA 2019). Project manager: Francesca De Serio (ICAR/01-DICATECh- Polytechnic University of Bari.
Work experience	From January 2015 to September 2018 I was a teaching support for the Chemistry and Chemistry complements course, in degree course of Mechanical Engineering and common courses (in Polytechnic University of Bari).

REFERENCES

REFERENCES

1 G. Rothenberg, Catalysis concepts and green applications, Weinheim: Wiley-VCH (2018).
2 P. I. Anastas, N. Eghbali, Chem Soc Rev 39 (2010) 301-312.
3 J. Hagen, Industrial Catalysis: A Practical Approach; Wiley-VCH: Weinheim, Germany (2006) 1-14.
4 P.T. Anastas, L.B. Bartlett, M.M. Kirchhoff, T.C. Williamson, Catalysis Today 55 (2000) 11-22.
5 Spent Nuclear Fuel and Radioactive Waste Inventories, Projections and Characteristics. Report Tennessee (1994).
6 A. Chrubasik. Proc. Conf. on Thermal Treatment o Radioactive Hazardous Chemical and Mixed Wastes (1991) 137.
7 Radioactive Tank Waste Remediation Focus Area. Technology Summary, DOE/EM-0255, Oak Ridge, TN, (1995).
8 S. Chapman, M. E. Potter, R. Raja, Molecules 22 (2017) 2127.
9 M. Rayner-Canham, G. W. Rayner-Canham, American Chemical Society (2001).
10 E. Farnetti, R. Di Monte, J. Kašpar, Life Support Syst. II (1999) 10.
11 W. Hunt, Journal of the Minerals Metals & Materials Society 56 (2004)13.
12 I.Y. Jeon, J.B. Baek, Materials 3 (2010) 3654-74.
13 T. K. Sau, A. L. Rogach, Adv. Mater 22 (2010) 1781–1804.
14 O. Masala, R. Seshadri. Annual Review of Materials Research 34 (2004) 41–81.
15 H.M. Chen, R.S. Liu, Journal of Physical Chemistry C 115 (2011) 3513–27.
16 D.K. Tiwari, J. Behari and P. Sen, World Applied Sciences Journal 3 (2008) 417-433.
17 M. Salavati-niasari, F. Davar and N. Mir, Polyhedron 27 (2008) 3514-8.
18 C.Y. Tai, C. Tai, M. Chang, H. Liu, Industrial & Engineering Chemistry Research 46 (2007) 5536-5541.
19 S. Bhaviripudi, E. Mile, S.A. Steiner, A.T. Zare, M.S. Dresselhaus, A.M. Belcher, J. Kong, J. Am. Chem. Soc. 129 (2007) 1516-1517.
20 R.M. Crooks, M. Zhao, L.I. Sun, V. Chechik and L.K. Yeung, Acc. Chem. Res. 34 (2001) 181-190.
21 F. Zaera, Chem. Soc. Rev 7 (2013).
22 Uyanik M., Synthesis and characterization of TiO2 nanostars, PhD Thesis. Saarland University, Saarbrucken (2008) 199.
23 R. R. Schrock, in Handbook of Metathesis, ed. R. H. Grubbs, Wiley-VCH, Weinheim 1 (2003) ch. 1.3 - 1.11.
24 D. Astruc, Anal Bioanal Chem 399 (2011)1811–1814.
25 S.J. Guo, E.K. Wang, Nano Today, 6 (2011) 240-264.
26 M. Cuia, Y. Chena, Q.F. Xiea, D.P. Yanga, M.Y. Han, Coordination Chemistry review (2019).
27 T.G.S. Neto, A.J.G. Cobo, G.M. Cruz, Appl. Catal. A: General 250 (2003) 331–340.
28 M. Zahmakiran, Dalton Transations 41 (2012) 12690-12696.
29 G. S. Fonseca, J. D. Scholten, J. Dupont, Synlett 9, 2004,1525-1528.
30 G. S. Fonseca, A. P. Umpierre, P. F. P. Fichtner, S. R. Teixeira, J. Dupont, Chem. Eur. J. 9 (2003) 3263 -3269.
31 M.J. Jacinto, P.K. Kiyohara, S.H. Masunaga, R.F. Jardim, L.M. Rossi, Applied Catalysis A: General 338 (2008) 52-57.
32 S. Akbayrak, Y. Tonbul, S. Ozkar, Applied catalysis B: Environmental 198 (2016)162-170.
33 J.L. Pellegatta, C. Blandy, V. Collière, R. Choukroun, B. Chaudret, P. Cheng, K. Philippot, Journal of molecular catalysis A 178 (2002) 55-61.
34 A. Javey, J. Guo, Q. Wang, M. Lundstrom, H. J. Dai, 424 (2003) 654–657.
35 H. U. Blaser, A. Indolese, A. Schnyder, H. Steiner, M. Studer, J. Mol. Catal. A-Chem. 173 (2001) 3–18.
36 Suzuki, J. Organomet. Chem. 576 (1999) 147–168.
37 M.L. Kantam, M. Roy, S. Roy, B. Sreedhar, S.S. Madhavendra, B.M. Choudary, R.L. De, Tetrahedron 63 (2007) 8002–8009.
38 J. Lemo, K. Heuze, D. Astruc, Chem. Commun. 42 (2007) 4351–4353.
39 N. Nakamura, Y. Tajima, K. Sakai, Heterocycles 17 (1982) 235-245.

40 M. Parsien, D. Valette, K. Fagnou, J.Org. Chem. 70 (2005) 7578-7584.
41 L. Joucla, L. Djakovitch, Adv. Syth. Catal. 351 (2009) 673-714.
42 S. Santoro, S.I. Kozhushkov, L. Ackermann, L. Vaccaro, Green Chem. 18 (2016) 3471-3493.
43 S. Mandal, D. Roy, R. V. Chaudhari, M. Sastry, Chem. Mater. 16 (2004) 3714-3724
44 D. Guin, B. Baruwati, S. V Manorama, Organic Letters 9 (2007) 1419-1421.
45 J.F.G.A. Jansen, E.W. Meijer, E.M.M. de Brabander-van den Berg, J. Am. Chem. Soc. 117 (1995) 4417-4418.
46 O. M. Wilson, M.R. Knecht, J.C. Garcia-Martinez, R.M. Crooks, J. Am. Chem. Soc. 128 (2006) 4510-4511.
47 S. Crossley, J. Faria, M. Shen, D. E. Resasco, Science 327 (2010) 68-72.
48 H.S. Nalwa, Handbook of Surfaces and Interfaces of Materials 1 (2001).
49 J. A. Schwarz, C. Contescu, A. Contescu, Chem. Rev. 95 (1995) 477–510.
50 P.E. De Jongh, T.M. Eggenhuisen, Adv. Mater. 25 (2013) 6672.
51 J. Park, J. Joo, S. G. Kwon, Y. Jang, T. Hyeon, Angew. Chem. Int. Ed. 46 (2007) 4630.
52 J. E. Mondloch, E. Bayram, R.G. Finke, J. Mol. Catal. A, 355 (2012) 1.
53 G. Prieto, J. Zečević, H. Friedrich, K. P. de Jong, P. E. de Jongh, Nat. Mater. 12 (2013) 34.
54 V. R. Calderone, N.R. Shiju, D. Curulla-Ferré, S. Chambrey, A.Y. Khodakov, A. Rose, J. Thiessen, A. Jess, G. Rothenberg, Angew. Chem. 52 (2013) 4397.
55 J.P. Collman, L.S. Hegedus, M.P. Cooke, J.R. Norton, G. Dolcetti, D.N. Marquardt, J. Am. Chem. Soc. 94 (1972) 1789.
56 A. Akaleh, D.C. Sherrington, Polymer 24 (1983) 1369.
57 B.C. Gates, Catalytic Chemistry, 4 (1992)182-253.
58 M.J. Sundell, J.H. Nasman, Chem tech 23 (1993) 16.
59 T. Nishikubo, A. Kamayana, C. Maejima, Y. Yamamoto, Macromolecules 27 (1994) 7240.
60 M.M. Dell'Anna, G. Romanazzi, P. Mastrorilli, Current Organic Chemistry, 17 (2013) 1236-1273.
61 M.M. Dell'Anna, M. Mali, P. Mastrorilli, A. Rizzuti, C. Ponzoni, C. Leonelli, Journal of Molecular catalysis A, Chemical 366 (2013) 186-194.
62 M.M. Dell'Anna, M. Mali, P. Mastrorilli, P. Cotugno, A. Monopoli, Journal of Molecular Catalysis A: Chemical 386 (2014) 114–119.
63 M.M. Dell'Anna, V.F. Capodiferro, M. Mali, D. Manno, P. Cotugno, A. Monopoli, P. Mastrorilli, Applied catalysis A: general 481 (2014) 89-95.
64 M.M. Dell'Anna, P. Mastrorilli, A. Rizzuti, C. Leonelli, Applied Catalysis A: General 401 (2011) 134–140.
65 M.M. Dell'Anna, S. Intini, G. Romanazzi, A. Rizzuti, C. Leonelli, F. Piccinni, P. Mastrorilli, Journal of Molecular Catalysis A: Chemical 395 (2014) 307-314.
66 T. Fujihara, Y. Horimoto, T. Mizoe, F.B. Sayyed, Y. Tani, J. Terao, S. Sakaki, Y. Tsuji, Org. Lett. 16 (2014) 4960-4963.
67 Z. Tasker, E.A. Standley, T.F. Jamison, Nature 509 (2014) 299-309.
68 A.J. Burke, C. Silva Marques, Wiley-VCH, Weinheim, (2015).
69 J.P. Klelman, M. Dubeck, J. Am. Chem. Soc. 85 (1963) 1544–15459.
70 L.C. Liang, P.S. Cheng, Y.L. Huang, J. Am. Chem. Soc. 128 (2006) 15562–15563.
71 J. Canivet, J. Yamaguchi, I. Ban, K. Itami, Org. Lett. 11 (2009) 1733–1736.
72 H. Hachiya, K. Hirano, T. Satoh, M. Miura, Org. Lett. 11 (2009) 1737–1740.
73 T. Yamamoto, K. Muto, M. Komiyama, J. Canivet, J. Yamaguchi, K. Itami, Chem. Eur. J. 17 (2011) 10113–10122.
74 N. Matsuyama, K. Hirano, T. Satoh, M. Miura, Org. Lett. 11 (2009) 4156–4159.
75 O. Vechorkin, V. Proust, X. Hu, Angew Chem. Int. Ed. 49 (2010) 3061–3064.
76 T. Yao, K. Hirano, T. Satoh, M. Miura, Chem. Eur. J. 16 (2010) 12307–12311.
77 H. Hachiya, K. Hirano, T. Satoh, M. Miura, Angew Chem. Int. Ed. 49 (2010) 2202–2205.
78 Z. Ruan, S. Lackner, L. Ackermann, Angew Chem. Int. Ed 55 (2016) 3153–3157.
79 V. Iaroshenko, I. Ali, S. Mkrtchyan, V. Semeniuchenko, D. Ostrovskyi, P. Langer, Synlett 23 (2012) 2603–2608.

80 K. Muto, T. Hatakeyama, J. Yamaguchi, K. Itami, Chem. Sci. 6 (2015) 6792–6798.
81 T. Yamamoto, A. Yamamoto, S. Ikeda, J. Am. Chem. Soc. 93 (1971) 3350.
82 K. Tamao, K. Sumitani, M. Kumada, J. Am. Chem. Soc. 94 (1972) 4374.
83 R.J.P. Corriu, J.P. Masse, J. Chem. Soc. Chem. Commun. 144 (1972).
84 M.R. Netherton, C. Dai, K. Neuschutz, G.C. Fu, J. Am. Chem. Soc. 123 (2001) 10099.
85 N. Hadei, E.A.B. Kantchev, C.J. O'Brien, M.G. Organ, Org. Lett. 7 (2005) 3805.
86 a) M.R. Netherton, G.C. Fu, Top Organomet. Chem. 14 (2005) 859. b) N. Kambe, T. Iwasaki, J. Terao, Chem. Soc. Rev. 40 (2011) 4937.
87 X. Hu, Chem. Sci. 2 (2011) 186718.
88 B.L.H. Taylor, E.R. Jarvo, Synlett (2011) 276119.
89 E.C. Swift, E.R. Jarvo, Tetrahedron 69 (2013) 57920.
90 S.Z. Tasker, E.A. Standley, T.F. Jamison, Nature 509 (2014) 299.
91 A. Devasagayaraj, T. Studemann, P. Knochel, Angew. Chem. Int. Ed. 34 (1995) 2723.
92 R. Giovannini, T. Studemann, G. Dussin, P. Knochel, Angew. Chem. Int. Ed. 3 (1998) 2387.
93 R. Giovannini, T. Studemann, A. Devasagayaraj, G. Dussin, P. Knochel, J. Org. Chem. 64 (1999) 3544.
94 M. Piber, A.E. Jensen, M. Rottlander, P. Knochel, Org. Lett. 1 (1999) 1323.
95 V.B. Phapale, E. Bunuel, M. Garcia-Iglesias, D.J. Cardenas, Angew. Chem. Int. Ed. 46 (2007) 8790.
96 M. Guisan-Ceinos, R. Soler-Yanes, D. Collado-Sanz, V.B. Phapale, E. Bunuel, D.J. Cardenas, Chem. Eur. J. 19 (2013) 8405.
97 T. Qin, J. Cornella, C. Li, L.R. Malins, J.T. Edwards, S. Kawamura, B.D. Maxwell, M.D. Eastgate, P.S. Baran, Science 352 (2016) 801.
98 R. Giovannini, P. Knochel, J. Am. Chem. Soc. 120 (1998) 11186.
99 M. Uemura, H. Yorimitsu, K. Oshima, Chem. Commun. (2006) 4726.
100 D.A. Powell, G.C. Fu, J. Am. Chem. Soc. 126 (2004) 7788.
101 D.A. Powell, T. Maki, G.C. Fu, J. Am. Chem. Soc. 127 (2005) 510.
102 S. Pisiewicz, D. Formenti, A.E. Surkus, M.M. Pohl, J. Radnik, K. Junge, C. Topf, S. Bachmann, M. Scalone, M. Beller, Chem. Cat. Chem. 8 (2016) 129–134.
103 P. Serna, A. Corma, ACS Catal. 5 (2015) 7114–7121.
104 P. Zhang, C. Yu, X. Fan, X. Wang, Z. Ling, Z. Wang, J. Qiu, Phys. Chem. 17 (2015) 145–150.
105 T. Wang, Z. Dong, T. Fu, Y. Zhao, T. Wang, Y. Wang, Y. Chen, B. Han, W. Ding, Chem. Commun. 51 (2015) 17712–1771.
106 S. Cai, H. Duan, H. Rong, D. Wang, L. Li, W. He, Y. Li, ACS Catal. 3 (2013) 608–612.
107 J.A. Johnson, J.J. Makis, K.A. Marvin, S.E. Rodenbusch, K.J. Stevenson, J. Phys. Chem. C 117 (2013) 22644–22651.
108 H. Ma, H. Wang, C. Na, Appl. Catal. B 163 (2015) 198–204.
109 S. Pandey, S.B. Mishra, Carbohydr. Polym. 113 (2014) 525–531.
110 P. Etayo, A. Vidal-Ferran, Chem. Soc. Rev. 42 (2013) 728–754.
111 S. Wesselbaum, T. vom Stein, J. Klankermayer, W. Leitner, Angew. Chem. 124 (2012) 7617–7620.
112 C. Lin, K. Tao, D. Hua, Z. Ma, S. Zhou, Molecules 18 (2013) 12609–12620.
113 T. Ji, L. Li, M. Wang, Z. Yang, X. Lu, RSC Adv. 4 (2014) 29591–29594.
114 A. Wang, H. Yin, M. Ren, H. Lu, J. Xue, T. Jiang, New J. Chem. 34 (2010) 708–713.
115 M. Ajmal, M. Siddiq, H. Al-Lohedan, N. Sahiner, RSC Adv. 4 (2014) 59562–59570.
116 D.F. Foster, D. Gudmunsen, D.J. Adams, A.M. Stuart, E.G. Hope, D.J. Cole-Hamilton, G.P. Schwarz, P. Pogorzelec, Tetrahedron 58 (2002) 3901–3910.
117 A. Sharma, C. Julcour-Lebigue, R.M. Deshpande, A.A. Kelkar, H. Delmas, Ind. Eng. Chem. Res. 49 (2010)10698–10706.
118 B. Cornils, Org. Process Res. Dev. 2 (1998) 121–127.
119 J.Manassen, in: F. Basolo, R.L. Burwell (Eds.), Catalysis Progress in Research (1973)177f.
120 E. Wiebus, B. Comils, Chem. Ing. Techn. 66 (1994) 916.
121 B. Comils, E. Wiebus, CHEMTECH 25 (1995) 33; E. Wiebus, B. Cornils, Hydrocarbon Process (1996) 63.

122 B. Cornils, W.A. Herrmann, Eds. Applied Homogeneous Catalysis with Organometallic Compounds; VCH: Weinheim, Germany 2 (1996).
123 C.W. Kohlpaintner, R.W. Fischer, B. Cornils, Appl. Catal. A 221 (2001) 219–225.
124 M. Deshpande, P. Purwanto, H. Delmas, R.V. Chaudhari, Ind. Eng. Chem. Res. 35 (1996) 3927–3933.
125 F.X. Legrand, F. Hapiot, S. Tilloy, A. Guerriero, M. Peruzzini, L. Gonsalvi, E. Monflier, Appl. Catal. A, 362 (2009) 62–66.
126 E. Hermanns, J. Hasenjaeger, B. Driessen-Hoelscher, Top. Organomet. Chem. 23 (2008) 53–66.
127 M.N. Khan, Micellar Catalysis (2006) 464.
128 V.C. Reinsborough, Micellar catalysis. In: Volkov AG (ed) Intercial catalysis (2002) 377-390.
129 M.N. Khan, Micellar catalysis (2006).
130 P. Cotanda, N. Petzetakis, R. K. O'Reilly, MRS Commun. 2 (2012) 119–126.
131 a) R.K. O'Reilly, C.J. Hawker, K.L. Wooley, Chem. Soc. Rev. 35 (2006) 1068 –1083; b) H. Gao, K. Matyjaszewski, Progr. Polym. Sci. (2009), 34, 317 –350.
132 T. Terashima, M. Ouchi, T. Ando, M. Kamigaito, M. Sawamoto, Macromolecules 40 (2007) 3581–3588.
133 T. Terashima, A. Nomura, M. Ito, M. Ouchi, M. Sawamoto, Angew. Chem. 123 (2011) 8038–8041.
134 T. Terashima, M. Ouchi, T. Ando, M. Sawamoto, J. Polym. Sci. Part A 49 (2011) 1061–1069.
135 J.T. Sun, C.Y. Hong, C.Y. Pan, Polym. Chem. 4 (2013) 873–881.
136 A.D. Levins, X.F. Wang, A.O. Moughton, J. Skey, R.K. O'Reilly, Macromolecules 41 (2008) 2998-3006.
137 A. Lu, D. Moatsou, D.A. Longbottomb, R.K. O'Reilly, Chem. Sci. 4 (2013) 965.
138 X. Zhang, A.F. Cardozo, S. Chen, W. Zhang, C. Julcour, M. Lansalot, J.F. Blanco, F. Gayet, H. Delmas, B. Charleux, E. Manoury, F. D'Agosto, R. Poli. Chem. Eur. J. 20 (2014) 15505-15517.
139 J. Ji, J. Wang, Y. Li, Y. Yu, Z. Xu, Ultrasonics 44 (2006) 411-4.
140 T. Terashima, T.A.M. Ouchi, M. Kamigaito, M. Sawamoto, Journal of Polymer Science Part A: Polymer Chemistry 44 (2006) 4966–4980.
141 T. Terashima, M. Kamigaito, K.Y. Baek, T. Ando, M. Sawamoto, J. Am. Chem. Soc. 125 (2003) 5288–5289.
142 A.F. Cardozo, C. Julcour, L. Barthe, J.F. Blanco, S. Chen, F. Gayet, E. Manoury, X. Zhang, M. Lansalot, B. Charleux, F. D'Agosto, R. Poli and H. Delmas, J. Catal. 324 (2015) 1-8.
143 E. Lobry, A.F. Cardozo, L. Barthe, J.F. Blanco, H. Delmas, S. Chen, F. Gayet, X. Zhang, M. Lansalot, F. D'Agosto, R. Poli, E. Manoury, C. Julcour, J. Catal. 342 (2016) 164-172.
144 J. Xu, X. Xiao, Y. Zhang, W. Zhang, P. Sun, J. Polym. Sci. Part A 51(2013) 1147–1161.
145 E. Velasquez, J. Rieger, F. Stoffelbach, B. Charleux, F. D'Agosto, M. Lansalot, P.E. Dufils, J. Vinas, Polymer 54 (2013) 6547–6554.
146 S. Chen, F. Gayet, E. Manoury, A. Joumaa, M. Lansalot, F. D'agosto, R. Poli, Chem. Eur. J. 22 (2016) 6302-6313.
147 A. Joumaaa, S. Chen, S. Vincendeau, F. Gayet, R. Poli, E. Manoury, Molecular Catalysis 438 (2017) 267–271.
148 F.R. Hartley, D. Reidel Publishing Company, Dordrecht, (1985).
149 J. Guzman, B.C. Gates, Dalton Trans. (2003) 3303-3318.
150 N.E. Leadbeater, M. Marco, Chem. Rev. 102 (2002) 3217.
151 C.A. Mc Namara, M.J. Dixon, M. Bradley, Chem. Rev. 102 (2002) 3275.
152 P. Mastrorilli, C.F. Nobile, Tetrahedron Lett. 35 (1994) 4193.
153 L. Lopez, P. Mastrorilli, G. Mele, C.F. Nobile, Tetrahedron Lett. 35 (1994) 3633.
154 N.M. Brunkan, M.R. Gagnè, J. Am. Chem. Soc. 122 (2000) 6217.
155 P. Mastrorilli, C.F. Nobile, G.P. Suranna, L. Lopez, Tetrahedron 51 (1995) 7943.
156 A.S. Rozenberg, A.V. Raevskii, E.I. Aleksandrova, O.I. Kolesova, G.I. Dzhardimalieva, A.D. Pomogailo, Russ. Chem. Bull. Int. Ed. 50 (2001) 901.
157 A.D. Pomogailo, V.F. Razumov, I.S. Voloshanovskii, J. Porphyrins Phthalocyanines 4 (2000) 45.
158 G.I. Dzhardimalieva, A.D. Pomogailo, Macromol. Symp. 186 (2002) 147.
159 K. Sreenivasan, J. Appl. Polym. Sci. 80 (2001) 2795.
160 A.M. Fiore, G. Romanazzi, M. Latronico, C. Leonelli, M. Mali, A. Rizzuti, P. Mastrorilli, Mol. Catal. 476

(2019) 110507.
161 M.M. Dell'Anna, P. Mastrorilli, C.F. Nobile, G.P. Suranna, J. Mol. Cat. A Chem. 103 (1995)17-22.
162 P.F. Vogt, J.J. Gerulis, Ullmann's Encyclopedia of Industrial Chemistry, in Aromatic Amines, Wiley-VCH Verlag GmbH & Co., Weinheim, (2005).
163 (a) S. Nishimura, Handbook of Heterogeneous Catalytic Hydrogenation for Organic Synthesis, John Wiley & Sons (2001); (b) R.A. Sheldon, H. van Bekkum (Eds.), Fine Chemicals through Heterogeneous Catalysis, Wiley-VCH, Weinheim, (2001); (c) R.V. Jagadeesh, A.E. Surkus, H. Junge, M.M. Pohl, J. Radnik, J. Rabeah, H. Huan, V. Schünemann, A. Brückner, M. Beller, Science 342 (2013) 1073–1076; (d) H.U. Blaser, H. Steiner, M. Studer, Chem. Cat. Chem 1 (2009) 210–221; (e) M.M. Dell'Anna, V. Gallo, P. Mastrorilli, G. Romanazzi, Molecules 15 (2010) 3311–3318; (f) R. Begum, R. Rehan, Z.H. Farooqi, Z. Butt, S. Ashraf, J. Nanopart. Res 18 (2016) 231.
164 D. Cantillo, M.M. Moghaddam, C.O. Kappe, J. Org. Chem. 78 (2013) 4530–4542.
165 K. Junge, B. Wendt, N. Shaikh, M. Beller, Chem. Commun. 46 (2010) 1769–1771.
166 D.M. Dotzauer, S. Bhattacharjee, Y. Wen, M.L. Bruening, Langmuir 25 (2009) 1865–1871.
167 T. Subramanian, K. Pitchumani, Chem. Cat. Chem 4 (2012) 1917–1921.
168 (a) J. Sun, Y. Fu, G. He, X. Sun, X. Wang, Catal. Sci. Technol. 4 (2014) 1742–1748; (b) O. Verho, A. Nagendiran, C.W. Tai, E.V. Johnston, J.E. Backvall, Chem. Cat. Chem. 6 (2014) 205–211.
169 X. Liu, S. Ye, H.Q. Li, Y.M. Liu, Y. Cao, K.N. Fan, Catal. Sci. Technol. 3 (2013) 3200–3206.
170 J.H. Kim, J.H. Park, Y.K. Chung, K.H. Park, Adv. Synth. Catal. 354 (2012) 2412–2418.
171 A.K. Patra, N.T. Vo, D. Kim, Appl. Catal. A Gen. 538 (2017) 148–156.
172 (a) H. Ma, H. Wang, T. Wu, C. Na, Appl. Catal. B Environ. 180 (2016) 471–479; (b) D. Formenti, C. Topf, K. Junge, F. Ragaini, M. Beller, Catal. Sci. Technol. 6 (2016) 4473-4477; (c) X. Wang, Y. Li, J. Mol. Catal. A Chem. 420 (2016) 56–65.
173 (a) R.J. Kalbasi, A.A. Nourbakhsh, F. Babaknezhad, Catal. Commun. 12 (2011) 955–960; (b) M.B. Gawande, A.K. Rathi, P.S. Branco, I.D. Nogueira, A. Velhinho, J.J.Shrikhande, U.U. Indulkar, R.V. Jayaram, C.A.A. Ghumman, N. Bundaleski, O.M.N.D. Teodoro, Chem. Eur. J. 18 (2012) 12628–12632; (c) G. Hahn, J.K. Ewert, C. Denner, D. Tilgner, R. Kempe, Chem. Cat. Chem. 8 (2016) 2461–2465; (d) Y. Qu, H. Yang, S. Wang, T. Chen, G. Wang, Catal. Commun. 97 (2017) 83–87.
174 A. Corma, P. Serna, Science 313 (2006) 332–334.
175 N.S. Chaubal, M.R. Sawant, J. Mol. Catal. A Chem. 261 (2007) 232–241.
176 L. Zhou, H. Gu, X. Yan, Catal. Lett. 132 (2009) 16-21.
177 A. Westerhaus, R.V. Jagadeesh, G. Wienhçfer, M.M. Pohl, J. Radnik, A.E. Surkus, J. Rabeah, K. Junge, H. Junge, M. Nielsen, A. Bruckner, M. Beller, Nat. Chem. 5 (2013) 537–543.
178 R.V. Jagadeesh, A.E. Surkus, H. Junge, M.M. Pohl, J. Radnik, J. Rabeah, H. Huan, V. Schnemann, A. Bruckner, M. Beller, Science 342 (2013) 1073–1076.
179 T. Stemmler, F.A. Westerhaus, A.E. Surkus, M.M. Pohl, K. Junge, M. Beller, Green Chem. 16 (2014) 4535–4540.
180 O. Beswick, I. Yuranov, D.T. Alexander, L. Kiwi-Minsker, Catal. Today 249 (2015) 45–51.
181 a) T. Fu, M. Wang, W. Cai, Y. Cui, F. Gao, L. Peng, W. Chen, W. Ding, ACS Catal. 4(2014) 2536–2543; b) P. Zhang, C. Yu, X. Fan, X. Wang, Z. Ling, Z. Wang, J. Qiu, Phys. Chem.Chem. Phys.2015,17, 145–150; c) T. Wang, Z. Dong, T. Fu, Y. Zhao, T. Wang, Y. Wang, Y. Chen, B. Han, W. Ding, Chem. Commun. 51 (2015) 17712–17715; d) X. Liu, X. Ma, S. Liu, Y. Liu, C. Xia, RSC Adv. 5 (2015) 36423–36427.
182 S. Cai, H. Duan, H. Rong, D. Wang, L. Li, W. He, Y. Li, ACS Catal. 3 (2013) 608–612.
183 G. Hahn, J.K. Ewert, C. Denner, D. Tilgner, R. Kempe, Chem. Cat. Chem. 8 (2016) 1-6.
184 W. Lin, H. Cheng, J. Ming, Y. Yu, F. Zhao, J. Catal. 291 (2012) 149–154.
185 H.A. Rojas, J.A. Cubillos, J.J. Martínez, D.C. Guerrero, P. Reyes, Curr. Org. Chem. 16 (2012) 2770–2773.
186 K.A. Kumar, K.S. Shruthi, N. Naik, C. Gowda, E.J. Chem. 4 (2008) 914–917.
187 A.S. Travis, Anilines: Historical Background. Z., Ed.; John Wiley & Sons (2007) 1-75.
188 P.F. Vogt, J.J. Gerulis, Ullmann's Encyclopedia of Industrial Chemistry, in Aromatic Amines, Wiley-VCH Verlag GmbH & Co., Weinheim, (2005).

189 F. Li, B. Frett, H.Y. Li, Synlett 25 (2014) 1403–1408.
190 K. Junge, B. Wendt, N. Shaikh, M. Beller, Chem. Commun. 46 (2010) 1769–1771.
191 L. Li, Z. Chen, H. Zhong, R. Wang, Chem. Eur. J. (2014) 3050–3060.
192 T. Subramanian, K. Pitchumani, Chem. Cat. Chem. 4 (2012) 1917–1921.
193 O. Verho, A. Nagendiran, C.W. Tai, E.V. Johnston, J.E. Backvall, Chem Cat Chem 6 (2014) 205–211.
194 X. Liu, S. Ye, H.Q. Li, Y.M. Liu, Y. Cao, K.N. Fan, Catal. Sci. Technol. 3 (2013) 3200–3206.
195 J.H. Kim, J.H. Park, Y.K. Chung, K.H. Park, Adv. Synth. Catal. 354 (2012) 2412–2418.
196 A.K. Patra, N.T. Vo, D. Kim, Appl. Catal. A Gen. 538 (2017) 148–156.
197 X. Wang, Y. Li, J. Mol. Catal. A Chem. 420 (2016) 56–65.
198 R.J. Kalbasi, A.A. Nourbakhsh, F. Babaknezhad, Catal. Commun. 12 (2011) 955–960.
199 M.B. Gawande, A.K. Rathi, P.S. Branco, I.D. Nogueira, A. Velhinho, J.J. Shrikhande, U.U. Indulkar, R.V. Jayaram, C.A.A. Ghumman, N. Bundaleski, O.M.N.D. Teodoro, Chem. Eur. J. 18 (2012) 12628-12632.
200 B. Sreedhar, P. Surendra Reddy, D. Keerthi Devi, J. Org. Chem. 74 (2009) 8806-8809.
201 X. Wang, M. Liang, H. Liu, Y. Wang, J. Mol. Catal. A Chem. 273 (2007) 160-168.
202 M. Liang, X. Wang, H. Liu, H. Liu, Y. Wang, J. Catal. 255 (2008) 335-342.
203 X. Yuan, N. Yan, C. Xiao, C. Li, Z. Fei, Z.Cai, Y. Kou, P.J. Dyson, Green Chem. 12 (2010) 228-233.
204 B.J. Zuo, Y. Wang, L. Wang, J.L. Zhang, N.Z. Wu, L.D. Peng, L.L. Gui, X.D. Wang, R.M. Wang, D.P. Yu, J. Catal. 222 (2004) 493-498.
205 O. Verho, A. Nagendiran, C.W. Tai, E.V. Johnston, J.E. Bäckvall, Chem. Cat. Chem. 6 (2014) 205–211.
206 O. Verho, K.P.J. Gustafson, A. Nagendiran, C.W. Tai, J.E. Back-vall, Chem. Cat. Chem. 6 (2014) 3153–3159.
207 C. Lu, M. Wang, Z. Feng, Y. Qi, F. Feng, L. Ma, Q. Zhang, X. Li, Catal. Sci. Technol. 7 (2017) 1581–1589.
208 W. Yu, L.L. Lou, S. Li, T. Ma, L. Ouyang, L. Feng, S. Liu, RSC Adv. 7 (2017) 751–757.
209 F. Alonso, I.P. Beletskaya, M. Yus, Chem. Rev. 102 (2002) 4009–4092.
210 M. Gruttadauria, F. Giacalone, R. Noto, Green Chem. 15 (2013) 2608–2618.
211 W. Lin, H. Cheng, J. Ming, Y. Yu, F. Zhao, J. Catal. 291 (2012) 149–154.
212 B.H. Liu, Z.P. Li, J. Power Sources 187 (2009) 527–534.
213 A. Saha, B. Ranu, J. Org. Chem. 73 (2008) 6867–6870.
214 A.K. Shil, D. Sharma, N.R. Guha, P. Das, Tetrahedron Lett. 53 (2012) 4858–4861.
215 K. Layek, M.L. Kantam, M. Shirai, D. Nishio-Hamane, T. Sasaki, H. Maheswarana, Green Chem. 14 (2012) 3164–3174.
216 E.A. Gelder, S.D. Jackson, C.M. Lok, Chem. Commun. (2005) 522–524.
217 A. Mahata, R.K. Rai, I. Choudhuri, S.K. Singh, B. Pathak, Phys. Chem. Chem. Phys. 16 (2014) 26365–26374.
218 Y. Du, H. Chen, R. Chen, N. Xu, Appl. Catal. A Gen. 277 (2004) 259–264.
219 I. Pogorelić, M. Filipan-Litvić, S. Merkaš, G. Ljubić, I. Cepanec, M. Litvić, J. Mol. Catal. A Chem. 274 (2007) 202–207.
220 P. Zhang, C. Yu, X. Fan, X. Wang, Z. Ling, Z. Wang, J. Qiu, Phys. Chem. Chem. Phys. 17 (2015) 145–150.
221 G. Wu, X. Liang, H. Zhang, L. Zhang, F. Yue, J. Wang, X. Su, Catal. Commun. 79 (2016) 63–67.
222 J. Xia, G. He, L. Zhang, X. Sun, X. Wang, Applied Catalysis B: Environmental 180 (2016) 408–415.
276 J. W. Wang, J.W. Liu, N.T. Yang, S.S. Huang, Y.H. Sun, Y. Zhu, Nano 8 (2016) 3949-3953.
277 J. Jiang, G. Li, L. H. Kong, Acta Phys. Chim. Sin. 31 (2015) 137-144.
278 Z.L. Liu, Y. Li, X.Y. Huang, J.I. Zuo, Z.Z. Qin, C.W. Xu, Catal. Commun. 85 (2016) 17-21.
223 M.L. Kantam, R. Chakravarti, U. Pal, B. Sreedhar, S. Bhargava, Adv. Synth. Catal. 350 (2008) 822-827.
224 M.Berger, B. Albrecht, A. Berces, P. Ettmayer, W. Neruda, M. Woisetschläger, J. Med. Chem. 44 (2001) 3031.
225 V. Gotor-Fernandez, P. Fernandez-Torres, V. Gotor, Tetrahedron: Asymmetry 17 (2006) 2558.
226 M. F. A. Adamo, V. K. 3.Aggarwal,; Sage, M. A. J. Am. Chem. Soc. 122 (2000) 8317.
227 R.N. Salvatore, C.H. Yoon, K.W. Jung, Tetrahedron 57 (2001) 7785–7811.
228 H.U. Blaser, H. Steiner, M. Studer, ChemCatChem 1 (2009) 210–221.

229 D.M. Roundhill, Chem. Rev. 92 (1992) 1–27.
230 K. Shimizu, Catal. Sci. Technol. 5 (2015) 1412–1427.
231 M.O. Sydnes, M. Isobe, Tetrahedron Lett. 49 (2008) 1199–1202.
232 J. Zhou, Z. Dong, P. Wang, Z. Shi, X. Zhou, R. Li, J. Mol. Catal. A 382 (2014) 15–22.
233 P. Zhou, Z. Zhang, ChemSusChem 10 (2017) 1892–1897.
234 F.G. Cirujano, A. Leyva-Perez, A. Corma, F.X. Llabres, i Xamena, ChemCatChem 5 (2013) 538–549.
235 L. Li, Z. Niu, S. Cai, Y. Zhi, H. Li, H. Rong, L. Liu, L. Liu, W. He, Y. Li, Chem. Commun. 49 (2013) 6843–6845.
236 L. Hu, X. Cao, D. Ge, H. Hong, Z. Guo, L. Chen, X. Sun, J. Tang, J. Zheng, J. Lu, H. Gu, Chem. Eur. J. 17 (2011) 14283–14287.
237 Y. Yamane, X. Liu, A. Hamasaki, T. Ishida, M. Haruta, T. Yokoyama, M. Tokunaga, Org. Lett. 11 (2009) 5162–5165.
238 P. Zhou, Z. Zhang, L. Jiang, C. Yu, K. Lv, J. Sun, S. Wang, Appl. Catal. B 210 (2017) 522–532.
239 T. Stemmler, A.E. Surkus, M.M. Pohl, K. Junge, M. Beller, ChemSusChem 7 (2014) 3012–3016.
240 T. Stemmler, F.A. Westerhaus, A.E. Surkus, M.M. Pohl, K. Junge, M. Beller, Green Chem. 16 (2014) 4535–4540.
241 X. Cui, K. Liang, M. Tian, Y. Zhu, J. Ma, Z. Dong, J. Colloid Interface Sci. 501 (2017) 231–240.
242 A.F. Abdel-Magid, K.G. Carson, B.D. Harris, C.A. Maryanoff, R. D. Shah, J. Org. Chem. 61 (1996) 3849–3862.
243 N. Ono, The Nitro Group in Organic Synthesis, Wiley, New York (2001).
244 E. A. Artiukha, A.L. Nuzhdin, G.A. Bukhtiyarova, V.I. Bukhtiyarov, RSC Adv. 7 (2017) 45856–45861.
245 Y. Yamane, X. Liu, A. Hamasaki, T. Ishida, M. Haruta, T. Yokoyama, M. Tokunaga, Org. Lett. 11 (2009) 5162–5165.
246 P. Zhou, Z. Zhang, *ChemSusChem* 10 (2017) 1892–1897.
247 A.L. Nuzhdin, E.A. Artiukha, G.A. Bukhtiyarova, E.A. Derevyannikova, V.I. Bukhtiyarov, Catal. Commun. 102 (2017) 108–113.
248 E.A. Artyukha, A.L. Nuzhdin, G.A. Bukhtiyarova, E.A. Derevyannikova, E.Yu. Gerasimov, A.Yu. Gladkii, V.I. Bukhtiyarov, Kinet. Catal. 59 (2018) 593–600.
249 R.V. Jagadeesh, T. Stemmler, A.E. Surkus, H. Junge, K. Junge, M. Beller, *Nat. Protoc.* 10 (2015) 548–557.
250 E. Byun, B. Hong, K.A. De Castro, M. Lim, H. Rhee, J. Org. Chem. 72 (2007) 9815–9817.
251 Y.J. Jung, J.W. Bae, E.S. Park, Y.M. Chang, C.M. Yoon, Tetrahedron 59 (2003) 10331–10338.
252 J.W. Bae, Y.J. Cho, S.H. Lee, C.O.M. Yoon, C.M. Yoon, Chem. Commun. (2000) 1857–1858.
253 B. Sreedhar, V.S. Rawat, Synth. Commun. 42 (2012) 2490–2502.
254 L. Hu, X. Cao, D. Ge, H. Hong, Z. Guo, L. Chen, X. Sun, J. Tang, J. Zheng, J. Lu, H. Gu., Chem. Eur. J. 17 (2011) 14283–14287.
255 L. Huang, Z. Wang, L. Geng, R. Chen, W. Xing, Y. Wang, J. Huang, RSC Adv. 5 (2015) 56936–56941.
256 C. del Pozo, A. Corma, M. Iglesias, F. Sánchez, J. Catal. 291 (2012) 110–116.
257 S. Ergen, B. Nişanci, O. Metin, New J. Chem. 42 (2018) 10000–10006.
258 Y.Z. Chen, Y.X. Zhou, H. Wang, J. Lu, T. Uchida, Q. Xu, S.H. Yu, H.L. Jiang, ACS Catal. 5 (2015) 2062−2069.
259 L. Li, Z. Niu, S. Cai, Y. Zhi, H. Li, H. Rong, L. Liu, L. Liu, W. He, Y. Li, Chem. Commun. 49 (2013) 6843–6845.
260 A. Cho, S. Byun, B. M. Kim, Adv. Synth. Catal. 360 (2018) 1253–1261.
261 D. Yin, C. Li, H. Ren, J. Liu, C. Liang, Chemistry Select 3 (2018) 5092–5097
262 I. Choi, S. Chun, Y. K. Chung, J. Org. Chem. 82 (2017) 12771–12777.
263 J.W. Park, Y.K. Chung, ACS Catal. 5 (2015) 4846−4850.
264 B. Nisanci, K. Ganjehyan, O. Metin, A. Dastan, B. Torok, J. Mol. Catal. A: Chem. 409 (2015) 191–197.
265 R.J. Kalbasi, O. Mazaheri, Catal. Commun. 69 (2015) 86–91.
266 R.J. Kalbasi, S.F. Rezayi, J. Porous Mat. 26 (2019) 641–654.
267 Y. Hayashi, Chem. Sci. 7 (2016) 866–880.

268 R.P. Tripathi, S.S. Verma, J. Pandey, V.K. Tiwari, Curr. Org. Chem. 12 (2008) 1093–1115.
269 H. Alinezhad, H. Yavari, F. Salehian, Curr. Org. Chem. 19 (2015) 1021–1049.
270 R. Retnamma, A.Q. Novais, C.M. Rangel, Int. J. Hydrog. Energy 36 (2011) 9772–9790.
271 D.M.F. Santos, C.A.C. Sequeira, Renew. Sust. Energ. Rev. 15 (2011) 3980–4001.
272 R. W. Layer, Chem. Rev. 63 (1963) 489–510.
273 L. D'Accolti, C. Annese, C. Fusco, Tetrahedron Lett. 46 (2005) 8459–8462.
274 F. Lo, K. Karan, B.R. Davis, Ind. Eng. Chem. Res. 48 (2009) 5177–5184.
275 a) R.E. Davis, J.A. Gottbrath, J. Am. Chem. Soc 84 (1962) 895-898; b) F. Lo, K. Karan, B.R. Davis, Ind. Eng. Chem. Res. 46 (2007) 5478-5484.
279 Z.S. Hou, N. Theyssen, A. Brinkmann,W. Leitner, Angewandte Chemie International Edition 44 (2005) 13465.
280 C.C. Luo, Y.H. Zhang, Y.G. Wang, Journal of Molecular Catalysis A: Chemical 229 (2005).
281 T.S. Huang, Y.H. Wang, J.Y. Jiang, Z.L. Jin, Chinese Chemical Letters 19 (2008).
282 X.M. Ma, T. Jiang, B.X. Han, J.C. Zhang, S.D. Miao, K.L. Ding, G.M. An, Y. Xie, Y.X. Zhou, A.L. Zhu, Catalysis Communications 9 (2008).
283 Y. D. Lu, Y. H. Wang , Z. L. Jin, Chinese Chemical Letters 21 (2010) 1067–1070.
284 Z. Sun, Y. Wang , M. Niu, H. Yi, Ji. Jiang, Z. Jin, Catalysis Communications 27 (2012) 78–82.
285 M. Niu, Y. Wang, P. Chen, D. Du, J. Jiang, Z. Jin, Catal. Sci. Technol. 5 (2015) 4746–4749.